



GP-RSS

International Joint Graduate Program in Resilience and Safety Studies



SyDE

WISE Program for
Sustainability in the
Dynamic Earth

変動地球共生学卓越大学院プログラム

**The 9th International Symposium
on Water Environment Systems
---with Perspective of Global Safety
(November 25th – 26th, 2021)**

**Department of Civil and Environmental Engineering
Graduate School of Engineering
Tohoku University**



**TOHOKU
UNIVERSITY**

Sponsors



**International Joint Graduate Program in
Resilience and Safety Studies of Tohoku University**

<http://gp-rss.tohoku.ac.jp/>



**WISE Program for Sustainability in the Dynamic
Earth of Tohoku University**

<https://syde.tohoku.ac.jp/>



**Department of Civil and Environmental
Engineering, Graduate School of Engineering,
Tohoku University**

<http://www.eng.tohoku.ac.jp/>

ORGANIZERS

- Dr. So KAZAMA (Professor, Tohoku University)
Dr. Yu-You LI (Professor, Tohoku University)
Dr. Daisuke SANO (Professor, Tohoku University)
Dr. Daisuke KOMORI (Associate Professor, Tohoku University)
Dr. Kengo KUBOTA (Associate Professor, Tohoku University)

SECRETARIATS

Assistant Professor, Dr. Yoshiya TOUGE
yoshiya.touge.a6@tohoku.ac.jp

Assistant Professor, Dr. Yu QIN
yu.qin.e8@tohoku.ac.jp

PARTICIPANTS

Tohoku university **Japan**

Name	Identity
Shuka KAGEMASA	Student
Luhur Akbar DEVIANTO	Student
Tianjie WANG	Student
Gaoxuefeng FENG	Student
Chen WANG	Student
Zibin LUO	Student
Kampachiro URASAKI	Student
Junhao SHEN	Student
Shitong ZHOU	Student
Ke Shi	Student
Vempi Satriya	Student
Mohammad Naser Sediqi	Student
Amalia Nafisah Rahmani Irawan	Student
Huang Qin	Student
Hayata Yanagihara	Student

The Hong Kong Polytechnic University **China**

Name	Identity
Hongxing YANG	Professor

Westlake University **China**

Name	Identity
Feng JU	Professor

University of Nottingham **UK, China, Malaysia**

Name	Identity
Chris Gibbins	Professor
Matthew Johnson	Associate Professor
Faith Chan	Associate Professor
Thomas Stanton	Lecturer

Kasetsart University **Thailand**

Name	Identity
Prem Rangsiwanichpong	Lecturer

Xi'an University of Architecture and Technology **China**

Name	Identity
Yu LI	Student
Ziwen JIA	Student

China Agricultural University **China**

Name	Identity
Mengmeng JIANG	Student
Zhiyue WU	Student

Shanghai University **China**

Name	Identity
Jinghuan LUO	Postdoctoral Researcher
Bohan YU	Student

Schedule (GMT+9)

25 Nov (Thu)

10:00 ~ 12:00 **Online Fieldwork**
Topic: AnMBR&Anammox pilot-scale plant

26 Nov (Fri)

9:00 ~ 9:05 **Opening speech**

9:05 ~ 9:10 **Group photo**

Session I Oral session I

9:10 ~ 9:40 The Power of Biology in River Environments
Matthew Johnson, University of Nottingham

9:40 ~ 10:10 Sustainable urban water management strategies in Chinese cities –
the Sponge City Program (SCP): the case of Ningbo
Faith Chan, University of Nottingham

10:10 ~ 10:40 Linking Remote Sensing Data and Soil-Bioengineering Technique for
Erosion Control in Sop Moei district, Thailand
Prem Rangsiwanichpong, Kasetsart University

10:40 ~ 10:50 **Coffee break**

10:50 ~ 11:10 Defining Global Fire Patterns and Quantifying Climate Influence on
Ke Shi, Tohoku University

11:10 ~ 11:30 The spatial and temporal response of wet crops to agricultural drought: A case
study in Indonesia
Amalia Nafisah Rahmani Irawan, Tohoku University

11:30 ~ 11:50 Evaluation of historical and future simulations of precipitation and
temperature in Afghanistan from CMIP6 climate models
Mohammad Naser Sediqi, Tohoku University

11:50 ~ 13:00 **Lunch break**

13:00 ~ 14:30 **Poster session**

Poster exhibition (Room A)

- Global-scale analysis of crop response pattern to different drought
timescales
Vempi Satriya, Tohoku University
- Evaluate the dynamic change of burn-ability by observing the fuel
moisture content in Japan
Huang Qin, Tohoku University
- Changes in exposed population to heavy rainfall disasters associated
with population decline in Japan
Hayata Yanagihara, Tohoku University

Poster exhibition (Room B)

- Assessment of long-term operation performance in mesophilic anaerobic co-digestion of Lipid and Food Waste
Chen WANG, Tohoku University
- Influence of ammonia concentration on the treatment performance of pilot-scale one-stage PN/Anammox process
Zibin LUO, Tohoku University
- Development of a BrISH for environmental microorganisms
Kampachiro URASAKI, Tohoku University
- Methane fermentation performance of pig manure treatment by a pilot-scale self-agitated anaerobic baffled reactor
Junhao SHEN, Tohoku University
- Enhancement Effect of Two Novel Pretreatment Methods on Anaerobic Digestion of Waste Activated Sludge with Thermophilic
Shitong ZHOU, Tohoku University

Session II Plenary lectures

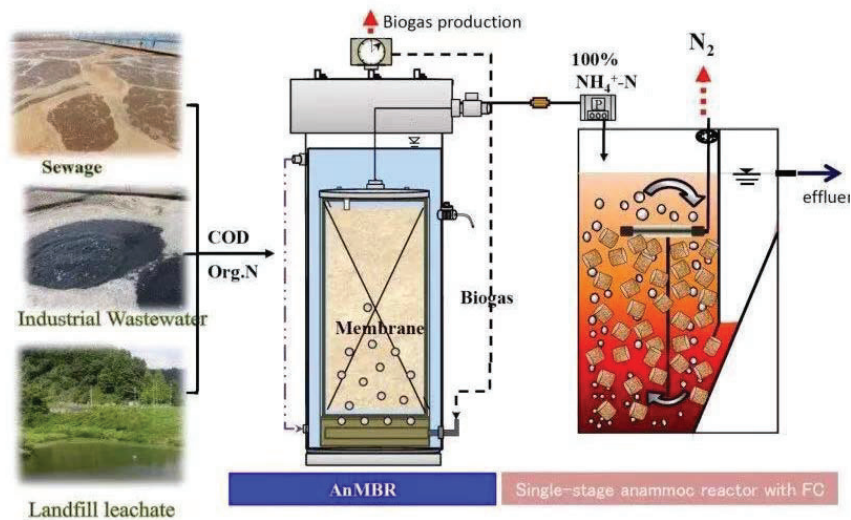
- 14:30 ~ 15:00 Applications of Solar Photovoltaics and Offshore Wind Power towards Carbon Neutrality in Coastline Cities
Hongxing YANG, The Hong Kong Polytechnic University
- 15:00 ~ 15:30 Exploring Microbiome Assembly and Antibiotic Resistome in Wastewater Treatment Plants
Feng JU, Westlake University

Session III Oral session II

- 15:30 ~ 15:45 Diversity and genomic information of Patescibacteria in activated
Shuka KAGEMASA, Tohoku University
- 15:45 ~ 16:00 Sewage concentration for detecting public health biomarkers in
Luhur Akbar DEVIANTO, Tohoku University
- 16:00 ~ 16:15 Influence of temperature on treatment performance of municipal wastewater by a pilot-scale Anaerobic Membrane Bioreactor (AnMBR)
Tianjie WANG, Tohoku University
- 16:15 ~ 16:30 AnMBR treating swine waste : from lab-scale to pilot-scale
Yu LI, Xi'an University of Architecture and Technology
- 16:30 ~ 16:45 Mitigation of membrane fouling in a thermophilic hybrid AnMBR treating food waste
Mengmeng JIANG, China Agricultural University
- 16:45 ~ 17:00 Elucidating fouling characterization in a high solid anaerobic membrane bioreactor treating OFMSW leachate
Zhiyue WU, China Agricultural University
- 17:00 ~ 17:15 Effective enrichment of anammox granules for high-loading landfill leachate treatment: Research progress
Jinghuan LUO, Shanghai University

- 17:15 ~ 17:30 | Biochar enhances partial denitrification/anammox by sustaining high rates of nitrate to nitrite reduction
Ziwen JIA, Xi'an University of Architecture and Technology
- 17:30 ~ 17:45 | Enhancing phosphorus recovery from sewage sludge using anaerobic-based processes: Current status and perspectives
Bohan YU, Shanghai University
- 17:45 ~ 18:00 | Mainstream Nitrogen Removal by a Partial nitritation-anammox Reactor with HAP Syntrophic Granules after an AnMBR
Gaoxuefeng FENG, Tohoku University
- 18:00 ~ 18:10 | **Closing speech**

Online fieldwork- AnMBR&Anammox pilot-scale plant



- New concept of organic wastewater treatment



- Pilot plant of AnMBR and One-stage Anammox in Senen sewage treatment plant

AnMBR and One-stage Anammox is a new technology to develop an energy-positive innovative sewage treatment system integrating an anaerobic membrane bioreactor (AnMBR) and anaerobic ammonium oxidation (Anammox) process. The pilot plant in Senen sewage treatment plant has a working volumes of 20 L for the AnMBR and 7 L for One-stage Anammox reactor and completed with a capacity of 20 m³/d after a 140-day operation.

The Power of Biology in River Environments

○ Matthew JOHNSON^{1*}

¹School of Geography, University of Nottingham, NG7 2RD, UK.

*E-mail: M.Johnson@nottingham.ac.uk

Abstract

Our knowledge of river processes is dominated by engineering and physics approaches focused on the hydraulic power of water and its ability to move the mineral sediment that constitutes river beds and banks. This excludes the role of living organisms, many of which burrow into river beds and banks, redistribute sediments when moving and foraging, or stabilize sediments through roots, mucous or silk. Here, experimental and field data are used to compare the energy in the biological community to the hydraulic energy to compare potential sources of power for geomorphological work. Experiments also show that Signal Crayfish, an invasive species, move sediment whilst expending much lower energy than would be expected by the hydraulic flow required to move equivalent grains. The paper discusses the implications of these findings to fluvial geomorphology and channel form.

Keywords: 1. Ecosystem engineering, 2. Biogeomorphology, 3. Signal Crayfish, 4. Stream Power, 5. Channel dynamics.

1 Introduction

Organisms living in rivers have adapted to survive, utilize and modify fluvial environment. There are numerous examples of living organisms altering river channels; however, that knowledge is not well integrated into geomorphological systems.

Sediment transport and channel change is typically related to the hydraulic power of water i.e. the stream power. It is proposed here that stream power is supplemented or retarded by biological power associated with, for example, burrowing animals and stabilization by plant roots, respectively. Framing the interaction of organisms and the environment as an energy transfer may be an informative way of integrating ecological processes into more established knowledge frameworks and assessing the relative significance of animals in comparison to purely physical processes.

2 Materials and methods

The potential relative significance of animals in controlling river processes was investigated at two scales. First, the stream power per unit width along three rivers was modelled using existing topographic, discharge and site survey data. In these rivers, there were also repeated species-level macroinvertebrate samples. Information on the calorific content of the collected species was collated from the literature, which was used to represent the theoretical maximal energy available for modifying environments. A comparison could then be made between the maximal biological power and the maximal hydraulic power, seasonally, at sites along rivers

Second, a higher resolution study was performed to investigate a specific example of a bio-geomorphic energy exchange. To further investigate the role of animals in sediment transport, Signal Crayfish (*Pacifastacus*

leniusculus) were investigated in mesocosm and field experiments. Signal Crayfish are an invasive species, native to the west coast of the USA, and invasive through northern Europe and Japan. They burrow extensively into river-beds and banks, causing bank collapse and damage to infrastructure including flood defenses. Past experiments have shown these animals can double bedload transport rates of gravels due to their redistribution of sediment grains across sediment surfaces [1] and field work has found they can increase fine sediment transport in rivers by 30% due to their burrowing activity [2].



Fig. 1. A Signal Crayfish on the experimental sediment.

Here, Signal Crayfish were held in sealed aquaria and their energy expenditure was estimated as a function of their respiration rate. As a validation, videography of grain movements was used to estimate energy expenditure associated with sediment reworking by multiplying the energy required to move a single grain by the estimated distance the grain was moved. By using an experimental

substrate where all grains were of identical weight and size, calculations could accurately estimate the energy required to modify sediment positions (Figure 1).

3 Results and discussion

The unit power (Watts/m²) associated with invertebrates at the sampling sites was consistently an order of magnitude higher than the stream power associated with Q10 flows. Only a small proportion of the biological energy associated with the invertebrate community would be used for sediment alterations; however, the same is also true of the unit stream power. Therefore, this result indicates the potential significance of invertebrate animals as a source of power for geomorphological work.

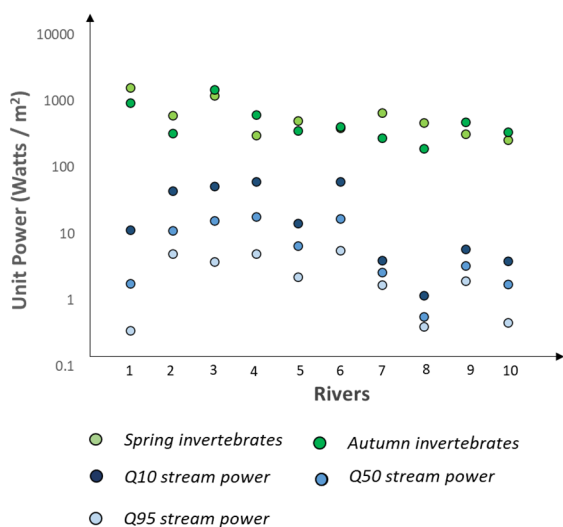


Fig. 2. The unit power associated with the invertebrate community in spring and autumn, and the equivalent stream power for the Q10, Q50 and Q95, representing the largest, median and lowest flows, respectively.

Oxygen measurements indicated that crayfish expended approximately 6 Joules per hour (i.e. 0.0017 Watts/m²), confirmed by videography that found crayfish moved 300 grains an average of 6 grain diameters, indicating a power of 0.0015 Watts/m². Extrapolating to crayfish populations recorded in the River Nene, UK, crayfish would expend 0.08 W m Watts/m² per night, which is much lower than the recorded stream power associated with the Q10 flow (37 W m Watts/m²). However, crayfish were found to move sediments up to 40 mm in diameter, which according to standard size-power relationships would require flows of 30 W m Watts/m² to mobilise. Therefore, crayfish are more efficient than the flow in moving sediments, requiring smaller powers to have the same geomorphological impact.

4 Conclusions

Biological power is much more efficient at moving sediment than stream power, complicating direct comparisons between biological and physical processes. However, it is clear that the biological power associated with invertebrate animals in rivers is substantial with the

potential to do significant geomorphological work, and that using metrics of energy expenditure and power may offer a useful framework for better integrating biological processes into river science.

References

- [1] Johnson, M.F., Rice, S.P. and Reid, I. (2011) Increase in coarse sediment transport associated with disturbance of gravel river beds by signal crayfish (*Pacifastacus leniusulus*). *Earth Surface Processes and Landforms* 36: 1680-1692.
- [2] .Rice, S.P., Johnson M.F., Mathers, K., Reeds, J., and Extence, C. (2016) The importance of biological biotic entrainment for base flow fluvial sediment transport. *Journal of Geophysical Research: Earth Surface* 121: 890-896.

Sustainable urban water management strategies in Chinese cities – the Sponge City Program (SCP): the case of Ningbo

○ Faith Ka Shun CHAN^{1,2*}, Lei LI¹ & Miran LU³

¹ School of Geographical Sciences, University of Nottingham Ningbo China, Ningbo 315100, China.

² Water@Leeds Research Institute, University of Leeds, Leeds LS29JT, United Kingdom.

³ Faculty of Science Department of Statistics and Applied Probability, National University of Singapore, Blk S16, Level 7, 6 Science Drive 2 Singapore 117546, Singapore.

*E-mail: faith.chan@nottingham.edu.cn

Abstract

‘*Sponge City*’ is the term used to describe the Chinese government’s approach to urban surface water management. The concept was conceived in 2014 in response to an increasing incidence of urban surface flooding in many Chinese cities. While ambitious and far-reaching in its aim (of reducing national flood risk, increasing water supply and improving water quality), the initiative must be implemented by individual sub-provincial or municipal-level government entities. Thus, while the concept is similar to Blue-Green Cities (BGCs). Indeed, the increasing use of national rather than international examples of best practice reflects a growing body of knowledge that has evolved since the start of the Sponge City initiative. In this session, we will discuss about the interpretation and development of the latest SCP guidelines by using the case of Ningbo, Zhejiang Province. In this study, we principally looking at the public perception and participation, and found that the influence on social media and communication channels between the according authorities have been initiated on the SCP development from the case of Ningbo. The communities have ways to express their opinions towards the SCP practice and operations for the improvements and adjustments. These findings will help to improve the current 3rd stage development of the Program until 2030s and beyond.

Keywords: Sponge City 1; Urban surface water flooding 2; Blue-Green Infrastructure 3; Climate Change 4; Public Participation 5.

1 Introduction

China has experienced rapid social-economic development in the recent decades. Substantial landuse changes and urbanisation enhanced several urban water issues, such as urban floods and water pollution (Xia et al., 2017). The natural hydrological cycle has been interrupted by removing green spaces (e.g. farmland, suburb land, wetland, etc.), which deficient 40-50% of stormwater intake in natural environment. Urban runoff coefficient has been significantly increased due to soil sealing and urban transformation with infrastructures (Yin et al., 2017). However, the existing land drainage system only withstand at 1-in-1 to 1-in-5 years return period. Unfortunately, Chinese cities suffer severe urban (surface water) floods because of insufficient drainage capacity. For example, Zhengzhou flood in July 2021,

Wuhan in 2020 and 2016, Ningbo in 2021 and 2013, Shenzhen in 2014 and 2013, and Beijing in 2012 (Griffiths et al., 2020, Xiao, 2021). These events caused casualties, injuries and huge economic impacts alarmed the Central National Government (CNG) to take according actions on urban flood relief.

The Sponge City Program (SCP) was initiated in 2013 and aimed to alleviate urban water floods, which reduce urban runoff discharge, infiltrate and storing urban stormwater by Blue-Green Infrastructure (BGI) to achieve 1-in-30 years protection level (Chan et al., 2018). Likewise, the SCP (selected 30 pilot cities across China) to restore natural hydrological function by improving soil infiltration, stormwater retention, storage, purification, but also retrofit to upgrade traditional engineering drainage systems via hybrid (green-grey) measures (e.g. artificial wetlands, ponds, green-

roofs, bio-swales, rain gardens, etc.) and achieving multiple benefits on improving the urban ecosystem services (Xie et al., 2020).

Ningbo is selected as one of the pilot cities in 2015 and undertaking several SCP infrastructure sites (e.g. Eco-corridor and Cicheng Park, etc.) (Fig.1). The city is frequently suffered with typhoon-enhanced storm surges and intensive rainstorms, over 80% of annual precipitation for about 1700-2200mm from May to September (Tang et al., 2015). The city was inundated severely in Typhoon Fitow during 2013, the municipal government integrated with the strategic scheme, namely “Five Water Management” Plan, which includes (i) sewage discharge treatment; (ii) flood control; (iii) waterlogging discharge; (iv) freshwater supply and (v) water conservation that is supported by the Zhejiang Provincial and Ningbo municipal governments. These practices co-produce with the SCP and targeting to deliver better urban water management and sustainability goals for the communities. These practices and policies have been established for several years and yet to know the conditions on public perceptions, understanding and awareness, but also the participation. The authorities have spent efforts on improving the communication channels (e.g. some popular social media platform in China).

This study aims to investigate current SCP and Five Water Management Plan in the case of Ningbo. We provide justification from our interviews and questionnaires and triangulate and validate current practices in Ningbo.



Fig. 1. SCP site locations in Ningbo as interviews and questionnaire sites for this study (Locations A: New East Town; B: Ci Cheng Park; C: Sanjiangkou Park; D: Yinzhou Park; E: Nan Tang Old Street) (Source: authors).

2 Materials and methods

In this study, we adopted the questionnaire survey and semi-structured interviews all conducted by face-to-face in the public space (e.g. surrounding the SCP parks, coffee shops, café, etc.). The survey sites for questionnaires were selected from the SCP projects location in Ningbo (see Fig.1) as for investigating the communities who are living in that area or commonly using these SCP facilities (e.g. Sponge urban parks, sponge healthy running tracks, Sponge artificial ponds and wetlands.). The survey was conducted from June to August 2017. Due to the limited labour resources and weather conditions, this study managed to conduct 110

questionnaires. All survey data were statistically analysed using Excel and R software.

Whilst, the interviews were helpful to understand more in-depth perspectives from the communities of the SCP and Five Water Management practices in Ningbo. The interviewees were selected randomly and each interview were about 10 minutes each conducted during November 2019 that aims to articulate the perception from the communities from the 2017 survey data set. The data was transcribed and translated. The analyses based on the ground theory, and the researchers undertook manual coding that match with the key research themes in this study. All data from the questionnaire survey and interviews have been undertaken the approved ethics application. All interviewees have been informed and agreed with the consent. All information to be deleted after the project completion.

Table 1 Interviewees' information

Participant ID (Interviewees)	Age, gender and occupation	Interviewees' home location (within 3km radius at the relevant SCP sites)
A	Elderly (F), 60, retired	NET Eco-corridor
B	Flower sales-person in South Business District, 35	Yinzhou Park
C	Elderly (F), 55, retired	Sanjiangkou Park
D	Housewife (F), 40	Cicheng Park
E	Primary school teacher (M), 30	Cicheng Park
F	Student (F), 20 in South Business District	Yinzhou Park
G	Waitress (F), 35 in Nantang Old Street	Nantang Old Street, Sanjiangkou Park
H	Elderly (M), 60, retired	Nantang Old Street, Sanjiangkou Park
I	Businessman (M), 55, at reside around the Tianyi Square	Nantang Old Street, Sanjiangkou Park
J	Student (M) 20, reside around the Tianyi Square	Nantang Old Street, Sanjiangkou Park

3 Results and discussion

In this questionnaire, we have conducted some other issues such as general information, perception on Fiver Water Management Plan, SCP, sustainability issues and future foresights about these programs.

In this section, we mostly focused on illustrating the results that responding our major research questions that conducted five specific questions in the questionnaire set on the perception issue (see Fig.2) and listed here:

“11. Ningbo has done a lot of works on urban river restoration under the 5-water management plan, are you familiar of this policy/what are the 5-water management about?

a. Not at all, b. little, c. modest, d. fully understood

12. Do you think it is useful to promote urban river restoration in Ningbo?

a. Not at all, b. a little, c. modest, d. very useful

13. Do you think there are any connections between Five Water Management Plan with sponge city projects?

a. Not at all, b. a little, c. modest, d. a lot of connections

14. Do you think more areas in Ningbo other than East town (Jiangdong) and North district (Jiangbei) need to be undertaken sponge city and urban river restoration projects?

a. No, b. Yes

15. Do you think current awareness and participation are enough to public for these projects?

a. Not at all, b. a little, c. modest, d. enough

We have found the results (see Fig.2) demonstrated the communities were not too familiar about the urban river restoration under Five Water Management Plan and urban river restoration (Q11) as 33.64% participants responded unfamiliar and another 44.55% respondent expressed with little understanding on the Five Water Management Plan.

In fact, we found that the communities also have rather conservative viewpoints on the usefulness of promoting urban river restoration in Ningbo (Q12) as only at about 9% participants expressed that promoting urban river restoration in Ningbo was very useful, but majority were expressed not useful or only little useful. Interestingly, we also found that majority of participants found no connection (3.64%) or only with little connection (about 27%) between Five Water Management Plan with SCP in Ningbo (Q13).

Participants believed it was not too useful to promote the urban river restoration and expressed only a little connection between Five Water Management Plan, urban river restoration and SCP as according to the analysis of the connection among these practices (Q12 and Q13), which reflected the public perception to the functions and benefits in urban ecology, water management and urban flood risk management and climate change adaption with these three main strategies from the data set in 2017 were yet understood the Science and technical aspects well.

That findings were implied by Q14 and Q15, which majority of community residents expressed that the SCP and urban river restoration should still be promoted and continuously expanded Five Water Management should still be undertaken (over 65%), but majority of participants admitted that their own awareness and participation were not enough (with about total 58% expressed not at all or a little awareness and participation) for these practices. That reflected the awareness and participation issues might influence the perceptions on the urban water management issues in Ningbo (include Five Water Management and SCP) from the 2017 questionnaire data set.

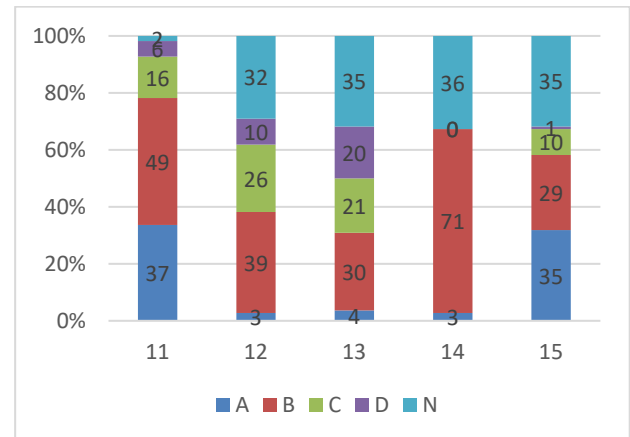


Figure 2 Public perception on urban river restoration, Sponge City Program and Five Water Management (note perception on these questions refer as above: Blue: Not at all (for Q11-13, 15)/Yes (Q14), Orange: a little (for Q11-13, 15)/No (Q14), Grey: Modest (Q11-13, 15), Yellow: fully understood (Q11)/very useful (Q12)/lots of connection (Q13)/enough (Q15), Green: Answer not valid/incomplete/not answered.

For such findings on public perceptions, we justified with the 2019 interview data with the local community and found that there were some evident afterwards. For some reasons, such as lacking of education and promotion, especially to elderlies, an elderly interviewee living around the Yinzhou Park responded (interviewee A): "...I have not heard too much on these programs, because I am getting old at this age, do not pay attention..." Another elderly interviewee (interviewee H) also responded: "...read and understood it (these programs/strategies) via the newspaper but can't remember it clearly, found these are helpful policies".

Moreover, we interviewed some interviewees who understood these schemes via social media channels, such as via the mobile apps that the elderlies might find their difficulties to adapt the implications from technology. Two students ex-pressed (interviewee F, resided at South Business district close to Yinzhou Park) "Heard it in the car radio and received relevant publicity via SMS."; another student (interviewee J, living around the Tianyi Square close to Sanjiangkou Park) expressed that "...Saw (these programs) on app news..."

For the work professional age that a flower-seller operated the shops at a shopping mall around the Yinzhou Park (interviewee B) expressed that: "...saw related information on mobile phone text messages..."; another interviewee working as a primary school teacher (interviewee E, Ci Cheng Park) expressed he understood about these urban water management strategies via television channels "...understanding (these programs) from TV news, three out of five water management are remembered: sewage, drainage water and flood."

From these justifications in the 2019 interviews, we can understand that the Municipal Government has actually used and adopted multiple channels on these urban water management strategies by TV, newspaper and lately via mobile apps, internet sources for enhancing promotion and improvement on public awareness and participation. We recommend the government may engage with the communities in several age groups for gathering them for

some local education activities or community engagement activities to enhance further public participation.

4 Conclusions

Ningbo Municipal Government has spent tremendous efforts on improving urban water issues by implementing SCP, Five Water Management and undertaking the large-scale urban river restoration schemes during the last few years. Despite more time is needed to see the performance and effects based on the regular monitoring and review. The optimistic effects at this early stage is reflected in the support of these schemes in 2017 from the communities and public. These showed the current challenges of reflecting the latest situation and phenomenon of these schemes as the data has been finalised after only a few years of implementation.

Public perception can be improved by using several channels and adopt “fit-for-purpose” approach such as looking after different age groups’ understanding and learning of these strategies (i.e. elderly and other age groups).

These lessons will be vitally important to improve urban water management strategies holistically providing good lessons for other Chinese cities that faced potential water risks from climate change and rapid urbanisation factors.

Reference

- CHAN, F. K. S., GRIFFITHS, J. A., HIGGITT, D., XU, S., ZHU, F., TANG, Y. T. & THORNE, C. R. 2018. “Sponge City” in China—A breakthrough of planning and flood risk management in the urban context. *Land Use Policy*, 76, 772.
- GRIFFITHS, J., CHAN, F. K. S., SHAO, M., ZHU, F. & HIGGITT, D. L. 2020. Interpretation and application of Sponge City guidelines in China. *Philos Trans A Math Phys Eng Sci*, 378, 20190222.
- TANG, Y.-T., CHAN, F. K. S. & GRIFFITHS, J. 2015. City profile: Ningbo. *Cities*, 42, Part A, 97-108.
- XIA, J., ZHANG, Y., XIONG, L., HE, S., WANG, L. & YU, Z. J. S. C. E. S. 2017. *Science China Earth Sciences*, 60, 652.
- XIAO, E. 2021. Death Toll From China Flood Jumps to More Than 300. *Wall Street Journal - Online Edition*, N.PAG-N.PAG.
- XIE, X., QIN, S., GOU, Z. & YI, M. 2020. Engaging professionals in urban stormwater management: the case of China’s Sponge City. *Building Research & Information*, 48, 719-730.
- YIN, H.-L., ZHAO, Z.-C., WANG, R., XU, Z.-X. & LI, H.-Z. 2017. Determination of urban runoff coefficient using time series inverse modeling. *Journal of Hydrodynamics*, 29, 898-901.

Linking Remote Sensing Data and Soil-Bioengineering Technique for Erosion Control in Sop Moei district, Thailand

○ Prem Rangsiwanichpong^{1*}, Chatchai Ngernsaengsaruy², Nisa Leksungnoen³,
and Apinit Jotisankasa⁴

¹Department of Water Resources Engineering, Faculty of Engineering,
Kasetsart University, Bangkok 19000, Thailand.

²Department of Botany, Faculty of Science, Kasetsart University, Bangkok 19000, Thailand.

³Department of Forest Biology, Faculty of Forestry, Kasetsart University, Bangkok 19000, Thailand.

⁴Department of Civil Engineering, Faculty of Engineering, Kasetsart University, Bangkok 19000, Thailand.

Correspondence to: Prem Rangsiwanichpong (Prem.R@ku.th)

Abstract

There is a potential for landslide hazards in the Sop Moei area, southernmost district of Mae Hong Son province, Thailand. Landslide happen by the combination factors such as earthquake, monsoon, and human activities. Water erosion is the one of main factors that leading to soil detachment and landslide event in high slope area. Therefore, the objective of this research is to estimation annual soil loss and generate a soil erosion potential map using GIS technique based on the Revised Universal Soil Loss Equation (RUSLE). The results shown that the high potential of soil erosion areas have also higher risk of landslide event. It involves identification of soil erosion hazard areas and rising community awareness of soil erosion risk, study of plants with potentials for bio-slope stabilization, in order better prepare the community for prevention and mitigation of soil erosion hazard in high slope areas of Thailand.

Keywords: GIS; Hazard map; RUSLE; Soil Bio-Engineering; Thailand.

1 Introduction

Soil Erosion is the first step in the sedimentation routes which consist of erosion, transportation and deposition of sediment [1]. Soil losses from water erosion, and the host of linked problems associated with occurred landslide events in high slope areas, are currently major environmental issues in Thailand. Therefore, the method for estimating soil erosion is an important for erosion control. In this century, numerical, empirical, and field experiments have been developed for assessing soil erosion. The RUSLE is widely used for estimating annual soil erosion rates. Several publications have used RUSLE method to estimate soil erosion rates for long term ([2], [3]). Currently, the erosion control using herbaceous and woody plants through soil bio-engineering remains a new challenge. Soil Bio-Engineering is the use of plants with engineering technique for control of landslide and erosion. Generally, plant life tend to be stronger and more stable with time as roots penetrate deeper, which engineering structure only deteriorates with time. Nevertheless, soil-bioengineering technique can be prevent only shallow landslide and surface erosion with depth of failure less than 3 meters [4].

This research aims to generate soil erosion hazard map by remote sensing data and using soil bio-engineering technique for erosion control in Sop Moei area. Moreover, this research also study plants which are of potential for preventing soil erosion and landslide in high land area with community participation.

2 Study Area

Sop Moei district is located on the south end of Mae Hong Son province. This area is 192 km. far from Mae Hong Son Mueang district (downtown). Topography, Most of Sop Moei area is a high mountain complex and still a richness natural

forest (Fig.1.). The area of forest is approximately 87.5% of the provincial area. There are mountains along the north-south parallel. (Fig. 2.)

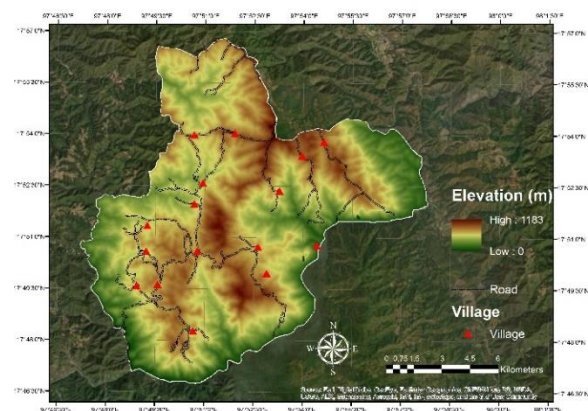


Fig. 1. Topography of Sop Moei district.

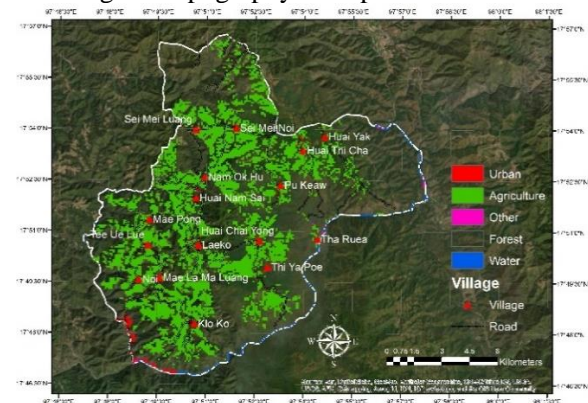


Fig. 2. Land use of Sop Moei district.

3 Methodology and Data

This research aimed to generate the soil erosion hazard map by remote sensing data and Geographic Information System (GIS) technique. The RUSLE method was used to analyze magnitude of soil erosion in each grid cell with 30 m. resolution. The RUSLE method is an empirical soil loss model [5] which can be expressed as:

$$A = R \times K \times LS \times C \times P \quad (1)$$

where:

A is the mean annual soil loss per unit area, R is the rainfall erosivity factor, K is the soil erodibility factor, LS is the topographic factor, C is the cover-management factor, and P is the conservation practice factor.

In this research, we used 20 rain gauge stations operated by the Highland Research and Development Institute (HRDI) to observe daily rainfall data during 2010 to 2020 (10 Years). The annual rainfall in Sop Moei is 1100 mm. per year. For extreme daily rainfall, we found that the extreme daily rainfall for Sop Moei ranges from 59 to 76 mm. with higher values occurring in the southern part of the district (Fig.3.). Moreover, Geologic map data obtained from the Land Development Department of Thailand (LDD).

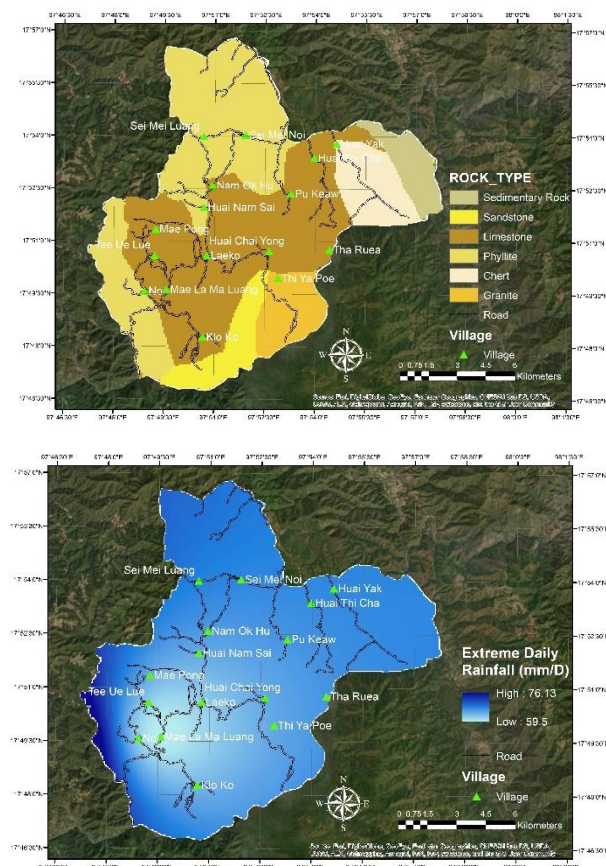


Fig. 3. Geological data and extreme daily rainfall map.

4 Results

The average annual soil erosion for each of the five studied areas was evaluated using the Revised Universal Soil Loss Equation (RUSLE) method with daily rainfall data between 2010 and 2020. The magnitude of erosion were divided into 5 levels: lowest, low, moderate, high and highest respectively.

The results indicate that the potential of average annual soil erosion rate in Sop Moei project is 86 tons/year. Furthermore, the erosion rate were correlated with topography and slope, with higher erosion rate associated with mountainous and higher slope areas. In addition, the results shown that different magnitudes of soil erosion occurring in every part of the studied areas but also significantly higher magnitudes occur in agriculture area without soil & water conservation practice, especially upland rice and maize (Fig.4.). Moreover, this research also compares the soil erosion hazard map with occurrence of landslides by the location of landslide areas from field survey data (Fig.9.). We found that the high potential of soil erosion have also greater risk of landslide occurrence. According to the highland community, the main reasons of such gully formations are agricultural activities, heavy rainfall, and lack of immediate treatment while gullies start to form. Fig.5. shows some of the gullies formed and soil being lost every year in the Sop Moei district. Moreover, the local community showed their good awareness of the local problems, as they were able to give useful information, guide the researchers and discuss about the way to mitigate the soil erosion problem (Fig. 8.)

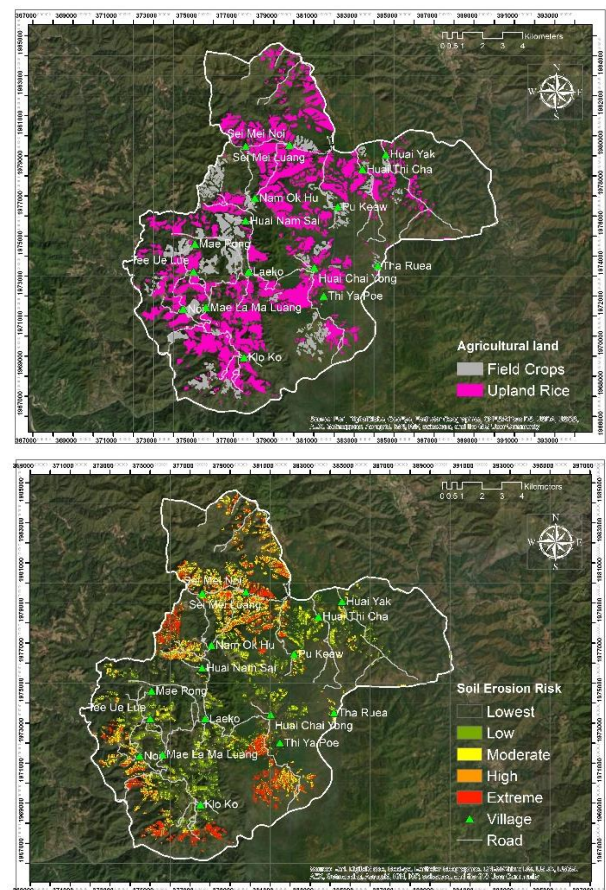


Fig. 4. Agricultural land and soil erosion hazard map.

In the studied area, the forest type is lower montane. The plant species were chosen to study root tensile strength. The criteria for species selection were based on the habitat of the species with both native and exotic species along with the observation of the farmers with the experiences of the HRDI officers. Moreover, the species selection for soil erosion

reduction has to be based on the benefits of the species on the timber, economic, as well as soil and water conservation. However, the native habitat of the species is equally important for consideration because even some species have high ability to reduce soil erosion, species introduced to the new area have to adapt to the new environments. They might adapt and survive but growth might not be normal or they might be able to adapt so well and rapidly take over the native species resulting in invasive species in the area.

Results from root tensile strength clarified that the strength decreased when the diameter of root increased. Root tensile strength also depended on root size, root moisture, root health and root storage, and root age etc.

Plants with high root tensile strength at root diameter of 1 millimeter were *Persea americana* (Avocado) (Fig.6.), *Litsea cubeba*, (Fig.7.), *Coffea arabica* (Arabian coffee), and *Prunus mume* (Plum) which most of them are exotic species that are not native to Thailand (apart from *L. cubeba*). The exotic species were introduced to Thailand for food with good economic benefits and they also serve the soil erosion control as well as soil and water conservation. We considered those species to have full potential for soil-bioengineering.



Fig. 7. Root of *L. cubeba* at Wadokro village (2/8/2020)



Fig. 5. Gully formations and surface soil loss at Sop Moei area (27/8/2020)



Fig. 8. Soil Erosion field survey at Huai Nam Sai village (27/8/2020)



Fig. 6. Root of *P. americana* (Avocado) at Wadokro village (1/8/2020)

The treatment of soil surface for protecting soil erosion in Sop Moei district can be done based on 2 levels of erosion problem as follows.

1. For areas where erosion just started or moderate erosion, vetiver system should be used along the contour, with 0.5m spacing between the rows, according to the standard drawing of Department of Highways or Department of Rural Roads.

2. For areas with severe erosion on side slope or back slope, soil bio-engineering technique including, flapped soil bag, micro pile with live stake can be used. More detailed soil

investigation, slope geometry and other limitations should be performed to make detail designs.

5 Conclusions

The result of soil erosion hazard map in the Sop Moei district Extension Areas indicated that high potential of soil erosion areas mostly occurred in high slope area especially 20 to 30 degrees with sedimentary rock geology, namely, siltstone, mudstone, and sandstone as well as igneous rock. The rainfall are under influence of the monsoon seasonal winds i.e. southwest monsoon and northeast monsoon as well as, orographic rainfall effect. These conditions accelerated

soil erosion leads to landslide events in this area. In studied area, soil erosion occurring in every part of the Sop Moei district but also significantly higher magnitudes occur in agriculture area without soil & water conservation and natural forest upstream with steep slope and high precipitation.

The recommended slope stabilization and erosion control techniques depends on the community conditions and other surrounding factors, which can be categorized in 3 groups, related to the level of engineering technique combined with plants (for lowest to highest), namely, 1) Vegetation technique 2) Soil bag and vegetation and 3) Engineering technique and vegetation.

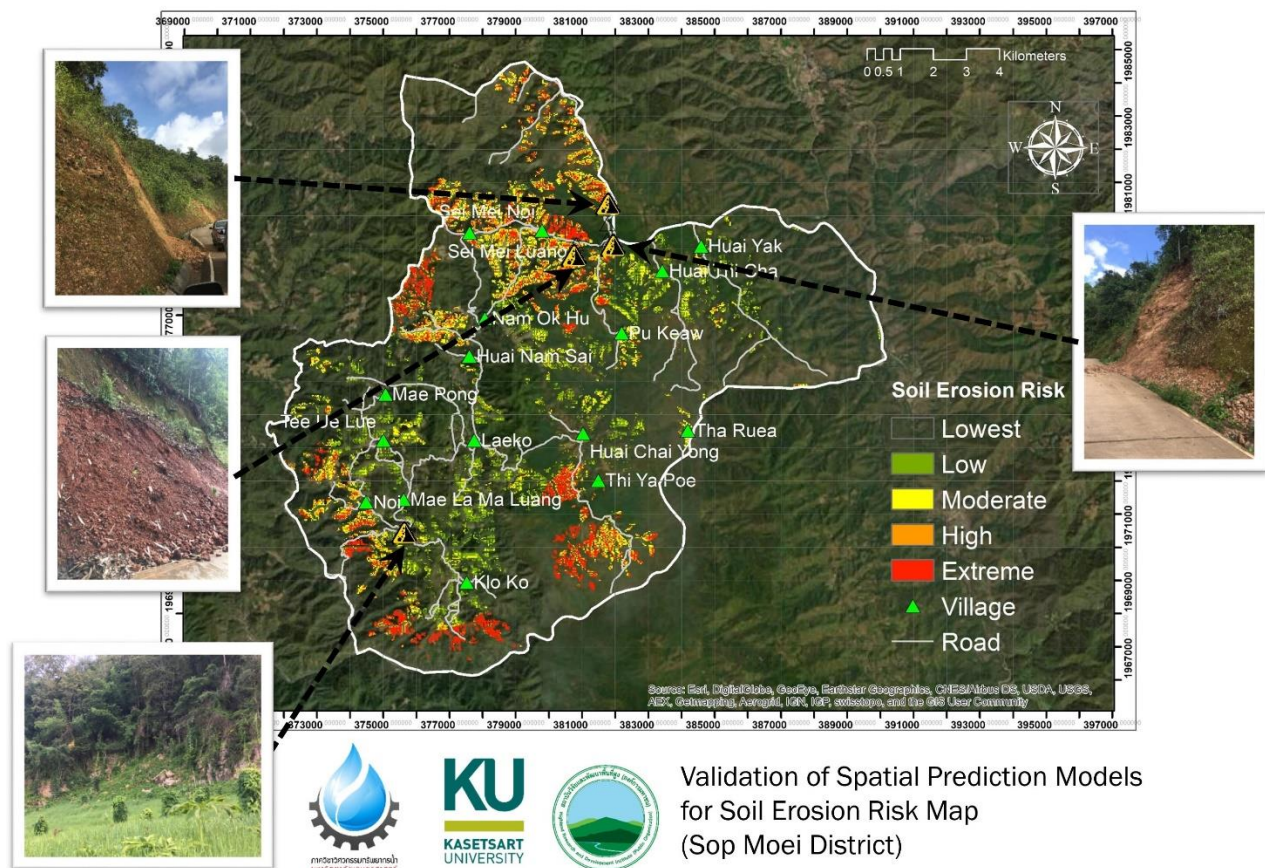


Fig. 9. Comparison of soil erosion risk map and location of landslide at Sop Moei district. (27-30/8/2020)

Acknowledgment

This project was supported by the Highland Research and Development Institute (HRDI). Valuable assistance provided by Dr. Jarunee Pilumwong and staffs at the HRDI. The authors wish to thank the Land Development Department of Thailand (LDD) for providing the geological data.

Reference

- [1] Ouyang D., Bartholic J., Predicting Sediment Delivery Ratio in Saginaw Bay Watershed, Proceedings of the 22nd National Association of Environmental Professionals Conference, Orlando, (1997), pp. 659-671.
- [2] Sahu, A., Baghel, T., Sinha, M. K., Ahmad, I., Verma, M.K., Soil Erosion Modeling using Rusle and GIS on Dudhawa Catchment, International Journal of Applied Environmental Sciences, 12(6), (2017), pp.1147-1158.
- [3] Rangsiwanichpong, P., Kazama, S., Gunawardhana, L., Assessment of sediment yield in Thailand using revised universal soil loss equation and geographic information system techniques, River Research and Application, 34(9), (2018), pp. 1113-1122.

[4] Jotisankasa, A., Taworn, D., Chumchey, N., Sukolrat, J., Quantification of root reinforcement in bio-slope stabilization: laboratory and field studies, Proceedings of the 4th International Conference on Rehabilitation and Maintenance in Civil Engineering (ICRMCE 2018), 195 (2018), pp. 1-11.

[5] Renard, K., Foster, G., Weesies, G., McCool, D., Yoder, D., Predicting soil erosion by water: a guide to conservation planning with the Revised Universal Soil Loss Equation (RUSLE), USDA Agriculture Handbook, 703. (1997)

Defining Global Fire Patterns and Quantifying Climate Influence on Fire

○ Ke SHI^{1*} & Yoshiya TOUGE¹

¹Department of Water Environment, Engineering University, Miyagi 980-8579, Japan.

*E-mail: shi.ke.s5@dc.tohoku.ac.jp.

Abstract

Fires are widespread disasters worldwide and are concurrently influenced by multiple global climatic drivers. The teleconnections between different regional fires and the underlying climatic cause mechanisms have not been fully explored. Determining a suite of global climatic drivers that explain most of the variations in different homogeneous fire regions will be of great significance for fire management, fire prediction, and global fire climatology. Therefore, this study first identified spatiotemporally homogeneous regions of burned area worldwide during 2001~2019 using a distinct empirical orthogonal function. Additionally, the cross wavelet transform and wavelet coherence were used to analyze the relationships between major patterns of fire burned area and various global climatic drivers. The three most significant global climatic drivers that strongly impacted each of the eight major fire patterns were identified. Then, the potential mechanisms of the global climatic drivers for specific regions were discussed. These results provide a reference for future exploration of the connection between fire and climate.

Keywords: Global fire patterns; Climate Influence; Teleconnection.

1 Introduction

Fire, which is strongly responsive to climatic drivers, is a critical component of the natural earth system's ecological process at scales ranging from local to global. Higher temperatures, more rain-free days, more fire events, and more fire-affected areas induce significant fire danger variations. An apparent increase in catastrophic fires has been found globally in recent years.

One of the critical factors affecting fires is climate. One of the best known of these mechanisms is the El Niño-Southern Oscillation (ENSO)-fire dynamic in Insular Southeast Asia [1]. Strong correlations were found between fires and the ENSO index (Southern Oscillation Index and Niño 3.4 index) in equatorial forests. The impact of the Arctic Oscillation (AO) pattern on interannual fire variability in Central Siberia was found by Balzter et al. [2].

Overall, climate variability could influence fire behavior and account for the variability in fire severity at various temporal and spatial scales. Therefore, substantial research has focused on the relationship between climate weather and fire from local to global levels. Aldersley et al. [3] analyzed the relationship between the burned area and meteorological elements such as high temperature and intermediate annual rainfall in fourteen global subcontinental regions. However, these studies mainly focused on gridpoint-specific meteorological elements and fire burned area relationship analysis. Global climatic drivers such were not considered from a more in-depth perspective in their global fire study. Indeed, global climatic drivers are often the most fundamental factor that affects meteorological elements such as precipitation and temperature, which in turn affects global fires. But there is still a gap in the comprehensive understanding of the relationship between global climatic drivers and fire, and even finding the teleconnections between different regional fires can be expected implying that same global climatic driver affecting fire in several regions.

Until now, previous studies have not filled gaps in exploring the spatiotemporally homogeneous regions of

global burned areas and multiple climatic influences. Therefore, a comprehensive study of global fire patterns will help us better understand global fires. Considering that the causes of fires are intricate and usually influenced by multiple factors, it is essential to study multivariable coherence to better reveal the salient features of fires from a global perspective. Therefore, the main aim of this study was to analyze the relationships between major fire patterns and various global climatic drivers.

2 Materials and methods

In this study burned area data is from Fire CCI v5.1 [4] dataset during 2001~2019 at the 1°×1° resolution on the monthly scale. Then, log-transformation was performed for burned area time series. Also, the monthly log-transformed burned area anomalies (logBAA) were subsequently calculated to indicate the abnormal fire condition every month. As for global climatic drivers, in this paper, sixteen global climatic drivers that may have impacts on fires were selected. To explore the diversity of climate causes, both oceanic indices such as the Oceanic Niño Index and continental teleconnection patterns such as the East Atlantic/Western Russia Pattern were considered. These global climatic drivers were sourced from the National Oceanic and Atmospheric Administration (NOAA): <https://www.noaa.gov/> (last access: 11 May 2021).

As for methods, the distinct empirical orthogonal function (DEOF) analysis was utilized to identify the global pattern of logBAA. In the DEOF, a continuous spectrum of spatial patterns resulting from a stochastic process can be represented by EOF modes, where some spatial structures will be more dominant than others. Based on the isotropic diffusion null hypothesis, the EOF modes (DEOFs) can be found by rotating the leading EOF modes, corresponding to the distinguished principal components (DPCs). The details about DEOF can be found in Dommengat [5]. Additionally, the cross wavelet transform (XWT) and wavelet coherence (WCO) [6] can examine the relationship between the DPCs and the global climatic driving factor. WCO reveals local similarities between two time series and may be found to be

a local correlation coefficient in the time-frequency plane; that is, their possible teleconnection can be identified by WCO [6]. The specific XWT and WCO analysis methods can also be found in Torrence et al. [6]. Notably, wavelet analysis brings about a cone of influence (COI) that delimits a region of the WPS beyond which the edge effects become significant, which means outcomes outside COI should be suspected [6].

3 Results and discussion

The DEOF calculation used the logBAA time series of each 1°×1° grid cell on a monthly scale. The first eight DEOFs represented 30.0% of the total variance. Figure 1 displays the spatial patterns of DEOF1~8. Different DEOFs represented different abnormal characteristics of fire burned areas. Specifically, EOF values greater than (less than) 80% of the total are considered high positive (low negative) loading. For example, in DEOF2, the spatial distribution illustrated that low negative loadings occurred in Part of Russia and Ukraine. Meanwhile, the high positive loadings were mainly concentrated in northern Kazakhstan, which also meant that these regions had opposite characteristics as those of the negative loading regions.

Figure 1 also shows the defined region of the three global climatic drivers that have the most significant influence on DEOF1~8. Some regions frequently appeared in different DEOF patterns. The hotspot-1 (around Ukraine and Kazakhstan) was found in DEOF1~3. Although the three most dominant global climatic drivers changed with the DEOF patterns, Atlantic multidecadal Oscillation (AMO), Pacific/North Pacific Oscillation (EP/NP) and Pacific North American Pattern (PNA) were the strongest influencing drivers among these five climatic drivers, indicating that these three global climatic drivers had a relatively strong impact on the hotspot-1. EP/NP, PNA, East Atlantic/Western Russia Pattern (EA/WR) were the dominant global climatic drivers among DEOF2, DEOF4 and DEOF8, where hotspot-2 (southern Africa) appeared concentrated. For DEOF3, DEOF5 and DEOF8, there were three different combinations of global climatic drivers affecting the hotspot-3 (Australia): Multivariate Niño/Southern Oscillation Index (MEI)-DEOF3, AO-DEOF5 and EA/WR-DEOF8. The global climatic drivers that affect the hotspot-4 (Brazil) have become very diverse, where they were found to be affected by ten different global climatic drivers. Affected by ten climatic drivers, PNA, Arctic Oscillation (AO), Polar/Eurasia Pattern (POL) and EA/WR were the dominant global climatic drivers in the hotspot-4 of DEOF4~7.

Overall, our teleconnection analysis has revealed how global climatic drivers affect global burned area patterns, which provides a possibility for informing the anticipation of burned area. As for global burned area patterns, regionality is greatly evident. These hotspots, such as around Ukraine and Kazakhstan, southern Africa, Australia and Brazil, frequently appear in different global burned area patterns. While, even if the around Ukrainian region did not show a large burned area, it showed significant burned area anomalies. Similarly, the United States, where fires frequently occurred, was also insignificant in our global burned area patterns. The study's limitations include the lack of validation for the physical mechanism between the

fire and global climatic drivers. Furthermore, some regions were ignored in our identified global fire patterns.

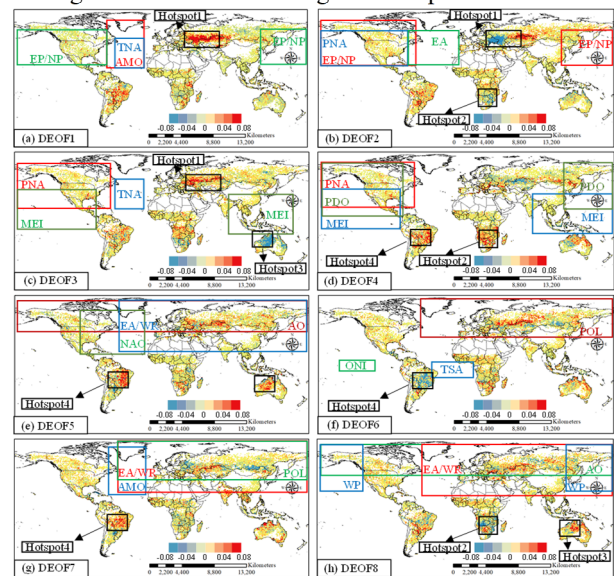


Fig. 1. The location distribution of the top three global climatic drivers with the strongest influence on DEOF patterns.

4 Conclusions

This paper establishes the teleconnection between global climatic drivers and logBAA patterns for the first time and explores the physical mechanism behind their teleconnection from a global perspective. The results of this paper are conducive to a better understanding of the spatiotemporal characteristics of global fire burned areas. Due to the changing climate, atmosphere and ocean scenarios, focusing on global climate drivers provides an efficient and promising reference for predicting fire burned area anomalies. The conclusions will also be valuable for fire management, fire prevention, and global fire ecological climatology.

Reference

- [1] Fuller, D. O. et al. The ENSO-fire dynamic in insular Southeast Asia. *Climatic Change*. 74(2006), 435–455.
- [2] Balzter, H. et al. Impact of the Arctic Oscillation pattern on interannual forest fire variability in Central Siberia. *Geophysical Research Letters*. 32(2005), 1–4.
- [3] Aldersley, A. et al. Global and regional analysis of climate and human drivers of fire. *Science of the Total Environment*. 409(2011), 3472–3481.
- [4] Chuvieco, E. et al. ESA Fire Climate Change Initiative (Fire_cci): MODIS Fire_cci Burned Area Pixel product, version 5.1[dataset]. Centre for Environmental Data Analysis: Didcot. (2018).
- [5] Dommengot, D. Evaluating EOF modes against a stochastic null hypothesis. *Climate Dynamics*. 28(2007), 517–531.
- [6] Torrence, C. et al. A Practical Guide to Wavelet Analysis. *Bulletin of the American Meteorological Society*. 79(1998), 61–78.

Acknowledgements

This study was jointly supported by Grant-in Aid for Scientific Research (B), 2020-2023 (20H02248, Yoshiya Touge).

The spatial and temporal response of wet crops to agricultural drought: A case study in Indonesia

○ Amalia Nafisah Rahmani IRAWAN^{1*}, Daisuke KOMORI^{1,2} & Vempi Satriya Adi HENDRAWAN¹

¹Graduate School of Environmental Studies, Tohoku University, Miyagi 980-8577, Japan.

²Department of Civil and Environmental Engineering, Tohoku University, Miyagi 980-8577, Japan.

*E-mail: amalia.nafisah.rahmani.irawan.q3@dc.tohoku.ac.jp.

Abstract

Wet crop (e.g., paddy) is one of the primary food sources in the world, including in Indonesia. Located in the tropical-humid region, as the main agricultural production, planting season for paddy is divided into the wet cropping season and the dry cropping season. The crop productivity is relatively higher in the dry cropping period due to the availability of sunlight and less clouds which support the crop growth. But there is a high risk of drought that could affect the crop production because the water supply often relies on precipitation especially during the rainy season. Standardized Precipitation Index (SPI) is a well-known drought assessment method found by McKee et al., in 1993 which only requires long term precipitation data for the input, and it can be used to assess the agricultural drought. The SPI analysis was conducted using GSMaP which has 0.1° x 0.1° spatial resolution. According to the correlation analysis between SPI index and drought affected areas on city-scale, SPI-3 in August is the most suitable to assess the agricultural drought in Indonesia. Based on the correlation analysis between SPI-3 and crop yield, the agricultural drought assessment is more suitable to be conducted on a grid-scale because of many local characteristics on fragmented agricultural areas which contribute to the response of wet crops to drought. For the spatial response, the lower crop yield loss is found in the area below the threshold value (r -value ≤ 0.6) or the region where drought is not the main driver of crop yield loss, even in the area that was hit by drought the hardest because there is the existence of irrigation system. But still in the region which more vulnerable to drought or has a high correlation (r -value > 0.6), the existence of irrigation systems cannot withstand the drought event resulting in higher crop yield loss when hit by more severe drought.

Keywords: Agricultural Drought; SPI; Wet Crop; Dry Cropping Season; Temporal Scale; Spatial Scale.

1 Introduction

Agricultural drought started from the lack of precipitation (meteorological drought) that damaged the agriculture area and affected the crop production. Standardized Precipitation Index (SPI) was found by McKee et al., in 1993 that it can be used for drought assessment and only needs the long-term precipitation data (minimum 20-30 years). By using the probability density function and normalization, the SPI can assess the wet and dry conditions over any regions (drought occurred where $SPI \leq -1$). Another benefit of SPI is the temporal versatility so it can be calculated for various timescale according to user's interest (WMO, 2012).

Many researchers have also used SPI for agricultural drought assessment, but there is no general agreement reached to determine the most appropriate timescale to be utilized. For example, Ali (2001) and Ji and Peters (2003) found that SPI-3 is suitable in Turkey and U.S. Great Plains respectively. Meanwhile Iglesias and Quiroga (2017) use SPI-12 as a climate indicator for measuring the climatic risk to cereal production. Still, there is less discussion related to the agricultural drought on wet crops (e.g., paddy). Located in the tropical-humid region, paddy is the main agricultural production in Indonesia. The crop productivity is relatively higher in the dry cropping period due to the availability of sunlight and less clouds which support the crop growth. But there is a high risk of drought that could affect the crop production because the water supply often relies on precipitation especially during the rainy season.

In this research, the objectives are i) to determine the most suitable SPI index to be utilized for agricultural application

in the tropical-humid region, ii) examine the spatial response of wet crop to agricultural drought on city-scale and grid-scale. Specifically, this study was focused on the wet crop during the dry cropping period.

This research was conducted in West Java as one of the largest rice producers in Indonesia with the rainy season from October - March and the dry season from April - September. According to the World Bank in 2016, 31.46% of the land is agricultural land, dominated by paddy fields, which is very vulnerable to drought events. The results of this study will be helpful to get a better understanding about agricultural drought impact on wet crops.

2 Materials and methods

The precipitation data collected from Japan Aerospace Exploration Agency (JAXA) provides near real-time rainfall data on their product called Global Satellite Mapping of Precipitation (GSMaP). The daily precipitation data are available from March 2000 - present date and were retrieved across West Java with 0.1° x 0.1° resolution. The agricultural statistical dataset in this study, drought-affected areas during the dry season and the crop yield (annually and monthly), were obtained from the Ministry of Agriculture and the Agricultural Agency of West Java respectively.

SPI was calculated based on the GSMaP precipitation dataset for various timescale (SPI-1, SPI-3, SPI-6, SPI-9, and SPI-12) with different month reference from January - December which is associated with the dry cropping season. To determine the most suitable SPI index, Pearson correlation analysis was assessed between various SPI index and drought-affected areas on the city-scale. For the

grid-scale analysis, crop yield estimation model was generated using stepwise multilinear regression model from the vegetation indices or the Normalized Difference Vegetation Index (NDVI) obtained from MODIS/TERRA with 250-m resolutions. Then, the correlation analysis was conducted between SPI-3 and detrended crop yield to assess the impact of drought on paddy in Indonesia.

3 Results and discussion

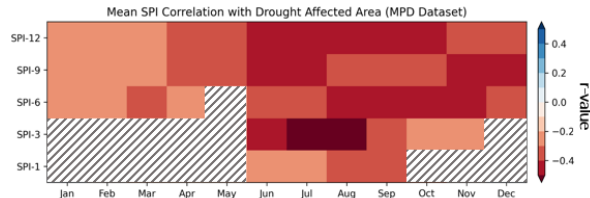


Fig. 1. Heatmap of Mean of Correlation Value between SPI Index and Drought-Affected Areas

Figure 1 showed the heatmap of average correlation value where vertical axis indicated the SPI aggregation timescale and horizontal axis indicated the month reference. The shaded area on the heatmap involved only a wet season which is not a target period of this study, so the result is not included. Based on the heatmap, the correlation resulted in negative values, indicated by the red colour, meaning that the decrease of SPI index, or a dry condition, is associated with the increase of drought-affected areas in the agriculture area. In addition, the highest correlation was found during the SPI-3 in August thus in this study SPI-3 was selected as the most suitable index to be utilized. This finding is consistent with study by Ali in 2013 which stated that SPI-3 is sensitive to the reduction in soil moisture that affects crop growth and with study by Ji&Peters in 2002 which stated that vegetation has a time lag response to precipitation and that the impact of water deficits is cumulative.

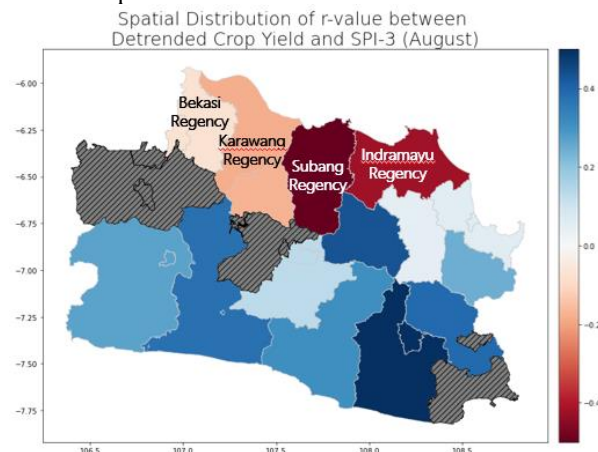


Fig. 2. Spatial Distribution of r-Value between Detrended Crop Yield and SPI-3 on City-Scale

After the most suitable SPI index was determined, the correlation between crop yield and SPI-3 was assessed on city scale. The result did not produce a high significant correlation caused by the spatial scale of the assessment and the uncertainty in the subround dataset. But the different response in the northern area (irrigated by dam) and southern area (irrigated by river or wells) was observed. This result indicates the importance of an advanced irrigation system. In the northern part, severe drought events did not result in a high crop yield loss because there is still water supply for agricultural activity resulted in negative correlation.

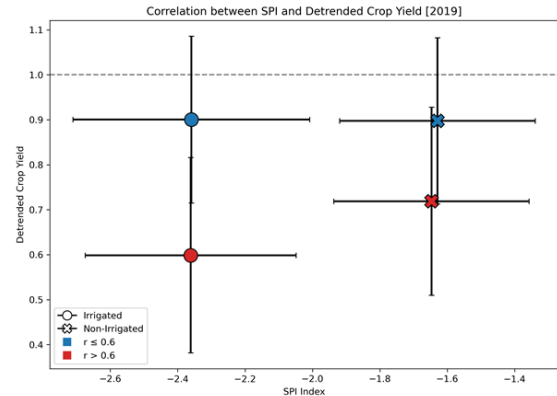


Fig. 3. Correlation between Detrended Crop Yield and SPI-3 in 2019 on Grid-Scale

For the grid-scale analysis, 2019 was selected to be the focus period because of the occurrence of most extreme drought year. Based on the characteristics of the data from grid-scale analysis, it was observed that almost all the grid located in region with r -value ≥ 0.6 experience crop yield loss with various SPI index values indicating the drought event as the main driver of crop yield loss, thus the threshold for r -value was set at 0.6. Figure 3 showed the result from grid-scale analysis with 4 main findings: (1) The irrigation system was installed in the area which was hit by drought the hardest (more to the left). (2) Region with r -value ≥ 0.6 was more vulnerable to drought proven by the red circle marker, the high crop yield loss occurred in the irrigated area when hit by the hardest drought meaning that there might be failure in delivering an adequate amount of water. (3) Region with r -value < 0.6 was more resilient to drought proven by the blue circle marker which has low crop yield loss even after hit by severe drought. (4) Meanwhile the region which is still irrigated by local water resources (cross shaped marker), even though it is not located in the extreme dry region, the water availability is still very dependent with precipitation that might be dangerous in the future because of climate change impact.

4 Conclusions

This study was conducted to assess the spatial and temporal response of the wet crop to the agriculture drought during the dry cropping season. SPI-3 in August is the most suitable index to be utilized and the assessment is recommended to be conducted on grid-scale because there are many local characteristics in fragmented agriculture areas. Based on the correlation between SPI-3 and crop yield, the threshold for r -value was set for 0.6. For the region which more vulnerable (r -value ≥ 0.6), the existence of irrigation systems cannot withstand the drought event resulting in higher crop yield loss when hit by more severe drought. Meanwhile, for the area which more resistant (r -value < 0.6), the low crop yield loss was observed both in irrigated and non-irrigated agricultural areas.

Reference

- [1] World Meteorological Organization, 2012: Standardized Precipitation Index User Guide (M. Svoboda, M. Hayes and D. Wood). (WMO-No. 1090), Geneva.
- [2] Ji, L., & Peters, A. J. (2003). Assessing vegetation response to drought in the northern Great Plains using vegetation and drought indices. Remote Sensing of Environment, 87(1), 85–98.

Evaluation of historical and future simulations of precipitation and temperature in Afghanistan from CMIP6 climate models

○ Mohammad Naser Sediqi^{1*}, Daisuke Komori^{1,2}

¹Graduate School of Environmental Studies, Tohoku University, Miyagi 980-0845, Japan.

² Graduate School of Engineering, Tohoku University, Miyagi 980-0845, Japan.

*E-mail: mohammad.naser.sediqi.p4@dc.tohoku.ac.jp.

Abstract

The coupled Model Intercomparison Project phase 6 (CMIP6) dataset was used to assess the spatio-temporal projected changes in precipitation and temperature over Afghanistan under latest three Shared Socioeconomic Pathways (SSPs) emission scenarios (SSP1-2.6, SSP2-4.5 and SSP5-8.5) for the three period, near future (2020-2044), mid future (2045-2067) and far future (2075-2099). Statistical metric was used for ranking the models to select appropriate GCMs based on their ability to simulate historical monthly average precipitation, maximum and minimum temperature for the period of (1990-2014). Three model namely MPI-ESM1-2-LR, ACCESS-CM2 and FIO-ESM-2-0 were found high ranked models based on past performance for simulating the all three variables. Mean ensemble of selected GCMs revealed an in-crease in maximum temperature in the range of 1.7-4.5 °C, 2.7-5.3 °C, and 4.5-6.8 °C and minimum temperature in the range of 1.8-9.8 °C, 3.2-9.9 °C and 5.6-10.7 °C and average precipitation change in the range of -4.9-10.23 %, -2.4-22.6 % and -1.4-29.8 % under SSP1-2.6, SSP2-4.5 and SSP5-8.5 scenarios, respectively during far future (2075-2099). Northeast of the country (Himalayas region) were projected higher increase in temperature, where, higher change in average precipitation were projected in the south and southwest (desert region) of Afghanistan.

Keywords: Climate projections; global climate model; CMIP6; Afghanistan

1 Introduction

Global Climate Models (GCMs) can be used to predict future climate information. The GCMs project future climate based on different assumptions of future changes of greenhouse gas (GHG) emissions, land use and socio-economy [1]. The change in global GHG re-releases and socioeconomic is related to the political strategies at national, regional and global levels.

Afghanistan is located in cross road of central and south Asia, and has divided to different climate zones (Figure 1). Decades of political fighting has faced many different environmental issues, mostly in water sector [2]. According global climate risk index (2017) ranked 12th most vulnerable to climate change and has already experienced prolonged droughts. i.e. drought 1998-2002 [3].

In Afghanistan 98 % of water resource is used for agriculture, similarly, more than 80 % of the population get their income from agricultural practices. Therefore, rapid declination of renewable water resources has caused a significant impact on water resources, agriculture and livelihood of the vast populace of the country.

The mean annual temperature in the country has increased by 0.13 to 0.29 °C/decade in the last five decades. Understanding possible climate changes are crucial for the country to anticipate future water stress, aridity and their implications to agriculture and economy.

The objective of the present study is to assess the relative historical performance and future projections of the CMIP6-GCMs in Afghanistan. Nineteen GCMs based on their availability for the study area are used for this purpose. The capability of the models was assessed in simulating the spatial and temporal variability of climate for annual scale.

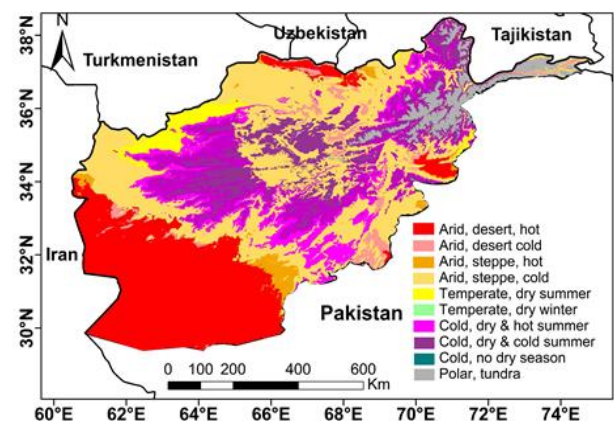


Fig. 1. Afghanistan with its different climate zones.

2 Materials and methods

CRU gridded dataset from the University of East Anglia Climatic Research Unit, was used for assessing GCM's performance in simulating historical monthly rainfall, maximum temperature (Tmax) and minimum temperature (Tmin) with resolution of 1.0 × 1.0.

Nineteen CMIP6 GCM's were used to assess the future climate projection for three different future scenarios over Afghanistan. The GCMs were selected based on availability of projections of three main climate variables rainfall, Tmax and Tmin, and their availability of future projection for SSP 1-2.6, SSP 2-4.5 and SSP 5-8.5.

The Kling-Gupta efficiency (KGE) [4] metrics were used to evaluate the association between gridded dataset (CRU) and GCMs and to select an ensemble of GCMs based on their past performance.

KGE range between 1 to $-\infty$, where 1 indicates a perfect association and can be calculated from equation (1). KGE metrics is a combination of combines Pearson's correlation (r), the ratio of spatial variability and the normalized difference between the gridded dataset (CRU) and each GCM model.

$$KGE = 1 - \sqrt{(r-1)^2 + \left(\frac{\mu_{GCM}}{\mu_{ref}} - 1\right)^2 + \left(\frac{\sigma_{GCM}/\mu_{ref}}{\sigma_{ref}/\mu_{ref}} - 1\right)^2}$$

where μ_{GCM} and μ_{ref} are the mean, and σ_{GCM} and σ_{ref} are the standard deviation for GCM and CRU data, respectively.

After the selection of high ranked GCMs based on KGE values, the ensemble of CMIP6-GCMs rainfall and temperature was bias corrected using quantile mapping (QM) bias correction approach. Bias corrected GCMs were compared to that of their reference period (1990-2015) for different SSP scenarios, and three future periods (2020-2044), (2045-2069) and (2075-2099) to assess the changes in Afghanistan future climate in desert and mountainous regions separately.

3 Results and discussion

The performances of CMIP6 GCMs based on KGE metric to reproduce the annual rainfall, Tmax and Tmin are shown in (figure 2). The figure revealed that based on combination of the rank of all variables using rating metric (RM) equation, FIO-ESM-2-0, ACCESS-CM2 and MPI-ESM1-2-HR has higher KGEs values between all models for all three variables.

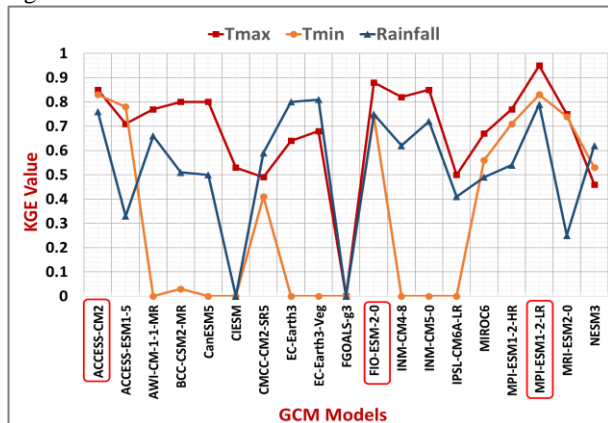


Fig. 2. KGE value for Tmax, Tmin and rainfall.

A multi-model mean ensemble (MME) was formed from the three models with highest KGE. Using the MME, the change in rainfall and temperature were calculated and presented spatially for three futures (near future 2020-2044, mid future 2045-2067 and far future 2075-2099). compared to the base period (1990 - 2014) for the SSP1-2.6, SSP2-4.5 and SSP5-8.5 emission scenarios.

It is projected that for both Tmax and Tmin (figure 3) the lowest change will be in SSP1-2.6, near future and the highest change is projected in SSP5-8.5 and far future. It's also predicted that future temperature changes in mountainous region for all SSPs and time periods is higher than desert region of the country.

On the other hand, the annual rainfall change (figure.4) was projected to have a positive in the range of (2 to 30 %) and the maximum changes is projected to the southwest of Afghanistan.

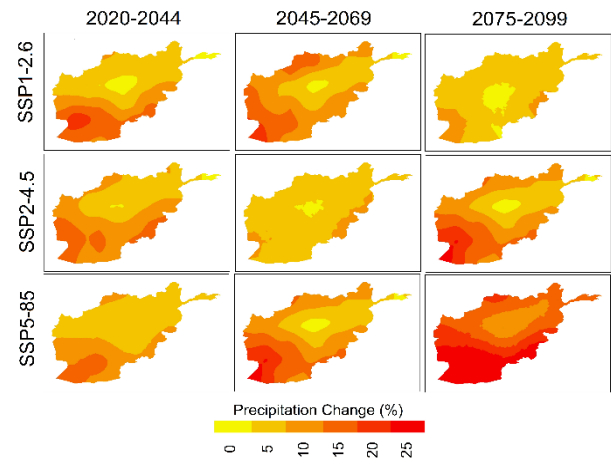


Fig. 3. Spatial patterns of changes in rainfall (%)

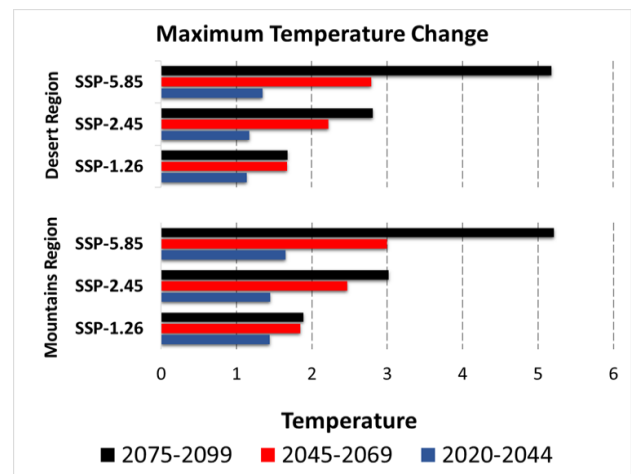


Fig. 3. Changes in Tmax (°C) for three futures and three scenarios in mountainous and desert region.

4 Conclusions

The statistical metric has been conducted in this study to evaluate the performance of CMIP6 GCMs in simulating historical climate. Besides, the MMEs were used to project the future climate for different scenarios. The study revealed a higher increase in rainfall and a significantly large rise in temperature for SSP scenarios.

Reference

- [1] Taylor KE, Balaji V, Hankin S, Juckes M, Lawrence B, Pascoe S. 2011. CMIP5 data reference syntax (DRS) and controlled vocabularies. San Francisco Bay Area, CA, USA.
- [2] Aich, V.; Akhundzadah, N.A.; Knuerr, A.; Khoshbeen, A.J.; Hattermann, F.; Paeth, H.; Scanlon, A.; Paton, E.N. Climate Change in Afghanistan Deduced from Reanalysis and Coordinated Regional Climate Downscaling Experiment.
- [3] Sediqi, M.N.; Shiru, M.S.; Nashwan, M.S.; Ali, R.; Abubaker, S.; Wang, X.; Ahmed, K.; Shahid, S.; Asaduzzaman, M.; Manawi, S.M.A. Spatio-Temporal Pattern in the Changes in Availability and Sustainability of Water Re-sources in Afghanistan. Sustainability 2019, 11, 5836.
- [4] H.V. Gupta, H. Kling, K.K. Yilmaz, G.F. Martinez. 2009. Decomposition of the mean squared error and NSE performance criteria: implications for improving hydrological modelling.

Global-scale analysis of crop response pattern to different drought timescales

○ Vempi Satriya Adi HENDRAWAN^{1,*}, Daisuke KOMORI¹

¹ Graduate School of Environmental Studies, Tohoku University, Sendai Miyagi 980-8579, Japan

*E-mail: vempi@dc.tohoku.ac.jp

Abstract

Drought is one of the extreme climate events lead by water deficit causing subsequent severe impacts. Different precipitation deficits over time can induce different responses to crops. Here, we identified the response pattern of crop yield anomaly to a different time scale of meteorological drought based on past events on a global scale. Standardized Precipitation Index based on ensemble precipitation dataset was used to identify drought episodes and severity from 1981 to 2016. The crop yield anomaly was estimated by detrending the gridded global dataset of crop yields for major crops (maize, rice, soybean, and wheat) in 0.5-degree resolution. The result indicates that crop yield loss is generally more sensitive to medium (5-8 months) to long (9-12 months) drought timescales globally, compared to short timescale (1-4 months). Various determinants might control the different spatial of crop response. This study contributes to an ongoing effort to assess crop vulnerability and possible mitigation and adaptation against climate change based on past understanding.

Keywords: agriculture, drought, SPI, timescale, yield

1 Introduction

IPCC (2013) reported that global warming would result in climate extremes inducing more frequent and severe natural disasters. Drought has contributed to some of the world's most severe famines (e.g. a severe drought in India affecting 300 million people in 2002). Agriculture is the most affected sector by drought in developing countries, absorbing about 80% of all direct impacts (FAO, 2017). Therefore, understanding drought and its impact are vital points towards the rising incidence of weather extremes and its negative impacts on agriculture.

The nature of drought impact on crops depends on how drought is defined (i.e., timescale, duration, and severity) (Mckee et al., 1993) and the characteristic of crop resistance (Daryanto et al., 2016). Numerous previous studies have assessed drought impact to crop by using multiple drought timescales (Peña-Gallardo et al., 2019). Drought timescale can be referred to as the length of time (e.g., months) during which the drought event develops (Hayes, 2001).

This study assesses crop sensitivity based on different drought timescales. This study aims to understand the global pattern of crop response to different drought timescales. This study contributes to existing drought-related studies for agricultural systems to understand how different drought timescales are associated with crop yield anomalies.

2 Materials and methods

The different drought timescale was modelled by a multiscalar meteorological drought index (i.e., SPI) with 1 – 12-month timescales based on the global gridded precipitation datasets. All analysis was done for each major crop (maize, rice, soybean, and wheat) in 0.5° grid resolution during 1981 – 2016 (36 years).

1.1 Materials

Datasets used in this study are shown in Table 1. The primary input dataset in this study is the global precipitation datasets for the drought model and crop yield data for assessing drought risk on crops.

Table 1 Dataset used in this study

Name	Data	Use	References
Drought Index (SPI)	Precipitation from ensemble historical global dataset	Drought model	(Hendrawan et al., 2021)
Crop calendar	Planting and harvesting date (Day of Year)	Exposure model	(Sacks et al., 2010)
The global dataset of historical yield (GDHY)	Crop yield (t/ha)	Risk model	(Iizumi & Sakai, 2020; Kim et al., 2019)

1.2 Methods

SPI was calculated by transforming monthly accumulated precipitation (i.e., within 1 – 12-month) to standardized value (mean 0 standard deviations 1) based on the specific distribution (i.e., gamma distribution) (Guttman, 1998).

Drought Index (DI) was then calculated based on the ensemble mean of several SPI data, obtained from the ensemble mean of several datasets (GPCC, CRU, PRECL, UDEL, CPC, MSWEP, MERRA-2, ERA-5, JRA-55). Then, Eq. 1 was used to convert monthly SPI to annual drought index based on harvesting month obtained from Sacks et al. (2010) dataset. To see the detailed method, refer to Hendrawan et al. (2021).

$$DI_{n,t} = \begin{cases} |SPI - n_{j,t}| & SPI < 0, \\ null & SPI \geq 0, \end{cases} \quad (1)$$

where $SPI_{n_{j,t}}$ is the SPI of n -month precipitation accumulation in harvested month j in year t . For example, $SPI_{n_{aug,2015}}$ is calculated using precipitation sum within 3-month: June, July, and August in 2015.

We assessed the relationship between each 12-timescales DI and crop yield anomaly estimated by detrending the gridded global dataset of crop yields for major crops (maize, rice, soybean, and wheat) for the four crops types using the Pearson correlation. Thus, we obtained 12 different correlations in each grid independently for each crop and obtained a DI timescale in which crop yield anomaly shows the highest correlation (Hendrawan et al., 2021; Peña-Gallardo et al., 2019).

3 Results and discussion

The result shows that medium timescale shows a stronger correlation for maize and soybean by around 24% and 31% of the total global crop area, respectively, followed by long and short timescale. Meanwhile, for wheat, long-timescale shows the highest global proportion by around 27%. In the case of rice, the dominant response is shown in the short timescale for around 17% global crop area. Medium responses to drought in maize and soybean are profound, while in contrast, wheat indicates a longer response to drought, and rice is more sensitive to short drought timescale despite its less share of global cropland (Fig. 1).

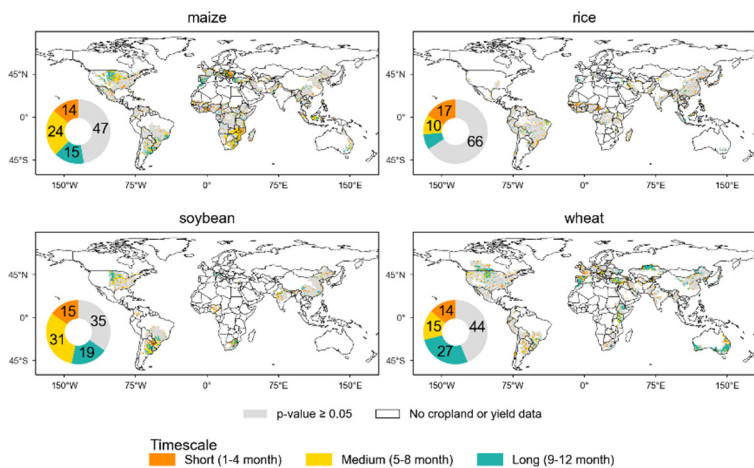


Figure 1 Drought time-scales (short, medium, and long) at which the most negative correlation between DI and crop yield anomaly is obtained.

Considering the different climatic regions that may govern the response of crop yield to drought, we summarized the results by categorizing cropland into the main classes (tropical, arid, temperate, cold, and polar) and the sub-types based on precipitation types (rainforest, monsoon, dry savannah, wet savannah, steppe, desert, dry summer, dry winter, without dry season, ice cap, and tundra) (Fig. 2). Results show that crop response to drought varies depending on the crop types among different climatic regions. For example, in the case of maize, medium response timescale become dominant for arid, cold, and temperate, followed by a long and short response. However, for the tropical region, the short response has more control in maize. Regarding the classification based on the sub-types, medium response timescale still dominates in all regions followed by a long and short response, except in savannah and wet region dominated by the short response. In dry summer, monsoon, and rainforest extended response slightly higher than short and medium timescale response.

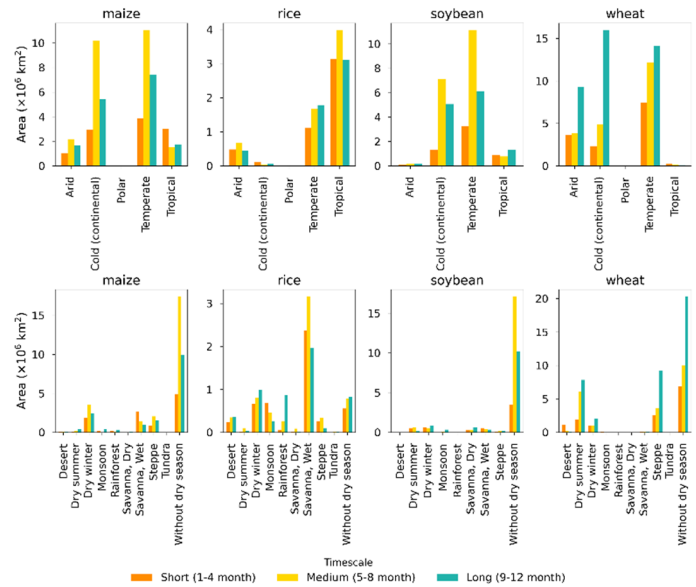


Figure 2 Area proportion of each different response timescale to drought (short, medium, and long) in different climatic regions based on Köppen-Geiger climate classification.

Conclusion

This study reveals that crop yield loss is generally more sensitive to medium (5-8 months) to long (9-12 months) drought timescales globally, compared to short timescale (1-4 months). Various determinants might control the different spatial of crop response which is essential for further consideration.

Selected references

Daryanto, S., Wang, L., & Jacinthe, P. A. (2016). Global synthesis of drought effects on maize and wheat production. *PLoS ONE*, 11(5), 1–15.

FAO. (2017). The Impact of disasters and crises on agriculture and Food Security.

Guttman, N. B. (1998). Comparing the palmer drought index and the standardized precipitation index. *Journal of the American Water Resources Association*, 34(1), 113–121.

Hayes, M. (2001). Revisiting the SPI : Clarifying the Process Revisiting the SPI : Clarifying the Process. *Drought Network News (1994-2001)*, 2000, 18–20.

Hendrawan, V. S. A., Kim, W., Touge, Y., Ke, S., & Komori, D. (2021). A global-scale relationship between a multiscale drought index and agricultural yield anomaly based on multiple precipitation data. Manuscript submitted for publication.

Iizumi, T., & Sakai, T. (2020). The global dataset of historical yields for major crops 1981–2016. *Scientific Data*, 7(1), 1–7.

IPCC Working Group 1, IPCC, 2013: Climate Change 2013: The Physical Science Basis. Contribution of Working Group I to the Fifth Assessment Report of the Intergovernmental Panel on Climate Change. *Ipcc*, AR5(May 2016), 1535.

Kim, W., Iizumi, T., & Nishimori, M. (2019). Global patterns of crop production losses associated with droughts from 1983 to 2009. *Journal of Applied Meteorology and Climatology*, 58(6), 1233–1244.

Mckee, T., Doesken, N., & Kleist, J. (1993). The relationship of drought frequency and duration to time scales. *Proceedings of the 8th Conference on Applied Climatology*, 17(22), 179–183.

Peña-Gallardo, M., Vicente-Serrano, S. M., Quiring, S., Svoboda, M., Hannaford, J., Tomas-Burguera, M., Martín-Hernández, N., Domínguez-Castro, F., & El Kenawy, A. (2019). Response of crop yield to different time-scales of drought in the United States: Spatio-temporal patterns and climatic and environmental drivers. *Agricultural and Forest Meteorology*, 264, 40–55.

Sacks, W. J., Deryng, D., Foley, J. A., & Ramankutty, N. (2010). Crop planting dates: An analysis of global patterns. *Global Ecology and Biogeography*, 19(5), 607–620.

Evaluate the dynamic change of burn-ability by observing the fuel moisture content in Japan

○ Qin HUANG^{1*}, Yoshiya TOUGE¹

¹Department of Environmental Engineering, Environmental University, Miyagi 980-8579, Japan.

*E-mail: huang.qin.p5@dc.tohoku.ac.jp.

Abstract

In recent years, big wildfire events are increasing. It is considered that the warming temperature caused by the climate change makes the dryness enhanced. Therefore, dryness is essential for evaluation of the wildfire. The measurement of dead fuel moisture content is a significant variable in determining fire danger since it is highly related to fire ignition and spread potential, and slight changes in moisture content can cause significant differences in fire behavior and effectiveness. From 21st February to 15th March 2021, a wildfire broke out in Ashikaga City, Tochigi Prefecture, Japan. Since the spread of the wildfire was affected by dry weather, to investigate the moisture status of the forest fuel, two field investigations were carried out. The Ashikaga wildfire observation results showed that the fuel moisture was below 10%, which is meaningful for evaluating burn-ability. The overall trend showed that, as the temperature increase and relative humidity decrease, the moisture content rise. It can be considered that the difference between the two species was greatly influenced by relative humidity. The main consideration was that the amount of radiation affected the evaporation rate of different densities. It is required to analyze the effect of condensation and evaporation on fuel moisture based on meteorological factors.

Keywords: dryness; wildfire; burn- ability; fuel moisture.

1 Introduction

Forests are a major component of the Earth's ecosystem and a fundamental resource on which human life depends. There have been several extreme fire incidents in the past two years. IPCC pointed out that under certain geographical conditions, there is a strong connection between climate change and wildfires. As the climate gradually becomes dry, we need quantitative and physical method to evaluate dryness. Combustibles, fire sources, and meteorological conditions are the primary factors affecting forest fire risk prediction [1]. Combustibles are the material basis for wildfires, they are the primary carrier for forest fire risk prediction research [2]. The occurrence and development of forest fires depend to a large extent on the fuel moisture content (FMC) and their duration [3,4]. Various meteorological factors directly or indirectly affect the changes in the moisture content of combustibles, which in turn affect the difficulty of combustibles on fire, that is, the size of the fire hazard. Studies on FMC dynamics can be divided into different time scales such as quarterly changes, daily changes, and hourly changes. However, few surveys are conducted on FMC during the fire period (indicating extremely dry weather). when a drought occurs, it is very likely that a fire will occur. The study of the dynamic changes of the fuel's moisture content is very indicative.

In Japan, wildfires are seasonal and regional. Due to Japan's humid climate, there are more small-scale fires. Japan has fewer wildfires than other countries, and the area burned is not large. However, because of the complex impact of fires on the ecosystem, wildfires capable of causing large-scale burns pose a greater threat to Japan than typhoon disturbance. From 21st February to 15th March 2021, a wildfire broke out in Ashikaga City, Tochigi Prefecture, Japan. This area is located at the intersection of mountains and plains and is one of the driest areas in Japan. Since the spread of the wildfire was affected by dry weather, in order to investigate the FMC

status of the forest fuel in this case, two field surveys were carried out.

The primary aim of this research is to determine the moisture content of forest surface fuel in Japan's driest region during the dry season, as well as to track intraday dynamic changes in FMC and conduct joint analyses with meteorological factors.

2 Materials and methods

2.1 Field sites

When sampling sites were chosen, mixed forests were avoided.

In the first investigation, samples were taken at three locations in Ashikaga City (Tochigi Prefecture) and Kiryu City (Gunma Prefecture). In Ashikaga City, surface dead fuel from broadleaf and cedar forests was collected, while in Kiryu City, surface dead fuel from cedar forest was used. The sampling sites.

The second investigation's sampling sites were in Ashikaga City, and gathered surface fuel from cedar forest as well as dense and loose areas in broadleaf forest. During the period, continued to collect samples at the site where we collected the broadleaf in Ashikaga City last time.

2.2 Sampling

All sampling days were rain-free. Dead fuel samples were collected from dispersed locations within study sites. In particular, intensive sampling of "easy to collect fuels" was avoided. The sample was the dead leaves of the corresponding tree species. Each sample was made up from three subsamples. In the second investigation, throughout the time of this intensive sampling run, samples were collected at 4-h intervals from 6am to 10pm (10pm only collect cedar). The samples were sealed in sealed bag for transport back to the laboratory. The field weight of samples was determined as soon as practical following collection. After back to the laboratory, oven-dry weights were obtained after drying

samples to constant weight at 60 °C. Due to the large number of samples collected during the second investigation, the samples were processed on the same day using a moisture analyzer (HE73, Mettler-Toledo, Switzerland).

3 Results and discussion

The FMC of the sample is low in first observation. Especially the FMC of the broadleaf measured in Ashikaga is as low as 7.6%. The value is meaningful for the description of dryness condition. The value will play a great role in evaluating burn-ability.

The FMC results and meteorological data obtained from the second investigation are shown in Fig.1. The overall trend showed that, as the temperature increase and relative humidity decrease, the FMC increase. The highest temperature was at 3 p.m. every day, after which the temperature began to decrease and the relative humidity began to rise, with the maximum humidity around 6 am.

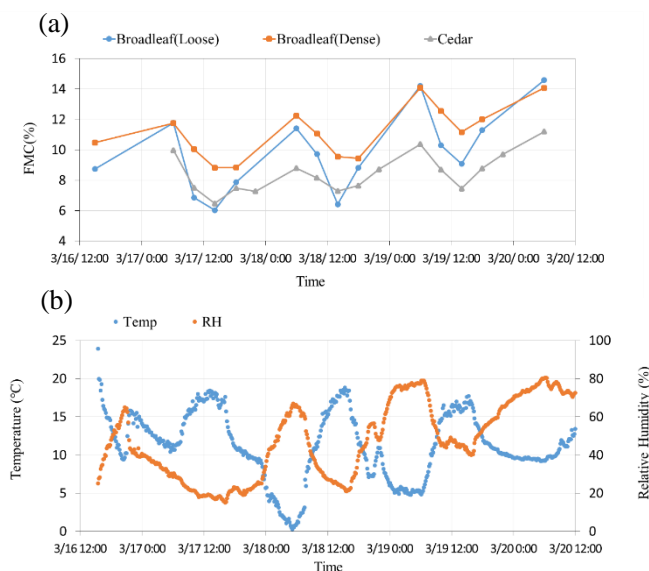


Fig.1. The time series of three sites of fuel moisture content (FMC) in the second investigation (a). Time series of meteorological observations (b).

FMC is primarily subject to change due to sorption processes. The gain and loss of moisture through vapor exchange occurs when the vapor pressure of the fuel surface differs from the surrounding air. This time, the dynamic change of FMC was mainly considered from two aspects of evaporation and condensation. FMC began to rise after two o'clock in the afternoon, indicating that condensation began to take effect between two and six o'clock in the afternoon.

Furthermore, the FMC was almost the same in the early mornings of March 19th and 20th, when the temperature difference was large and the relative humidity was almost the same. Given that relative humidity had a greater influence on FMC during the adsorption process, condensation played a significant role. The overall FMC is higher in the early mornings of March 18th and 19th, when the humidity is higher.

When comparing cedar and broadleaf, the figure shows that the time when the FMC differs the most was around 6 a.m., and the relative humidity at this time was also the highest in a day. When the relative humidity was at its lowest, the gap in FMC was nearly the smallest. Because adsorption was primarily affected by condensation at night, it was assumed

that the difference in FMC between the two fuels was greatly influenced by relative humidity. Particle density is another physical factor that influences fuel moisture content. In general, higher density particles (e.g., oak) absorb or lose moisture more slowly than lower density fuel particles.

The downward trend of FMC shows that the rate of decline in loose areas was much greater than that in dense areas. Indeed, canopy shading reduces incoming solar radiation and wind flow in denser stands. According to some studies, moisture loss from understory fuels is greatly accelerated in less dense canopies. The main consideration was the difference in the amount of radiation. Fuel that is in direct sunlight will not only change the microclimate of the air immediately surrounding the fuel but can also increase the fuel temperature that can reach up to 70°C when in direct sunlight. At 2pm, the value of FMC in the loose site was much lower than that in the dense site. When condensation began, the adsorption rate of broad leaves in loose site was much higher than that in dense site. Due to the fact that the capacity of fuel particles to absorb moisture is primarily determined by the pressure difference between the inside and outside, it was determined that the FMC was much smaller than the EMC at this time, resulting in a greater pressure gradient. And the FMC of two sites were nearly identical at 6 am. It can be shown that even though the variation in the previous day was significant, the final adsorption process remained unaffected. It was discovered that condensation could return FMC to an equilibrium state. This shelter effect has been incorporated into some fuel moisture models by incorporating variables such as the leaf area index (LAI) or stand density, which change dynamically with the seasons and vary depending on the forest species.

4 Conclusions

The FMC results obtained in the first investigation are all less than 10%. The second investigation results showed that even in dry periods, FMC would vary greatly with meteorological factors such as temperature and humidity throughout the day. In the adsorption process, the relative humidity had a greater influence on FMC, and the condensation took a major role. The difference between different species was also considered to be affected by relative humidity. For forests of different densities, FMC varied greatly. At 2 pm, the FMC value of the loose site was much lower than that of the dense site. However, even though the previous day's changes were great, the final adsorption process was still unaffected. It was considered that condensation could recover FMC to an equilibrium state.

Reference

- [1] K. Anderson, D. L. Martell, M. D. Flannigan, and D. Wang, *Modeling of Fire Occurrence in the Boreal Forest Region of Canada*, Springer, New York, NY, 2000, pp. 357–367.
- [2] S. Matthews, Effect of drying temperature on fuel moisture content measurements, *Int. J. Wildl. Fire*, vol. 19, no. 6, pp. 800–802, 2010.
- [3] R. C. Rothermel, How to predict the spread and intensity of forest and range fires., US Dep. Agric. For. Serv. Gen. Tech. Rep., no. INT-143, 1983.
- [4] A. G. and A. McArthur, *Fire Behaviour in Eucalypt Forests*. Forestry and Timber Bureau Canberra, 1967.

Changes in exposed population to heavy rainfall disasters associated with population decline in Japan

○ Hayata YANAGIHARA^{1*}, So KAZAMA¹ & Seiki KAWAGOE²

¹Department of Civil Engineering, Graduate School of Engineering, Tohoku University, Miyagi 980-8579, Japan.

²Faculty of Symbiotic Systems Science, Fukushima University, Fukushima 960-1296, Japan.

*E-mail: yanagihara.hayata.r1@dc.tohoku.ac.jp

Abstract

This study evaluated the changes in the exposed population to river flooding, inland flooding, and slope failure from 2015 to 2100 with population changes by shared socioeconomic pathways (SSPs). The exposed population to river and inland flooding was defined as the population living in the area where inundation of 45cm or more (above the floor level of general houses). The exposed population to slope failure was defined as the population living in the area where the probability of slope failure exceeds 80%. Although there were differences in population distribution among the SSPs, such as urban concentration and decentralization, the magnitude relation of the total exposed population to the three disasters by SSPs was the same as the magnitude relation of the total population by SSPs in 2100. The SSPs with the largest number of prefectures with the increase in the ratio of the exposed population to population were estimated to be SSP4 to river flooding, SSP1, SSP2, and SSP5 to inland flooding, SSP4 to slope failure, and SSP4 and SSP5 to the three disasters.

Keywords: river flooding; inland flooding; slope failure; shared socioeconomic pathways; disaster risk.

1 Introduction

In recent years, record-breaking rainfall has happened every year, causing river flooding, inland flooding, and sediment disaster. There are concerns that the damage caused by river flooding, inland flooding, and sediment disaster will increase due to climate change. Therefore, further disaster management measures based on quantitatively evaluating the disaster risk are required. Many previous studies estimated the disaster risk using the exposed population (e.g., Ward *et al.*, 2013^[1]). Matsunaka *et al.* (2021)^[2] estimated the exposed population to river flooding and sediment disaster in two population migration scenarios, one with more concentrated population to the three major metropolitan areas and one with more dispersed population to local areas. However, although shared socioeconomic pathways (SSPs) were developed, there are no studies of changes in the exposed population with population change by SSPs in Japan. This study evaluated the changes in the exposed population to river flooding, inland flooding, and slope failure from 2015 to 2100 with population changes by SSPs.

2 Datasets

2.1 Inundation depth data of river flooding

As hazard data of river flooding, this study used the inundation depth data of river flooding throughout Japan computed by Yamamoto *et al.* (2021)^[3] using a two-dimensional unsteady flow model (Tezuka *et al.*, 2014^[4]). The spatial resolution of the inundation depth data is the fifth-order mesh (approximately 250m×250m). The inundation depth data of river flooding with return periods of 30, 50, 100, and 200 years were used. The inundation depth data reflects the capacity of flood control facilities in each water system and river section utilizing the method of Tanaka *et al.* (2019)^[5].

2.2 Inundation depth data of inland flooding

As hazard data of inland flooding, this study used the inundation depth data of inland flooding throughout Japan under the poor drainage condition computed by Yanagihara *et al.* (2020)^[6] using a two-dimensional unsteady flow model (Tezuka *et al.*, 2014^[4]). This inundation depth data assume that precipitation with a return period of 5 years can drain. The inundation depth data under the poor drainage condition was used because actual inland flooding is often accompanied by poor drainage. The spatial resolution of the inundation depth data is the fifth-order mesh. The inundation depth data of inland flooding with return periods of 5, 10, 30, 50, 100, and 200 years were used.

2.3 Probability data of slope failure

As hazard data of slope failure, this study used the probability data of slope failure throughout Japan computed by Kawagoe *et al.* (2010)^[7]. The spatial resolution of the probability data is the third-order mesh. The probability data of slope failure with return periods of 5, 10, 30, 50, 100, and 200 years were used.

2.4 Population data

As the reference population data, this study used the population data of the third-order mesh based on the national census in 2015 (Statics Bureau of Japan, 2017^[8]). As the population data in 2100, this study used the population data by SSPs developed by the National Institute for Environmental Studies^[9]. The image of the population distributions by SSPs is as follows: SSP1: compact + network; SSP2: maintenance of the status quo; SSP3: blight and slums; SSP4: concentration in urban centers and decline of suburbs; SSP5: concentration in metropolitan areas.

3 Method for estimating the exposed population

The exposed population to river and inland flooding was defined as the population living in the area where

inundation of 45cm or more (above the floor level of general houses). The exposed population to slope failure was defined as the population living in the area where the probability of slope failure exceeds 80%. The hazard data used to calculate the future exposed population did not consider changes due to climate change. The annual expected exposed population (AEEP) was computed using Eq.1.

$$E = \sum_{i=1}^n \frac{(1/m_i - 1/m_{i+1})(x_{m_i} + x_{m_{i+1}})}{2} \quad (1)$$

where E is the AEEP, n is the number of return periods, m_i is the return period, x_{m_i} is the exposed population with a return period of m_i .

4 Results and discussion

4.1 Changes in the exposed population with population changes in Japan

The AEEP in 2015 was estimated to be 0.66 million people/year to river flooding, 0.83 million people/year to inland flooding, and 0.74 million people/year to slope failure. The total AEEP to the three disasters in 2100 was estimated to be 1.2 million people/year in SSP1, 0.99 million people/year in SSP2, 0.63 million people/year in SSP3, 0.78 million people/year in SSP4, and 1.3 million people/year in SSP5. Although there were differences in population distribution among SSPs, such as urban concentration and decentralization, the magnitude relation of the total AEEP to the three disasters by SSPs was the same as the magnitude relation of the total population by SSPs. Fig.1 shows the AEEP decline rate by SSPs from 2015 to 2100 in Japan. For comparison, Fig.1 also shows the population decline rate. Like the population decline rate, the AEEP decline rates to river flooding, inland flooding, and slope failure were the largest in SSP3, followed by SSP4, SSP2, SSP1, and SSP5.

4.2 Changes in the ratio of the exposed population to population by prefecture

When the ratio of the AEEP to population increases, the AEEP decline rate is lower than the population decline rate. The number of prefectures with the increase in the ratio of the AEEP to population was counted for each SSPs to river flooding, inland flooding, and slope failure. The SSPs with the largest number of prefectures with the increase in the ratio of the AEEP to population were estimated to be SSP4 to river flooding, SSP1, SSP2, and SSP5 to inland flooding, SSP4 to slope failure, and SSP4 and SSP5 to the three disasters.

5 Conclusions

This study estimated the changes in the exposed population to heavy rainfall disasters with population change by SSPs. As a result, the SSPs with the largest number of prefectures with the increase in the ratio of the AEEP to population were SSP4 to river flooding, SSP1, SSP2, and SSP5 to inland flooding, SSP4 to slope failure, and SSP4 and SSP5 to the three disasters.

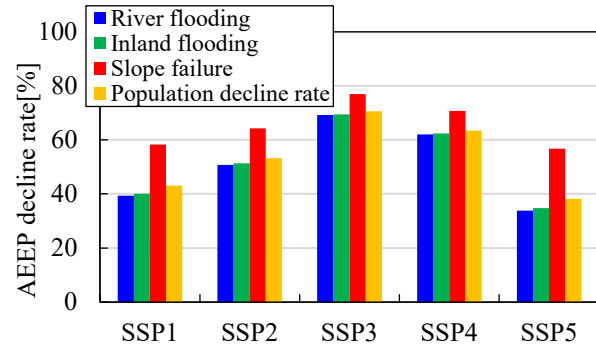


Fig. 1. The AEEP decline rate by SSPs from 2015 to 2100 in Japan

Table 1 The number of prefectures with the increase in the ratio of the AEEP to population

	SSP1	SSP2	SSP3	SSP4	SSP5
River flooding	26	25	24	27	26
Inland flooding	21	21	20	17	21
Slope failure	1	1	3	5	2
Total	48	47	47	49	49

Reference

- [1] Ward, P.J. *et al.*, Assessing flood risk at the global scale: model setup, results, and sensitivity, *Environmental Research Letters*, Vol.8, No.4 (2013), 040019.
- [2] Matsunaka *et al.*, Analysis of future disaster risk based on population exposure to disasters, *Journal of the City Planning Institute of Japan*, Vol.56, No.1 (2021), pp.73-84 (in Japanese).
- [3] Yamamoto, T. *et al.*, Evaluation of flood damage reduction throughout Japan from adaptation measures taken under a range of emissions mitigation scenarios, *Climatic Change*, Vol.165 (2021), Article: 60.
- [4] Tezuka, S. *et al.*, Estimation of the effects of climate change on flood-triggered economic losses in Japan, *International Journal of Disaster Risk Reduction*, Vol.9 (2014), pp.58-67.
- [5] Tanaka, Y. *et al.*, Assessment of the risk of flood and storm surge with flood control facilities, *Journal of Japan Society of Civil Engineers*, Ser.B1 (Hydraulic Engineering), Vol.75, No.2 (2019), pp.I_109-I_114 (in Japanese).
- [6] Yanagihara, H. *et al.*, Estimation of the risk of inland flood based on extreme precipitation data considering climate change in Japan, *Journal of Japan Society of Civil Engineers*, Ser.B1 (Hydraulic Engineering), Vol.76, No.2 (2020), pp.I_85-I_90 (in Japanese).
- [7] Kawagoe, S. *et al.*, Probabilistic modeling of rainfall induced landslide hazard assessment, *Hydrology and Earth System Sciences*, Vol.14 (2010), pp.1047-1061.
- [8] Statics Bureau of Japan, e-Stat, <https://www.e-stat.go.jp/gis/statmap-search?page=1&type=1&toukeiCode=00200521> (2017).
- [9] NIES, Results of Environment Research and Technology Development Fund 2-1805, <https://adaptation-platform.nies.go.jp/socioeconomic/population.html> (2021).

Assessment of long-term operation performance in mesophilic anaerobic co-digestion of lipid and Food Waste

○ Chen WANG^{1*}, Yuanyuan REN¹, Yu QIN^{1,2} & Yu-You Li^{1,2}

¹Department of Civil and Environmental Engineering, Tohoku University, Miyagi 980-8579, Japan.

²Department of Frontier Science for Advanced Environment, Tohoku University, Miyagi 980-8579, Japan.

*E-mail: wang.chen.q6@dc.tohoku.ac.jp.

Abstract

In this study, long-term operation performance of mesophilic anaerobic co-digestion system of lipid and food wastes was investigated. The experiment run in a semi-continues mesophilic CSTR reactor with the HRT of 30 days. It included 6 operating phases, and lipid/TS ratio of each phase was from 10% to 60%. With the increase of the lipid/TS ratio, the biogas production and the proportion of methane gradually increased, and the maximum biogas production could reach 2.43L/L/d, the proportion of methane could account for up to 66.95%. The removal efficiency of TS, VS and COD was as high as about 80%, and the removal efficiency of carbohydrate and lipid could reach 90%. When the ratio of lipid/TS reached 60%, the system broke down, which indicated that the system could operate stably below the lipid/TS ratio of 50%. The results of this experiment could provide a constructive basis for the establishment of a stable, low-cost anaerobic co-digestion system of lipid and food waste.

Keywords: Mesophilic anaerobic co-digestion; Food waste; Lipid; CSTR.

1 Introduction

With the increase of the world's population and the advancement of agricultural processing technology, food waste (FW), including food loss is increasing year by year. At present, 13 billion tons of food are discarded every year in the world^[1], which is equivalent to one-third of food production. A survey shows that by 2025, the production of food waste will increase by 30% compared to 2020^[2]. Similarly, as people's dietary structure changes, the world's production and consumption of edible oil are also increasing year by year, which has led to an increase in the amount of edible oil waste. In view of this situation, the disposal of food and oil waste has become an important topic.

Compared with traditional landfilling, burning and other treatment methods, anaerobic digestion has shown a strong advantage in the treatment of FW and lipid^[3]. It degrades the waste while generating usable green gas energy.

In addition, the physiochemical characteristics of FW and edible oil are very suitable for use as raw materials for anaerobic digestion. Anaerobic digestion is a process in which organic matter and water are degraded into methane under the effect of microorganisms. For FW, more than 90% of it is composed of organic matter, and its moisture content is also around 70%-90%. And the theoretical methane conversion rate of lipid is as high as 94.8%. The anaerobic fermentation system combining FW and lipid is expected to achieve higher methane production and conversion rate while reducing total operating costs.

2 Materials and methods

2.1 Substrate and inoculum

The FW used in this experiment was made in the laboratory, according to the survey about the ingredients and proportion of Japanese food waste, and then stored in the refrigerator at 4°C. The lipid used in the experiment was prepared by mixing several kinds of oil according to the edible oil consumption survey. The anaerobic sludge was collected from an anaerobic reactor treating sewage sludge.

2.2 Anaerobic co-digestion experiment

This semi-continuous long-term experiment was carried out in a continuous stirred tank reactor (CSTR) with an effective volume of 12L. The operating temperature of the reactor was 37°C, and the hydraulic residence time (HRT) of the reactor was constant at 30 days. The detail operation conditions were shown in Table 1.

Table 1 Experimental parameters of 6 phases.

Phase		I	II	III	IV	V	VI
HRT	Days	30	30	30	30	30	30
Substrate	%(TS)	10	10	10	10	10	10
Lipid/TS ratio	%	10	20	30	40	50	60
TS loading rate	g-TS/L/d	3.3	3.3	3.3	3.3	3.3	3.3
OLR	g-COD/L/d	4.7	5.5	5.7	6.21	6.3	7.0

3 Results and discussion

3.1 Biogas production

The rate of biogas production rate is the most important indicator to evaluate the performance of an anaerobic digestion system. The detail results were shown in the Figure 1 and Figure 2.

When the Lipid/TS ratio was 10%, the biogas production rate was 2.74L/L/d, and the methane production rate was 1.64L/L/d. When the Lipid/TS ratio reached 50%, the biogas production rate was 3.63L/L/d, an increase of 32.48%. The methane production rate was 2.43L/L/d, an increase of 48.17%. This results showed that when the Lipid/TS ratio was less than 50%, the co-digestion of lipid and FW could increase the biogas production rate and methane production rate, and the entire anaerobic system had a better performance. When the Lipid/TS ratio reached 60%, as the

entire anaerobic digestion system broke down, the biogas production rate and methane production rate dropt sharply, becoming 0.86L/L/d and 0.38L/L/d, a decrease of 68.61% and 76.83%. To obtain higher gas production rate while maintaining the stable operation of the system, it could be roughly inferred that the optimal Lipid/TS ratio was 50% or less.

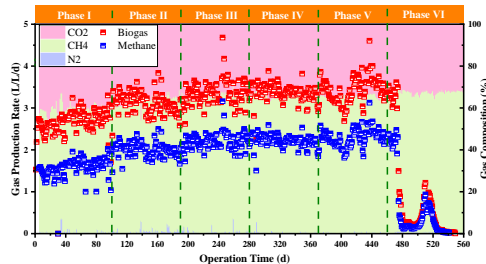


Fig. 1. The gas production rate

At the same time, the proportion of methane in the biogas produced in the anaerobic reactor also increased obviously. As shown in the Figure 2(b), during the operation with lipid/TS ratio of 50% or less, the proportion of carbon dioxide dropped from about 40% at the beginning to about 33%, while the content of methane rose from about 60% at the beginning to about 67%.

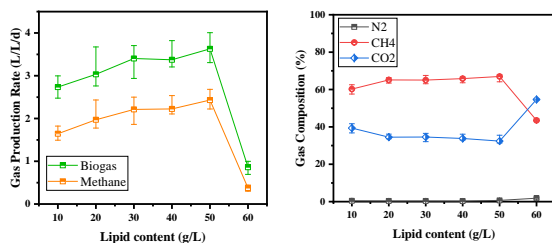


Fig. 2. Gas production rate in each phase ((a) Gas production; (b) Gas composition)

3.2 Sludge characteristics

In an anaerobic digestion system, pH, alkalinity and total ammonia nitrogen are usually indicators of the stability, while these three indicators also influence each other. During the long-term operation, the characteristics of the sludge were shown in the Figure 3.

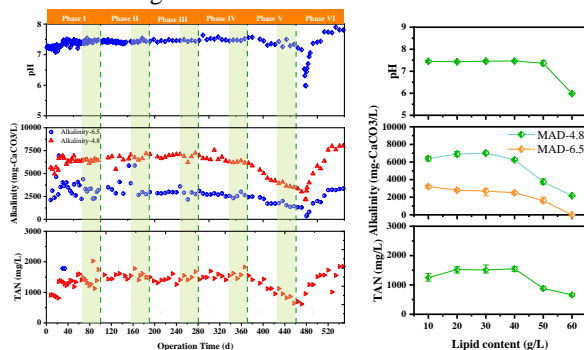


Fig. 3. Sludge characteristics ((a) During long-term operation; (b) In each phase)

It could be seen from the figure that in the first four phases, when the lipid/TS ratio was lower than 40%, the pH, alkalinity, and total ammonia nitrogen content of the system

were relatively stable, which showed strong buffering capacity of the system. With the lipid/TS ratio increasing to 50%, alkalinity had dropped from 6130 mg-CaCO₃/L to 3350 mg-CaCO₃/L. And it can be seen that there were slight fluctuations around 7.5 in pH. The reason for the decrease was that the total ammonia nitrogen as the buffering materials began to decrease. After continuing to increase the ratio of lipid/TS to 60%, the alkalinity was reduced to 2180 mg-CaCO₃/L, the pH was only 5.99, and the system was completely acidified.

3.3 Organic removal efficiency

The organic removal efficiency represented the metabolic capacity of the system, and generally the more organic matter was degraded, the higher the methane production would be. Through experimental determination, it could be obtained that when the lipid/TS ratio was less than 50%, the reactor could be operated stably, the degradation rate of TS, VS and COD has been stable at about 80%, and the degradation rate of carbohydrates and lipid could reach about 90%.

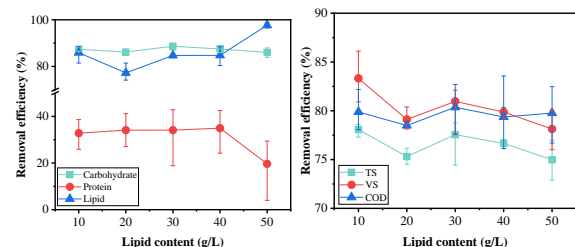


Fig. 4. Organic removal efficiency in each operation phase

It shows that this anaerobic co-digestion system can achieve an ideal degradation effect of organic matter.

4 Conclusions

For mesophilic anaerobic co-digestion of food waste and lipid, the system could be operated successfully in the case of 50% Lipid/TS ratio, from the perspective of system performance and stability. When the concentration of lipid/TS ratio reached 50%, the removal efficiency of lipid could reach 90%, biogas production rate of 3.63L/L/d and methane production rate of 2.43L/L/d can be achieved at OLR of 6.39 g-COD/L/d.

Reference

- [1] 農林水産省, 食品ロスの現状を知る, aff (あふ), 2020年10月号.
- [2] Yuanyuan Ren, Miao Yu, Chuanfu Wu, Qunhui Wang, Ming Gao, Qiqi Huang, Yu Liu, A comprehensive review on food waste anaerobic digestion: Research updates and tendencies, Bioresource Technology, 247 (2018) 1069-1076.
- [3] M.F.M.A.Zamri, Saiful Hasmady, Afifi Akhbar, Fazril Ideris, A.H. Shamsuddin, M. Mofijur, I. M. Rizwanul Fattah, T.M.I.Mahlia, A comprehensive review on anaerobic digestion of organic fraction of municipal solid waste, Renewable and Sustainable Energy Reviews, 137 (2021) 110637.

Influence of ammonia concentration on the treatment performance of pilot-scale one-stage PN/Anammox process

○ Zibin LUO^{1*}, Chao Rong², Tianjie Wang¹, Yan Guo¹, Yu Qin¹ & Yu-You Li^{1,2}

¹Department of Civil and Environmental Engineering, Tohoku University, Graduate School of Engineering, Miyagi 980-8579, Japan

²Department of Frontier Science for Advanced Environment, Graduate School of Environmental Studies, Tohoku University, Miyagi 980-8579, Japan.

*E-mail: luo.zibin.q1@dc.tohoku.ac.jp.

Abstract

A pilot-scale novel wastewater treatment system combining an anaerobic membrane bioreactor (AnMBR) and a one-stage partial nitrification-anammox (PN/A) reactor was set up to verify the application of this brand new system on real wastewater. The biofilm-based PN/A reactor was started up successfully and quickly in the first year of running. However, anammox biofilm, one of the critical points in the system, did not proceed well enough as the studies before. This study focuses on biofilm formation and reactor performance in dealing with wastewater of different ammonia concentrations after biofilm is formed. Through 164-days cultivation, biofilm was obviously observed. With a stable nitrogen loading rate (NLR) of 0.3 g-N/L/d and decreasing influent ammonia concentration from 5000 mg-N/L to 100 mg-N/L, the nitrogen removal efficiency dropped from 94.8% to 74.1%. The results confirm that the system has the great potential to be widely applied in wastewater with different nitrogen concentrations.

Keywords: Partial nitrification; Anammox; Biofilm; Municipal wastewater.

1 Introduction

The anaerobic ammonia oxidation (anammox), where ammonium could be combined with nitrite to generate nitrogen, was a great discovery in recent years. For the reason that the traditional nitrification/denitrification process has been blamed for the disadvantage of being too energy-intensive, this brand new technology is expected to be used as an alternative to conventional denitrification for the treatment of nitrogen in wastewater. Since the anammox reaction has been found, a number of researchers are working on basic research related to anammox and trying to get the technology into practical application.

Up to now, the anammox-based research has proceeded into full scale, and a large number of full-scale implementations of the one-stage nitrification/anammox process have been conducted. However, seldom of them are primarily related to the treatment of low-strength municipal wastewater in mainstream^[1].

According to the Environment Bureau of Aichi Prefecture data, 46% of the total nitrogen released by human activities comes from household water. Applying this energy-saving anammox process as a mainstream process in the nitrogen treatment of domestic water is necessary from a sustainable development perspective.

In this study, a pilot-scale PNA reactor was started up with an anaerobic membrane bioreactor (AnMBR) to verify the feasibility of this brand-new system in treating wastewater of different nitrogen concentrations in the mainstream, which can provide a reference for subsequent practical studies.

2 Materials and methods

2.1 Reactor Setup and Operation

The moving bed biofilm reactor (MBBR) possesses a working volume of 1.67 m³, equipped with a stirrer, a pH

sensor, and an NH₄⁺-N sensor. Hollow cylinder carriers, made of hydrophobic polypropylene resin, were added into the reactor until the filling rate of 15%. Air would be pumped intermittently into the bottom of the reactor to supply the oxygen, which could be regulated by a rotameter attached. Artificial influent was transferred by a peristaltic pump, while an impeller pump provided the effluent of AnMBR. Mixed liquid from the PN/A reactor would flow into a 1.92 m³ radial-flow sedimentation tank, and the collected sludge in the bottom was refluxed into the PNA reactor through an impeller pump. The operation temperature was set at around 23 degrees centigrade. The activated sludge containing ammonia-oxidizing bacteria (AOB) and anammox seed sludge were inoculated in the reactor and supplied with synthetic wastewater for proliferation. In the start-up stage, nitrite-oxidating bacteria (NOB) that remained in the sludge were inhibited. DO concentration and pH in the effluent were regularly measured using a DO meter (HORIBA HC-200NH, Japan) and a portal pH meter (HORIBA D-71, Japan), respectively.

The operation condition is shown in Table 1.

Table 1 Operation Conditions

Stage	I	II	III	IV	V
Duration (day)	1-164	165-180	181-214	215-236	237-264
Influent ammonia concentration (mg-NH ₄ ⁺ -N/L)	30-440	5000	1000	500	100
HRT (Days)	0.11-0.87	16.70	3.30	1.67	0.33
NLR (g-N/L/d)	0.2-0.5		0.3		
MLVSS (mg/L)	1766	2471	2361	1876	2179

2.2 Sampling and analytical methods

All of the samples of influent and effluent were analyzed after being filtrated through Millipore filter units with 0.45 μm pore size. The $\text{NH}_4^+\text{-N}$, $\text{NO}_2^-\text{-N}$, and $\text{NO}_3^-\text{-N}$ concentration was measured by capillary electrophoresis (Agilent 7100, Agilent Technologies, USA).

3 Results and discussion

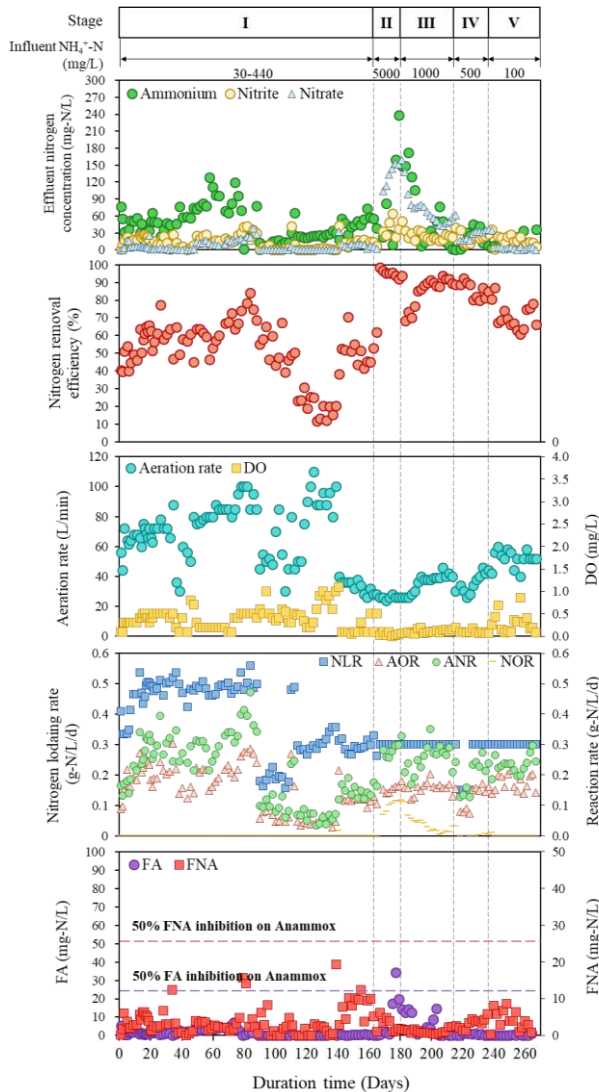


Fig. 1. Reactor performance

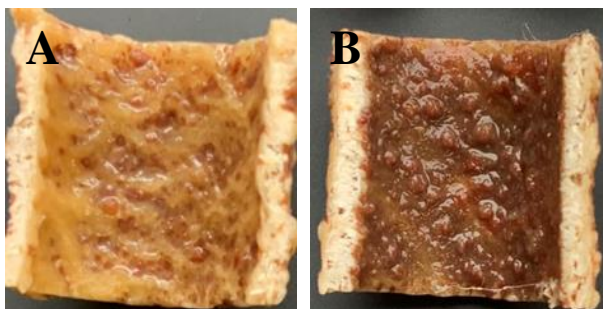


Fig. 2. Biofilm on (A) Day 1 and (B) Day 102

This study is divided into five stages, containing the biofilm-forming stage and the experiment stages. In Stage I, several strategies were adopted for the growth of anammox bacteria. As shown in Fig. 1, reactor performances were unstable. The nitrogen removal efficiencies were quite different while treating wastewater of 30-440 mg-N/L due to the sparse and thin biofilm and the impact from the actual sewage. However, the maximum removal efficiency of 84.2% can be achieved when the influent concentration is 440 mg-N/L. More importantly, the anammox biofilm, the main target of this stage, has clearly formed as Fig. 2.

In order to further understand the effect of influent nitrogen concentration on the PN/A reactor performance, the reactor was maintained at a nitrogen loading rate of 0.3 g-N/L/d, and the influent ammonium concentration was gradually reduced from 5000 mg-N/L in Stage II to 100 mg-N/L in Stage V. As with the results of many studies, the anammox process was very effective in treating wastewater with high ammonium concentrations. When the reactor was fed with 5000 mg-N/L sewage in Stage II, a 94.8% nitrogen removal was achieved. Once the influent nitrogen concentration dropped to 1000 mg-N/L in Stage III, the nitrogen removal efficiency decreased to 88.5%. With a further halving of the influent ammonium concentration to 500 mg-N/L in Stage IV, a removal rate of 84% could still be achieved. Finally, in stage V, when the influent ammonium concentration became 100 mg-N/L, relatively low compared with stage II, the reactor performance became unstable, and nitrogen removal efficiency declined to 76.1%. From the result above, it was evident that as the influent $\text{NH}_4^+\text{-N}$ concentration got lower, the nitrogen removal efficiencies of the reactor were with varying degrees of decline. Moreover, the trend line fit revealed that the ammonium concentration might be logarithmically or power functionally related to the nitrogen removal efficiency in this case. Meanwhile, the anammox biofilm in Stage V became denser and thicker compared with the former stage.

After all, in this pilot plant study, it is confirmed that the biofilm-based one-stage PN/Anammox process showed an excellent performance with a wide range of concentrations of nitrogen wastewater.

4 Conclusions

(1) In a pilot-scale PN/A reactor, anammox bacteria can be proliferated using real wastewater, and anammox biofilms have been successfully formed on the hollow cylinder hydrophobic polypropylene resin carriers.

(2) At the same nitrogen loading rate, the nitrogen removal efficiency of the PN/A reactor decreases to varying degrees as the influent ammonium concentration decreases and the actual wastewater ratio increases. However, the results of studies at the pilot-scale show that the biofilm-based one-stage PN/Anammox process has great potential to treat a wide range of concentrations of ammonia nitrogen wastewater.

Reference

[1] Rong Chen, Using Partial Nitrification and Anammox to Remove Nitrogen from Low-Strength Wastewater by Co-immobilizing Biofilm inside a Moving Bed Bioreactor, ACS Sustainable Chemistry & Engineering (2019) 1353-1361.

Development of a BrISH for environmental microorganisms

○ Kampachiro URASAKI^{1*}, Yu-You LI¹ & Kengo KUBOTA²

¹Department of Civil and Environmental Engineering, Graduate School of Engineering, Tohoku University, Miyagi 980-8579, Japan.

²Department of Frontier Sciences for Advanced Environment, Graduate School of Environmental Studies, Tohoku University, Miyagi 980-8579, Japan.

*E-mail: kampachiro.urasaki.p1@dc.tohoku.ac.jp

Abstract

Fluorescence *in situ* hybridization is a convenient tool for understanding microbial community because it can visualize microorganisms at single cell resolution. FISH has a lot of variants that uses the heavy element instead of the fluorophore for the X-ray detection. X-ray based techniques can detect with high resolution; therefore, have a technical potential for the single cell detection. In this study, we attempted to develop a novel bromine labeling method, “BrISH.” BrISH employs TSA (tyramide signal amplification) reaction to enhance the intensity of the labeled element. Two candidates of the tyramide-Br compound (tyramide-Br-1, C₁₀H₁₂O₂NBr; tyramide-Br-2, C₇H₆O₂NBr) were synthesized, nevertheless, tyramide-Br-1 (C₁₀H₁₂O₂NBr) yield was low and another tyramide compound added Cl was obtained. Tyramide-Br-2 (C₇H₆O₂NBr) was not obtained. BrISH using tyramide-Br-1 was applied to the pure cultures however Br signal wasn't obtained so far.

Keywords: CARD-ISH; Bromine; X-rays detection; Scanning electron microscope.

1 Introduction

FISH (fluorescence *in situ* hybridization) is widely used in various fields because it can detect microorganisms at single-cell resolution without cell cultivation and DNA/RNA extraction. FISH is an attractive tool for understanding microbial community structure because it can detect target microorganisms phylogenetically. In recent years, detection using X-ray-based techniques, e.g., SEM (scanning electron microscopy), are becoming mainstream due to their high resolution. For X-rays detection, labeling the microbial cells with heavy elements is necessary. Gold (Au) is commonly used as a labeling element for the X-ray detection [1]. For multicolor staining, a novel labeling method that uses heavy elements other than Au is promised. In this study, bromine (Br) was focused on as the cell labeling element. In order to label cells with high density Br, TSA (tyramide signal amplification) reaction was employed. TSA reaction is the peroxidase-catalyzed reaction to bind the tyramide compounds with the aromatic amino acids in the cell tissue. The reaction was employed highly sensitive FISH method (TSA-FISH), ELISA and etc. In this study, a novel Br labeling method employing TSA reaction, named “BrISH,” was attempted to develop.

2 Materials and methods

2.1 Sample preparation

The strains used in this study were *Comamonas testosteroni* and *Escherichia coli*. Both strains were cultivated in LB medium at 37°C with agitation. During exponentially growth phase, these cells were fixed in a 4% paraformaldehyde solution in phosphate buffered saline (PBS; 150 mM NaCl, 20 mM PO₄³⁻ [pH7.4]) for 12 h at 4°C, and stored in ethanol/PBS solution at -20°C.

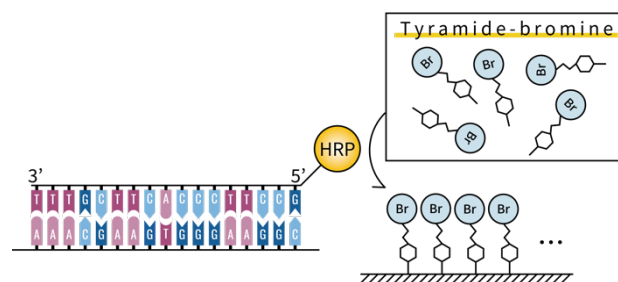


Fig.1 Scheme of TSA-Br-ISH

2.2 Tyramide synthesis

First, a synthesis reaction of tyramide compounds was investigated. Two candidates of tyramide-Br compounds were prepared which were tyramide-Br-1 (C₁₀H₁₂O₂NBr, MW 258) and tyramide-Br-2 (C₇H₆O₂NBr, MW 216). Tyramide compounds were synthesized in accordance with the previous report with some modifications [2]. Tyramide-Br-1 was synthesized from tyramine-HCl and 2-bromoisobutanoic acid NHS ester, and tyramide-Br-2 was synthesized from tyramine-HCl and bromoacetic acid NHS ester. NHS esters were dissolved in DMF (10 mg/ml) to obtain the stock solution A. Tyramine-HCl was dissolved in DMF containing TEA (10 µl/ml) to obtain the stock solution B. Then the stock solution A was added in 1.1 times equimolar amounts to the stock solution B. The mixture of the stock solution A and B was incubated for two hours in the dark with mild stirring. Obtained compounds were analyzed by GC-TOF/MS (JEOL, JMS-T100GCV).

2.3 BrISH

The scheme of BrISH was shown in Fig.1. First, cell wall treatment was performed using lysozyme solution (10 mg/ml). *In-situ* hybridization with BET42a-HRP (5'-GCCTTCCCAC TTCGT TT-3') was performed as described previously [3]. After *in-situ* hybridization, TSA reaction was

carried out using the working buffer (10% dextran sulfate and 0.0015 % [v/v] H₂O₂ 0.1% [w/v] blocking reagent in PBS) containing 20 µg/ml of tyramide-Br-1 compound for 15 min at room temperature. Then, the samples were equilibrated in 0.05% [v/v] PBSX for 15 min at room temperature. For microscopic observation, digital photograph, and EDX measurement, scanning electron microscope (JEOL, JSM-7100F) was used.

3 Results and discussion

3.1 Analysis of the synthesized tyramides

Fig.2(A) shows the TOF/MS spectrum analyzing the obtained tyramide-Br-1 solution. The low intensity of tyramide-Br-1 was detected (m/z 257). The highest signal (m/z 213) was estimated “C₁₀H₁₂O₂NCl.” It was speculated that Cl in tyramine-HCl (C₈H₁₁NO · HCl) was replaced with tyramide-Br-1’s Br among the synthesis. **Fig.2(B)** shows the TOF/MS spectrum analyzing the obtained tyramide-Br-2 solution; however, tyramide-Br-2 was not detected. The highest peak is estimated “C₁₂H₁₆O₂NBr” (m/z 285). Tyramide-Br-2 was failed to synthesize; therefore tyramide-Br-1 was used for BrISH.

3.2 BrISH

Fig.3 shows the *C.testosteroni* by BrISH of (A) secondary electron image and (B) EDX measurement by scanning electron microscope (SEM). For EDX measurement, Br peak (1s; 1.60 keV, 2s; 1.78 keV) was not observed from the target microorganism (*C. testosteroni*). Only C peak (1s; 0.28 keV) and O peak (1s; 0.54 keV) were observed that were from the cell’s organic matter. Br was not detected from the nontarget microorganism (*E. coli*, data not shown). Cl peak (1s; 2.82 keV) wasn’t observed thus “C₁₀H₁₂O₂NCl” didn’t deposit to the cell tissue. Those results indicated that synthesized compounds didn’t have the function of the tyramide compounds.

4 Conclusions

We attempt to develop the novel phylogenetically specific Br labeling method, “BrISH.” Tyramide-Br was synthesized from 2-bromoisobutanoic acid NHS ester and tyramide-HCl, however sufficient yield was not obtained. BrISH was applied to the pure cultures and detected by SEM, but any Br signals were not obtained so far.

Reference

- [1] Schmidt H, Eickhorst T, Musmann M. Gold-FISH: a new approach for the in situ detection of single microbial cells combining fluorescence and scanning electron microscopy. *Syst Appl Microbiol.* 35(8) (2012):518-25.
- [2] Hopman AH, Ramaekers FC, Speel EJ. Rapid synthesis of biotin-, digoxigenin-, trinitrophenyl-, and fluorochrome-labeled tyramides and their application for In situ hybridization using CARD amplification. *J Histochem Cytochem.* 46(6) (1998):771-7.
- [3] Kubota K, Imachi H, Kawakami S, Nakamura K, Harada H, Ohashi A. Evaluation of enzymatic cell treatments for application of CARD-FISH to methanogens. *J Microbiol Methods.* 72(1) (2008):54-9.

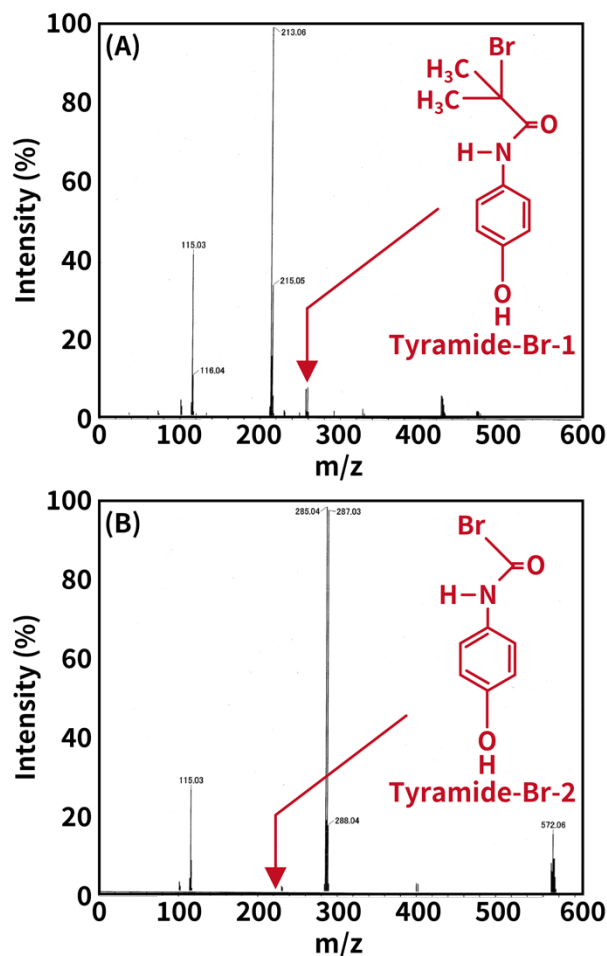


Fig.2 GC-TOF/MS spectrum of the tyramide compounds (A) tyramide-Br-1 and (B) tyramide-Br-2

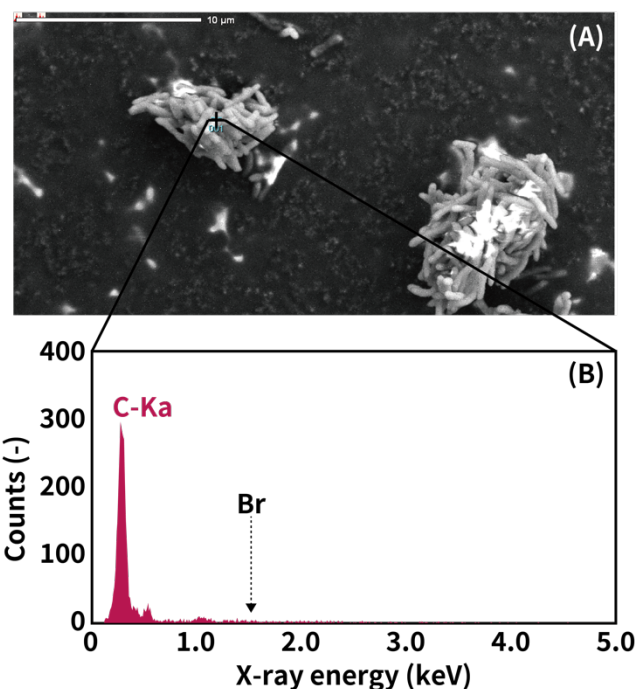


Fig.3 Detection *C.testosteroni* by BrISH (A) secondary electron image and (B) EDX measurement by SEM

Methane fermentation performance of swine wastewater treatment by a pilot-scale self-agitation anaerobic baffled reactor

○ Junhao SHEN¹, Yunzhi QIAN¹, Yan GUO¹, Fuqiang CHEN¹, Yu-You LI^{2*}

¹Dept. of Frontier Sciences for Advanced Environment, Tohoku University, Sendai, 980-8579, Japan.

²Dept. of Civil and Environmental Engineering, Graduate School of Engineering, Tohoku University, Sendai 980-8579, Japan.

*E-mail: shen.junhao.q2@dc.tohoku.ac.jp
gyokuyu.ri.a5@tohoku.ac.jp

Abstract

In the context of the intensification of pig production and consequent higher animal densities, the environmental effects have to be considered. Swine Wastewater (SW), as the main direct environmental impact pig production, can be removed by biological treatment, which is called methane fermentation. In this research, SA-ABR (Self-Agitation Anaerobic Baffled Reactor) is used in the treatment of SW to save energy as the goal. The performance, in term of gas production, organic removal, and the stability of the system in practical applications were investigated during 400 days by changing the hydraulic retention time (HRT) and organic loading rate (HRT) from 60 to 7.5 days and from 0.18 to 7.16 g/L/d. SW which had TCOD, proteins and carbohydrates of 22.4, 6.34 and 1.48g/L, respectively, was used as substrate. COD removal efficiency reaches a maximum of 65% when the organic load on HRT 10 days is 1.14g/L/d, and COD removal efficiency is maintained at 50% or more until the organic load on HRT 10 days is 1.85 g/L/d, but after the OLR exceeded 2, it was going to drop more and more. The biogas production was about 100 L / day, and a maximum of 544.2 L / d was recorded when the organic load was 4.8g/L/d.

Keywords: Swine Wastewater; Methane Fermentation; Self-Agitation Anaerobic Baffled Reactor (SA-ABR).

1 Introduction

Recent years, in the context of the intensification of pig production and consequent higher animal densities, the environmental effects have to be considered. Global issue such as greenhouse gas emission from livestock production are becoming internationally recognized. Swine wastewater (SW), as the main direct environmental impact pig production, can release the production of combustibles through bio-digestion which can help to make optimum use of the natural resources involved in the production cycle. (FAO, 2021).

A common treatment process in SW is an anaerobic-aerobic treatment system. The processing capacity of this process is low depending on the volume of the processing equipment and is expensive in terms of investment, maintenance and operation. Therefore, we are keenly aware of the need to improve the efficiency of removing SW and to find a treatment process that can be applied to the recovery of resources. On another hand, anaerobic digestion (AD) has presented high effectiveness in the elimination of biodegradable pollutants from complex agro-industrial effluents, as well as bioenergy production through biogas (G. Lourinho, 2020).

Various of anaerobic bioreactor were developed for anaerobic digestion, such as up-flow anaerobic sludge blanket (UASB), continuously stirred tank reactor (CSTR), anaerobic membrane bioreactor (AnMBR) and baffled reactor. The first anaerobic baffled reactor (ABR) was developed by Bachmann (1983). Then, many researchers have been working on baffled reactor and found its several advantages. ABR has faster granulation process (Hutnán, M. et al., 1999), higher microbial diversity in every chamber,

good resilience to hydraulic and organic shock loads, prevent the sludge wash-out (Tanikawa, D., 2017 and Motteran et al., 2013), high resistance in environmental parameters such as pH and alkalinity (Rongrong et al., 2011; Zhong and Yang, 2012), simple design low cost for construction and operating (Tanikawa, D., 2017; Ji et al., 2009). Moreover, it is lauded for its simple design and the low construction and operating costs (Ji et al., 2009).

With the advantages of the ABR, Previous researchers developed a new ABR called self-agitation anaerobic baffled reactor (SA-ABR). The SA-ABR has been investigated and the result show that SA-ABR is comparable in digestion performance to the completely stirred tank reactor (CSTR) (Kobayashi and Li, 2011). In addition, subsequent experiments were carried out on a laboratory scale with actual fish processing wastewater as the substrate. The experimental results showed that SA-ABR showed good processing performance in the treatment of fish processing wastewater (Eli, 2020). In another study by Qiao, a higher methanogenic performance was achieved by the SA-ABR than the CSTR in treating swine wastewater. In that study, at an HRT of 1 day, the specific methane yield of the SA-ABR was 0.43 L/g, while the CSTR failed to produce biogas due to the sludge washout, and stable biogas production was achieved at a short HRT of 0.5 days for the SA-ABR (Qiao et al., 2018).

Therefore, based on previous studies, in this study, we designed a pilot-scale SA-ABR system for anaerobic fermentation of swine wastewater and urine. The purpose of this research is to investigate the performance of SA-ABR in methane fermentation of SW in term of COD conversion; biogas production and the stability of SA-ABR.

2 Materials and methods

2.1 Reactor design and operation

The reactor design is shown on Fig.1 with working volume 1000 L (total volume 1050 L), setting temperature 35±1°C. The seed sludge was taken from anaerobic wastewater treatment Jnex Waste recycling factory. The reactor is set up in the Za-O pig farm, and samples are taken twice a week and taken back to the laboratory for measurement and analysis.

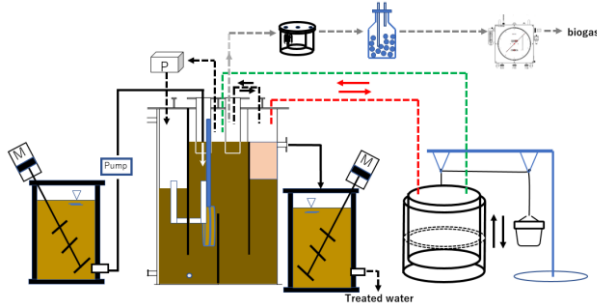


Fig.1 SA-ABR system Design

2.2 Analysis

Analyses of pH, alkalinity, COD, protein, carbohydrate, lipid, NH₄⁺, TS, VS, MLSS, MLVSS were performed according to the Japan standard methods (JSWA, 1997). VFA was determined by gas chromatography (Agilent-6890). Biogas composition was measured by a gas chromatograph (SHIMADZU GC8A).

3 Results and discussion

3.1 Substrate profile

Characteristics of swine wastewater, such as pH, TAN is determined with the average 7.78, 2.967g/L. On the other hand, the averages of alkalinity, protein, carbohydrate, TS, VS, SS, VSS were 12.26g/L, 6.34g/L, 1.48g/L, 24.7g/L, 12.48g/L, 13.82g/L and 7.49g/L. In addition, the fluctuation of COD is relatively large, between 8.0g/L to 56.3g/L and the average is 22.4g/L.

3.2 Performance and stability of fermentation process

In general, the performance of SA-ABR in treatment of swine wastewater was good. Organic loading rate (OLR) increased from 0.18 g/L/d to 7.16g/L/d with the decrease of Hydraulic Retention Time (HRT). COD removal efficiency reaches a maximum of 65% when the organic load on HRT 10 days is 1.14g/L/d, and COD removal efficiency is maintained at 50% or more until the organic load on HRT 10 days is 1.85 g/L/d, but after the OLR exceeded 2, it was going to drop more and more. And with regard to biogas production, the amount of biogas produced was about 100L/day, and a maximum of 544.2L/d was recorded when the organic load was 4.8 g/L/d. To look for optimal operating conditions, calculated COD balance, the result showed when OLR was 1.90g/L/d, the COD balance reached over 90% and the methane conversion efficiency exceeded 20%.

About the stability of system, when HRT was 15days with OLR of 0.5±0.05g/L/d, the performance of system was very good that can be applied to various conditions, such as low temperature, extremely high concentration of COD. But if take consideration such as biogas production, COD removal

efficiency, the optimal operating condition was OLR 1.75±0.25g/L/d in HRT of 10 days.

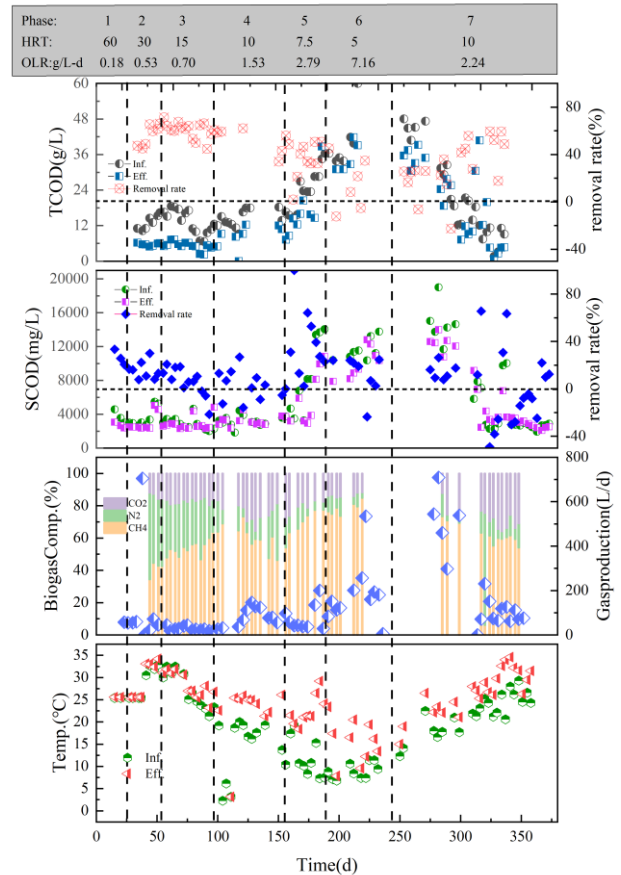


Fig.2 SA-ABR Performance in Swine Wastewater Fermentation

4 Conclusions

The content of components such as the content of organic matter in swine wastewater was extremely unstable, which influenced the research. But even if in this situation, the SA-ABR showed satisfying stability. Biogas production recorded a maximum of 544.2L/d with an OLR of 4.8g COD/L/d on the HRT of 10 days. However, it is still necessary for advanced studies of SA-ABR for COD removal efficiency and higher methane conversion efficiency.

Reference

- [1] Eli Hendrik Sanjaya, Mesophilic methane fermentation performance and ammonia inhibition of fish processing wastewater treatment using a self-agitated anaerobic baffled reactor, *Bioresource Technology* 313 (2020) 123644.
- [2] G. Lourinho et al., Recent advances on anaerobic digestion of swine wastewater, *International Journal of Environmental Science and Technology* volume 17, pages 4917–4938 (2020).
- [3] Qiao et al., Continuous anaerobic treatment of swine wastewater by using self-agitation anaerobic baffled reactor, *Nongye Gongcheng Xuebao Transactions Chin. Soc. Agric. Eng.* 34, 210–215.

Enhancement Effect of Two Novel Pretreatment Methods on Anaerobic Digestion of Waste Activated Sludge with Thermophilic AnMBR

○ Shitong ZHOU^{1*}, Guangze GUO¹, Yemei LI^{2,3}, Yu-You LI^{1,2}

¹Department of Frontier Science for Advanced Environment, Graduate School of Environment Studies, Tohoku University, 6-6-06 Aoba, Aramaki-Aza, Sendai, Miyagi 980-8579, Japan.

²Department of Civil and Environmental Engineering, Graduate School of Engineering, Tohoku University, 6-6-06 Aoba, Aramaki-Aza, Sendai, Miyagi 980-8579, Japan.

³Material Cycles Division, National Institute for Environmental Studies, Tsukuba 305-8506, Japan

*E-mail: zhou.shitong.q2@dc.tohoku.ac.jp.

Abstract

Two novel integrated pretreatment methods called venturi tube combined with steam injection (VT-SI) and inflow heating steam injector (IHSI) were firstly applied to increase the sludge solubility of waste activated sludge (WAS). Both methods innovatively combined hydrodynamic cavitation (HC) and steam. All the untreated sludge and pretreated sludge were digested in a thermophilic anaerobic membrane bioreactor (ThAnMBR) respectively under the high solid condition with TS = 30 and 40 g/L for a long term. Both VT-SI and IHSI proved effective in sludge solubility enhancement, with COD disintegration degree (DD) of 11.2% and 11.0% respectively. Besides, biogas yield increased by 5.4% and 7.0%, and methane conversion efficiency increased by 6.9% and 9.0% through VT-SI and IHSI pretreatment, respectively. In addition, the ThAnMBR was operated stably for a long term under the condition that TS was 30 g/L with the average flux of 6 L/m²/h (LMH). However, when the TS continued increased to 40 g/L, the filtration performance showed a great reduction. Membrane cleaning was conducted and membrane resistance of each foulant layer was calculated. And cake layer was considered as the biggest contributor to membrane fouling.

Keywords: Pretreatment; ThAnMBR; Waste activated sludge; Hydrodynamic cavitation; Membrane Performance

1 Introduction

During the municipal wastewater treatment, a large amount of WAS is produced. Anaerobic digestion (AD) has been widely used for WAS treatment. However, microbial flocs can be discharged with the effluent, resulting in bad effluent quality and low methane conversion efficiency. AnMBR is an emerging treatment process to solve this problem with several merits. Combining the membrane filtration technology, AnMBR realizes the complete separation of HRT and SRT, thus effectively maintaining the microorganism in the reactor, reducing the sludge discharge, guaranteeing excellent effluent quality, and improving the organic conversion efficiency.

Another problem lies in AD of WAS is known as the slow hydrolysis rate due to the recalcitrant substances and complex structure. To increase the biodegradability, pretreatment has been proposed accordingly. There are various pretreatment methods, which can be classified as thermal hydrolysis, mechanical pretreatment, chemical pretreatment, and biological pretreatment. Nowadays, mechanical pretreatment has attracted more and more interest because it is energy-saving, convenient, and is easy of operation with good enhancement performance as well. The principle of hydrodynamic cavitation (HC) has commonly applied in mechanical pretreatment, which takes advantage of the local pressure drop resulted from the change of cross section. During the HC process, cavitation bubbles produce, grow and finally implosive break to release huge kinetic energy and heat near the local area. In this way, it disrupts the sludge structure, increases solubility and accomplishes homogenization.

In this study, the enhancement effect of two novel pretreatment methods on the AD of WAS in a ThAnMBR was first investigated, especially the sludge solubility, biogas production and organic conversion efficiency. In addition, the feasibility of stable operation of AnMBR under high solid condition for a long term was also explored.

2 Materials and methods

2.1 Substrate and Pretreatment methods

The WAS was collected from S municipal wastewater treatment plant in Japan. Then part of WAS was pretreated by VT-SI and IHSI, respectively. In VT-SI, pre-heated WAS was added to pass through a venturi tube which had a throat with narrowed diameter. In venturi throat, pressure dramatically decreased due to the increase of velocity, leading to the production of cavities. In the downstream area, the pressure recovered and caused the cavitation bubbles breaking. At the same time, steam was injected in a speed of sound to promote the cavitation (Fig.1a).

As for IHSI, it also took advantage of HC and had a narrowed cross section as well, but with a different application method of steam. The steam was input to mix with sludge so that it realized simultaneous cavitation promotion and sludge heating. The temperature of outflow WAS was 70 °C while that of inflow was 30 °C. Due to adjustment of the configuration of steam injector, IHSI could achieve great mixture effect (Fig.1b).

2.2 Experimental Device and Operation Conditions

The ThAnMBR system used in this study was external submerged AnMBR composed of one continuous stirred tank reactor (CSTR) of 13 L and one membrane unit of 2 L (Fig.1c). The membrane was hollow fiber membrane with

pore size of 0.1 μm and effective membrane area of 0.1 m², the material of which was polytetrafluoroethylene (PTFE).

There were five stages in the whole operation period, with the HRT kept as 15 days. In the first three stages, three different types of sludge were fed as substrate, which were untreated WAS, pretreated WAS by VT-SI and pretreated WAS by IHSI, respectively. And the total solid (TS) concentration of bulk sludge in reactor was kept at 30 g/L. In the later two stages, the TS was increased to 40 g/L, and untreated WAS and pretreated sludge by IHSI were used as substrate respectively.

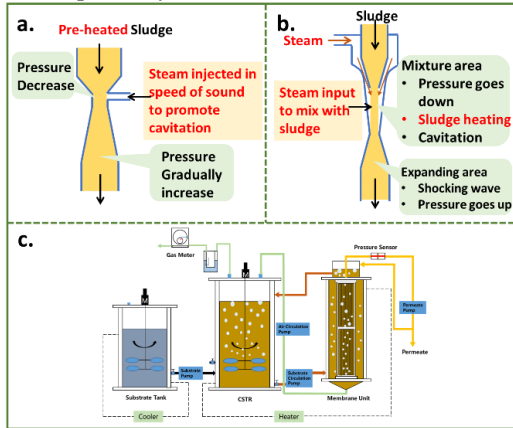


Fig. 1. The schematic diagram of the pretreatment methods and experimental device. a) VT-SI; b) IHSI; c) ThAnMBR

3 Results and discussion

3.1 Sludge Solubility

Since most of anaerobic microorganisms only ingest soluble organics, converting large-size organic substances into small ones, namely increasing sludge solubility will lead to biodegradability improvement. The suspended solids (SS) and volatile suspended solids (VSS) concentration decreased while soluble substances going up. Disintegration degree (DD) is commonly used to evaluate the solubility enhancement performance. A modified DD was used in this experiment because the concentrations of total organic substances were detected not the same in different stages, which was calculated in the following equation (1).

$$\text{Modified DD}(\%) = \frac{\frac{\text{Soluble}_{x,i}}{\text{Total}_{x,i}} - \frac{\text{Soluble}_{0,i}}{\text{Total}_{0,i}}}{1 - \frac{\text{Soluble}_{0,i}}{\text{Total}_{0,i}}} \times 100\% \quad (1)$$

The results showed DD (%) of COD, carbohydrates and proteins were 11.7%, 3.48%, 11.2% respectively after VT-SI, while that of IHSI were 10.9%, 7.39%, and 11.0%, respectively. Both pretreatment methods proved effective in increasing sludge solubility.

3.2 Biogas Production

These three types of sludge were fed as substrate in each stage and biogas yield, and biogas composition as well as methane conversion efficiency were analyzed and calculated (Tab 1). In general biogas composition is rather stable in each stage. Methane took up 63.1%-65.0%, while carbon dioxide accounted for 33.6%-34.7%. As for biogas yield, it increased from 12.9 L/d to 13.6 L/d and 13.8 L/d after VT-SI and IHSI pretreatment, respectively. When it comes to methane conversion efficiency, it increased from 0.233 L-CH₄/g-COD to 0.249 and 0.254 L-CH₄/g-COD after VT-SI and IHSI pretreatment, improving by 6.9% and 9.0%, respectively. The improvement effect was not that

significant, which was because thermophilic AD posed higher hydrolysis rate and better disintegration efficiency itself compared with mesophilic AD. Thus, the enhancement effect seemed to be weakened accordingly.

Table 1 The biogas yield and methane conversion efficiency in each stage

Items	Unit	Stage 1	Stage 2	Stage 3	Stage 4	Stage 5	
Biogas yield							
	L/d	13.6	13.8	12.9	13.9	13.2	
Biogas composition							
	CH ₄	%	65.0	63.3	63.1	64.5	63.6
	CO ₂	%	33.6	34.4	34.3	33.8	34.7
	H ₂ S	ppm	527	588	500	769	667
Methane conversion efficiency							
	L-CH ₄ /g-TS	0.354	0.361	0.297	0.355	0.316	
	L-CH ₄ /g-VS	0.510	0.488	0.413	0.468	0.409	
	L-CH ₄ /g-COD	0.249	0.254	0.233	0.255	0.242	

3.3 Organic Removal and COD Balance

Due to membrane rejection, ThAnMBR successfully realized high removal efficiency with excellent effluent quality. The removal efficiency of COD, carbohydrates and proteins were all above 92%. Besides, material flow analysis was also conducted by comparing the COD mass in system input (substrate) and output (digested sludge, permeate and biogas). And the results showed nearly half of the COD remained in the digested sludge with 42%-47% COD converted into methane, indicating the great energy recovery potential of digested sludge.

3.4 Membrane Performance and Membrane Fouling

Membrane fouling is an important issue in AnMBR system. It was discovered that when filtration mode was 1 min filtration and 1 min relaxation with the average flux was 6 L/m²/h (LMH), membrane could work stably under the high solid condition of TS 30 g/L (Fig.2). However, when the TS concentration continuously increased to 40 g/L in stage 4 and 5, there was a great reduction in filtration performance. The filtration mode could not be maintained as that in first three stages and had to be adjusted into 1.6 LMH, indicating solid concentration was an important constraint in AnMBR application. In addition, membrane cleaning as well as clean water filtration test were conducted to calculate membrane resistance of each foulant layer. The results showed that cake layer was the largest contributor to membrane fouling, which accounted for nearly half of the resistance.

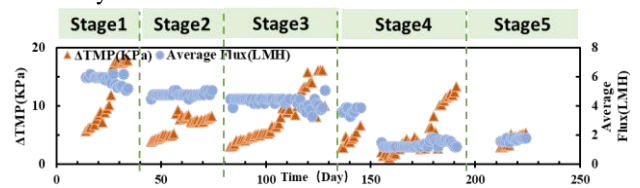


Fig. 2. Membrane filtration performance in ThAnMBR

4 Conclusions

- VT-SI and IHSI greatly improved the sludge solubility, with the DD of COD at 11.2% and 11.0%, separately.
- VT-SI and IHSI also enhanced the biogas yield and methane conversion efficiency.
- ThAnMBR operated stably in long term under high solid condition of TS=30 g/L with the average flux of 6 LMH. But filtration performance greatly reduced when TS increased to 40 g/L.

Reference

[1] Mancuso, G., Langone, M., & Andreottola, G. (2020). A critical review of the current technologies in wastewater treatment plants by using hydrodynamic cavitation process: principles and applications. *Journal of Environmental Health Science and Engineering*, 18(1), 311–333.

Applications of Solar Photovoltaics and Offshore Wind Power towards Carbon Neutrality in Coastline Cities

Hongxing Yang

Department of Building Environment and Energy Engineering,
The Hong Kong Polytechnic University, Hong Kong, China
E-mail: hong-xing.yang@polyu.edu.hk

Abstract

Renewable energy applications are playing an important role for achieving the carbon neutral targets in the world. Solar photovoltaic power generation and offshore wind power generation are the main renewable energy resources for most coastline cities, especially in Hong Kong and the Greater Bay Area of China. This presentation will focus on our research and development of solar photovoltaic applications, especially building-integrated solar photovoltaics (BIPV), and offshore wind power production. The world development trends of these two main renewable energy resources are introduced first and our research efforts are then presented. In Hong Kong, the Feed-in-Tariff policy has greatly promoted the BIPV power generation in the territories, but less development in wind power. It is estimated that the potential annual power generation from these two renewable energy resources are about 30% of local annual power demand in Hong Kong. In Chinese mainland, BIPV is a hot topic nowadays due to the pressures to realize carbon neutrality in 2060. Our research projects in solar photovoltaic façade, wake model development of wind farms and hybrid solar-wind power generation will be briefly introduced. The local policy towards renewable energy applications will be discussed. A new development project in Hong Kong will be used as a sample project to highlight the importance of solar photovoltaic and offshore wind power generations for achieving carbon neutrality in Hong Kong by the year 2050.

Exploring Microbiome Assembly and Antibiotic Resistome in Wastewater Treatment Plants

Feng Ju^{1,2}

¹ Environmental Microbiome and Biotechnology Laboratory (EMBLab), School of Engineering, Westlake University, Hangzhou 310012, China; ² Institute of Advanced Technology, Westlake Institute for Advanced Study, Hangzhou 310024, China.

*E-mail: jufeng@westlake.edu.cn

Abstract

Microbiome, which encompasses microbial communities (i.e., microbiota) and their ‘theatre of activity’, plays a central role in the success of biological wastewater treatment plants (WWTPs). Our and other researches have fully acknowledged that WWTPs microbiome not only contains diverse beneficial microbes that convert and remove various wastewater pollutants or produce biomethane, but also harbors a proportion of detrimental microbes and genes responsible for common operational problems (e.g., bulking and foaming) and/or hygienic issues (human pathogens and antibiotic resistance). More importantly, new progress has also been achieved to resolve the patterns and processes underlying microbiome assembly and antibiotic resistome in WWTPs, providing a theoretical basis for targeted microbiome-based control and regulation of process functioning.

Keywords: Wastewater Treatment Plant; Activated sludge; Anaerobic digestion; Microbiome; Resistome.

1 Introduction

Activated sludge (AS) and anaerobic digestion (AD) are the most popular bioreactors in municipal WWTPs worldwide with microbes as the key driver to their success in wastewater de-contamination and sludge resourcization. However, they frequently suffer from operational problems such as sludge bulking and foaming [1]. Worse still, in contrast to their contribution in environmental protection, municipal WWTPs are increasingly criticized as a hotspot for the release of antibiotic resistant genes (ARGs) and bacteria (or pathogens) into the environment [2]. Because of the importance of microbiome for the bioreactor functioning, it is therefore crucial to investigate on the microbiome structure and function, and link them to environmental (i.e., wastewater and operational) parameters and bioreactor performance, which should inform on the management strategies and engineering measures for the targeted microbiome control to optimize WWTPs operation.

2 Materials and methods

16S rRNA gene amplicon sequencing was used to profile microbial community diversity, composition, and temporal dynamics in full-scale WWTPs or lab-scale bioreactors. Microbial interactions and the MEP nexus between microbiota (M), environment parameters (E), and process performance (P) were explored by co-occurrence network and multi-variate analyses [1]. Moreover, quantitative meta-omics (i.e., metagenome and metatranscriptome) were co-used to quantify ARGs and ARG transcripts in 12 WWTPs [2], achieving a systematic view of the fate, *in-situ* expression, and influential factors of ARGs of over 20 classes of antibiotics throughout WWTP compartments: i) clarified influent, ii) denitrification stage, iii) nitrification stage, and iv) secondary effluent.

3 Results and discussion

The results showed WWTP microbiome is non-randomly assembled by taxonomic relatedness and driven by multiple deterministic processes, e.g., habitat filtering, immigration,

and biotic interactions [1-2]. In one WWTP with seasonally occurring foaming events, AS community shows limited seasonal succession over 5 years. Biotic interactions are revealed as important drivers of microbiota assemblage [1], whereas sludge retention time (SRT) and inorganic nitrogen, partially explain phylogenetic and quantitative variances of community patterns (Fig. 1). Moreover, antibiotic resistome (i.e., the collection of all ARGs) greatly varies throughout WWTPs (Fig. 2), and its composition strongly correlate with bacterial composition. Although no strong drivers of resistome composition could be identified among the chemical stressors analyzed, the sub-inhibitory level of macrolide antibiotics in wastewater appears to select for macrolide and vancomycin resistance genes and induce their expression. Notably, pathogenic and indigenous denitrifying bacteria are found as transcriptionally active and key multi-antibiotic-resistant players, and a small proportion of persistent ARGs traverse WWTPs and show upregulated expression in the secondary effluent [3].

4 Conclusions

Multiple deterministic processes (e.g., habitat filtering and biotic interactions) co-drives microbiome assembly and dynamics in WWTPs, where antibiotic resistome is shaped by bacterial composition, genetic exchange, and upregulated expression in the effluent microbiomes.

Reference

- [1] Ju F and Zhang T*. 2015. Bacterial assembly and temporal dynamics in activated sludge of a full-scale municipal wastewater treatment plant, ISME J. 9: 683-695
- [2] Ju F, Helmut Bergmann* et al. 2019. Wastewater treatment plant resistomes are shaped by bacterial composition, genetic exchange and up-regulated expression in the effluent. ISME J. 13 (2): 346-360
- [3] Yuan L, Ju F* et al., 2021. Pathogenic and Indigenous Denitrifying Bacteria are Transcriptionally Active and Key Multi-Antibiotic-Resistant Players in Wastewater Treatment Plants. Environ. Sci. Technol. 55 (15): 10862-10874

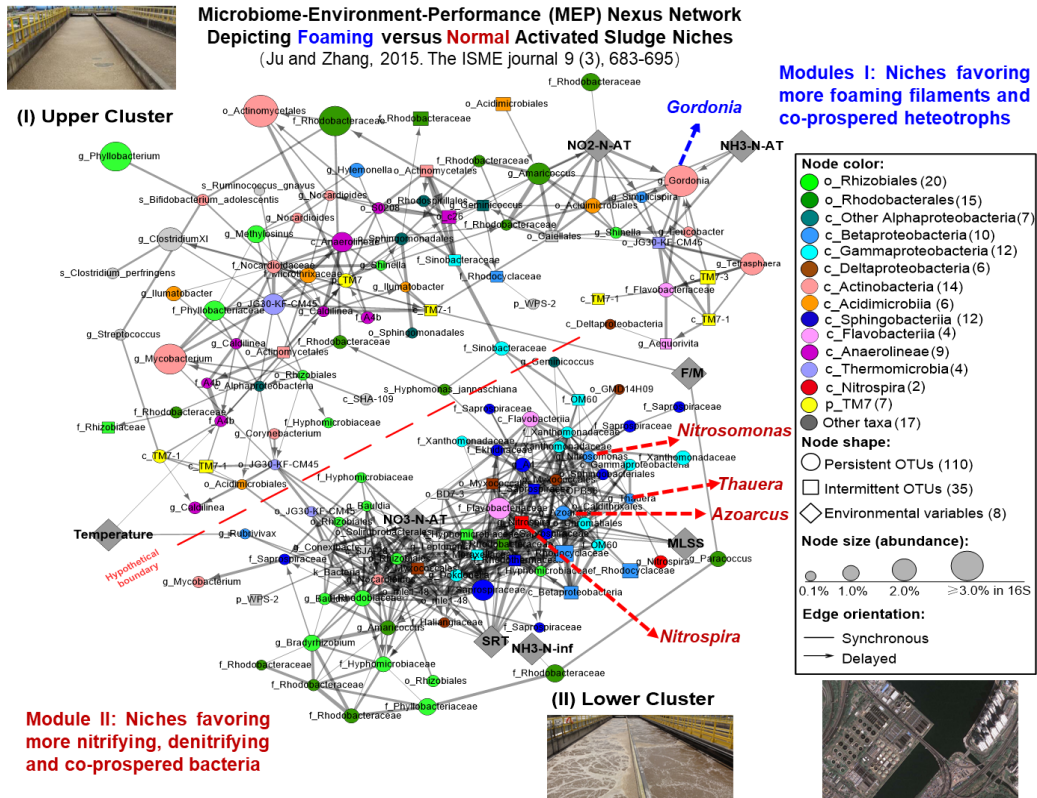


Fig. 1. Bacteria-bacteria and bacteria-environment co-occurrence network reveals distinct niches of foaming-thrived bacteria versus nitrogen-removing bacteria [1]. An edge represents a statistically significant and strong correlation between a bacterial OTU, and a wastewater or an environmental parameter.

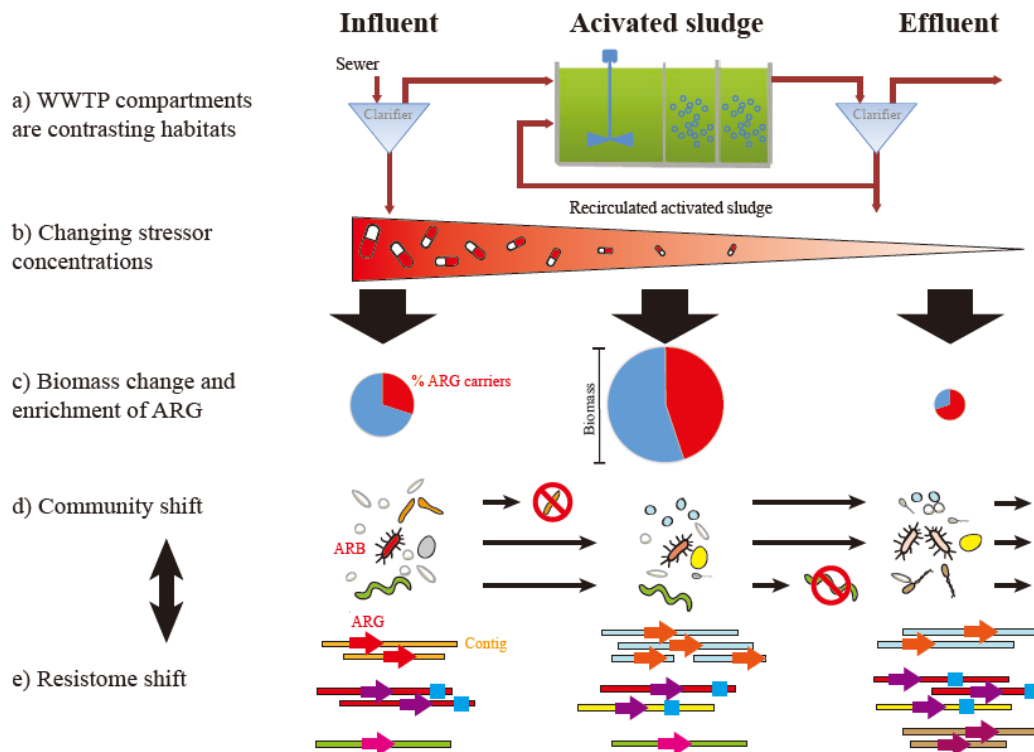


Fig. 2. Key hypotheses about processes affecting the resistome (resistance genes of microbiome) during passage of a WWTP. Conventional WWTPs consist (a) of primary and secondary treatment compartments with contrasting environmental conditions including (b) changing concentrations of stressors (e.g., antibiotics and metals) that may act as drivers on microbial biomass (c), community assembly (d) and resistome (e) [2].

Diversity and genomic information of *Patescibacteria* in activated sludge

○ Shuka KAGEMASA^{1*}, Kyohei KURODA², Ryosuke NAKAI², Yu-You Li^{1,3},
Kengo KUBOTA^{1,3}

¹ Department of Civil and Environmental Engineering, Tohoku University, Miyagi 980-8579, Japan.

² Bioproduction Research Institute, National Institute of Advanced Industrial Science and Technology (AIST), Hokkaido 062-8517, Japan.

³ Department of Frontier Sciences for Advanced Environment, Tohoku University, Miyagi 980-8579, Japan

*E-mail: shuka.kagemasa.t2@dc.tohoku.ac.jp

Abstract

Uncultured microorganisms make it difficult to understand the mechanisms of biological wastewater treatment processes. The candidate division, *Patescibacteria*, is always present in sludge treating wastewater (~10%), but their roles remain unknown. The purpose of this study is to reveal the diversity and obtain genomic information of *Patescibacteria* in activated sludge treating sewage for understanding their ecophysiology and roles in treatment processes. Very small cell sizes characterize *Patescibacteria*. In this study, microorganisms were fractionated by size for the enrichment of *Patescibacteria*, and metagenomic analysis was conducted using the size-fractionated sample. The size fractionation enriched *Patescibacteria* (*Saccharimonadia*, *Parcubacteria*, *Gracilibacteria*, *Microgenomatia*, and *ABY1*). The richness of *Patescibacteria* species detected by size fractionation of activated sludge also increased. In addition, we successfully obtained metagenome-assembled genomes of *Patescibacteria* and were able to infer metabolic pathways from the genomic information. This study deepened our understanding of *Patescibacteria* ecophysiological characteristics in activated sludge treating sewage.

Keywords: *Patescibacteria*; Filtration fractionation; Metagenomic analysis; Metabolic pathways; Activated sludge.

1 Introduction

Bacteria belonging to the superphylum *Patescibacteria* is universally found in sludge treating wastewater. *Patescibacteria* is part of a large bacterial phylogenetic group called candidate phyla radiation (CPR), a group of uncultured bacteria at the phylum level [1]. *Patescibacteria* have been inferred to contribute to wastewater treatment [2, 3]. However, when we analyze *Patescibacteria* by metagenomics analysis, there is often not enough *Patescibacteria* to construct MAGs (metagenome-assembled genomes) for functional analysis in sludge. In this study, we focused on the size fractionation of samples as a method of *Patescibacteria* enrichment. *Patescibacteria* is characterized by small cell size (about 0.2 μm in diameter) [4] and small genome size (about 1 Mbp) [5]. By size-fractionation of sludge treating wastewater, *Patescibacteria* is enriched, and their diversity in sludge treating wastewater was clarified. In addition, we attempted to obtain genomic information of *Patescibacteria* by metagenomic analysis.

2 Materials and methods

2.1 Sample and sample treatment

Activated sludge in the reaction tank of a sewage treatment plant was centrifuged, and the supernatant was size-fractionated in the order of filter pore sizes of 0.45 μm , 0.22 μm , and 0.1 μm (Stericup, Merck Millipore). Filters with pore sizes of 0.22 μm and 0.1 μm were collected as fractionation samples (referred to as 0.45-0.22 μm fraction and 0.22-0.1 μm fraction).

2.2 Microbial community structure analysis

PCR amplification used the 341F-806R-mix primer set, and

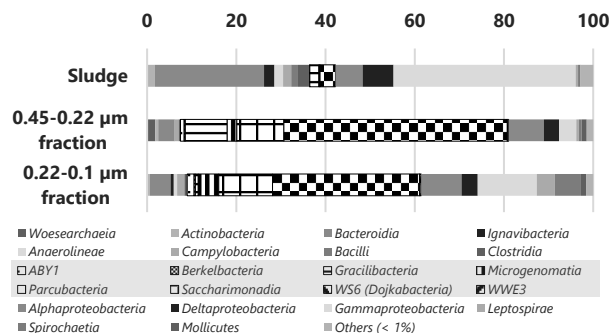


Fig.1 Microbial community structure analysis result of the size-fractionated activated sludge
(%, the gray area indicates *Patescibacteria*)

sequencing was performed using MiSeq (Illumina, Inc.). The sequence data were analyzed using QIIMETM (database: silva132) after removing a single read. Assigned as "None" and "No blast hit" operational taxonomic units (OTUs) were excluded from the analysis. They randomly selected 7,000 reads that were subjected to microbial community structure analysis. The coverage was 96.4~98.3%. The beta diversity and alpha diversity for *Patescibacteria* was calculated using QIIMETM.

2.3 Metagenomic analysis

Metagenomic analysis was performed using 0.45-0.22 μm fractions. Library preparation was performed using the Nextera XT DNA Library Preparation Kit (Illumina, Inc.) and sequenced using MiSeq. The sequencing data were binned (MetaBAT2, MaxBin2, vamb, MyCC) to obtain genomic bins, and the bins were quality-checked by CheckM (CPR maker gene) and phylogenetically classified (GTDB-tk ver. 1.5.1).

Table 2 Genomic information of *Patescibacteria* recovered in the 0.45-0.22 μm fraction

	<i>Saccharimonadia</i>	<i>Gracilibacteria</i>	<i>Paceibacteria</i> ^{*1}	<i>Microgenomatia</i>	ABY1
Relative abundance (%) Microbial community structure analysis (Sludge)	50.1 (3.5)	9.4 (2.1)	10.6 (0.2)	2.2 (0.03)	0.8 (0.07)
Metagenomic analysis	49.0	1.6	41.0	1.3	5.9
Number of Bin ^{*2}	7	1	13	1	2
Completeness (%, Min ~ Max)	73.6 (55.2~84.3)	76.7	66.3 (52.6~83.8)	58.5	85.8 (84.5~87.1)
Contaminations (%, Min ~ Max)	2.2 (0~6.3)	1.9	2.5 (0~6.9)	0.2	1.0 (0~2.0)
Genome size (%, Min ~ Max)	0.92 (0.46~1.32)	1.09	0.70 (0.39~0.91)	0.76	0.94 (0.93~0.94)

*1 *Parcubacteria* in the silva132 database. *2 Bin with completeness $\geq 50\%$ and contamination $\leq 10\%$.

3 Results and discussion

3.1 Microbial community structure analysis

The results of microbial community structure analysis are shown in Figure 1. In the unfractionated activated sludge, *Proteobacteria* and *Bacteroidia* were dominant in the samples, while *Patescibacteria* is dominant in the size-fractionated samples. The relative abundance of *Patescibacteria* in the samples was 69.9% in the 0.45-0.22 μm fraction and 51.1% in the 0.22-0.1 μm fraction, compared to 5.8% in the activated sludge. *Saccharimonadia*, *Gracilibacteria*, *Parcubacteria*, *Microgenomatia*, and ABY1 were detected in more than 1% of the size-fractionated samples. In particular, *Saccharimonadia* was the most dominant *Patescibacteria* in activated sludge, accounting for 59.7~68.1% of the *Patescibacteria* detected regardless of size fractionation or fraction size. *Saccharimonadia* and *Gracilibacteria* had a higher percentage in the 0.45-0.22 μm fraction than in the 0.22-0.1 μm fraction, and *Parcubacteria*, *Microgenomatia*, and ABY1 had a higher percentage in the 0.22-0.1 μm fraction than in the 0.45-0.22 μm fraction. This result indicates that by changing the pore size of the filter, different *Patescibacteria* can be enriched.

The number of OTUs of *Patescibacteria* was significantly increased by size fractionation of activated sludge. A total of 388 OTUs of *Patescibacteria* were detected in all samples, but only 46 OTUs were detected in activated sludge, and about 88% of total OTUs were detected only in size-fractionated samples. About 70% of the OTUs detected in activated sludge were also detected in the size-fractionated samples. These results suggest that *Patescibacteria* can be enriched by size-fractionation of activated sludge and that there may be a greater variety of *Patescibacteria* than previously thought.

3.2 Metagenomic analysis

As a result of metagenomic analysis, we obtained 25 bins with completeness $\geq 50\%$ and contamination $\leq 10\%$, of which 24 bins were *Patescibacteria*. In addition to *Saccharimonadia*, we obtained the genomes of several other *Patescibacteria* (Table 1). We obtained multiple bins for *Paceibacteria*, *Saccharimonadia*, and ABY1 which differed at the family level. As for the completeness of Bin, 14 bins were $\geq 70\%$ ~90% and 11 bins $\geq 50\%$ ~ 70%. 21 bins were $\leq 5\%$ (4 bins of them 0%), and 4 bins were 5% ~ $\leq 10\%$. Although the completeness values varied, we were able to obtain genomes with low contamination.

The predicted genome size of *Patescibacteria* for which we were able to obtain genome information was around 1 Mbp, and some species, such as *Saccharimonadia* with 0.46 Mbp (completeness: 69.8%, contamination: 0%) and *Paceibacteria* with 0.39 Mbp (completeness: 55.3%, contamination: 0%), which may have a minimal genome size.

We obtained eighteen 16S rRNA gene sequences (*Paceibacteria*, *Saccharimonadia*, ABY1, *Gracilibacteria*, *Microgenomatia*) from 15 bins of the total of 24 bins of *Patescibacteria*. These 16S rRNA gene sequences and OTUs (by amplicon analysis) with high relative abundance within the phylogenetic group belong to *Patescibacteria* were highly identified. We obtained genomes close to the major species in the phylogenetic group belonging to *Patescibacteria* detected in the 0.45-0.22 μm fraction.

Patescibacteria, for which we could obtain genomic information, lacked genes involved in metabolic pathways such as glycolysis and were consistent with the report [5]. These characteristics suggest that they are dependent on other microorganisms for metabolic resources.

4 Conclusions

By size-fractionating the activated sludge and applying it to the analysis, it was shown that a wide variety of *Patescibacteria* existed in the activated sludge and that it was possible to obtain their genomic information. The enrichment and analysis techniques of *Patescibacteria* established in this study are expected to deepen our understanding of the contribution of *Patescibacteria* to the degradation of organic compounds and the material cycle and conversion processes in wastewater treatment.

Reference

- [1] Castelle, J.C. *et al.*, Major New Microbial Groups Expand Diversity and Alter our Understanding of the Tree of Life Cell, 172 (6) (2018) 1181-1197.
- [2] Kandaichi, T. *et al.*, Phylogenetic diversity and ecophysiology of Candidate phylum Saccharibacteria in activated sludge, FEMS Microbiology Ecology 92 (6) (2016).
- [3] Kuroda, K. *et al.*, Patterns of uncultured bacteria phyla in different wastewater treatment sludges, Journal of japan society of civil engineers G (Environment), 70 (3) (2014) 42-52 (in Japanese).
- [4] Beam, P. J. *et al.*, Ancestral absence of electron transport chains in *Patescibacteria* and DPANN, Frontiers in Microbiology (2020).
- [5] Brown, C.T. *et al.*, Unusual biology across a group comprising more than 15% of domain Bacteria, Nature 523 (2015) 208-211.

Sewage concentration for detecting public health biomarkers in wastewater

○ Luhur Akbar DEVIANTO^{1*}, Yifan ZHU¹ & Daisuke SANO^{1,2}

¹Department of Frontier Sciences for Advanced Environment, Tohoku University, Miyagi 980-8579, Japan.

²Department of Civil and Environmental Engineering, Tohoku University, Miyagi 980-8579, Japan.

*E-mail: luhur.akbar.devianto.r1@dc.tohoku.ac.jp

Abstract

Sewage, mixture of water from domestic activity and possibly run-off water, is not only containing pollutants but also including biomarkers that would be useful as public health surveillance tool. One of the potential biomarkers is human immunoglobulin A (IgA). Biomarkers from urine and fecal samples have a broad range of concentration from ng/mL to mg/mL, but those biomarkers will be diluted in the wastewater. In this research we employed 4 different methods: filtration-ultrafiltration, filtration, ammonium sulphate precipitation, and polyethylene glycol 6000 precipitation. The human IgA in concentrated samples was detected using commercial human IgA enzyme-linked immunosorbent assay (ELISA) kit and western blotting. The highest recovery of human IgA (22.7%) was achieved by filtration-ultrafiltration using 0.22 µm PVDF membrane with Amicon® Ultra 15K centrifugation filter with 100kDa molecular weight cut-off (MWCO). Also, the detection of human IgA from real wastewater was achieved by using Amicon® Ultra 15K with 30kDa MWCO that was confirmed by western blotting.

Keywords: biomarkers; ultrafiltration; IgA; precipitation; sewage concentration.

1 Introduction

Sewage contains nutrients (nitrogen and phosphorus), organic matter, and pathogens and includes biomarkers, which are biological molecules that could be found in blood, saliva, urine, and feces. Recently in wastewater-based epidemiology (WBE), we can monitor health indicators and population behavior by using biomarkers in wastewater [1]. Biomarkers in wastewater were used as a non-invasive diagnosis of respiratory diseases [2], infectious diseases [3], and other diseases analyzed from serum or blood. One of the potential biomarkers that we can detect from sewage is Immunoglobulin A (IgA). IgA has functions ranging from protection against enteric pathogens to maintaining host-commensal symbiosis. Through adsorption and agglutination to the mucosal surface, IgA prevents pathogens' penetration [4]. Furthermore, IgA also contributes to intestinal homeostasis by inhibiting virulence or promoting symbiosis among bacteria and shaping microbiota composition [5].

However, the quantification of human IgA in sewage samples is challenging. Protein biomarkers concentration varies from mg/mL to ng/mL in urine samples that possibly is diluted into hundred-fold dilution in wastewater [6]. The concentration method to improve human IgA detectability from wastewater is very important. In the previous study, the viral particle of severe acute respiratory syndrome coronavirus 2 (SARS-CoV-2) was able to be detected from stool and sewage [7]. The presence of the viral particle was confirmed by the detection of specific viral RNA sequences by qPCR. Several pretreatment methods such filtration - precipitation, centrifugation - ultrafiltration, centrifugation - precipitation in order to concentrate virus particles have been applied to improve detection [7,8]. Fortunately, similar methods were utilized for the protein purification and concentration [9]. In this research, we conduct preliminary research for the detection of potential public health biomarkers from sewage by employing various concentration methods.

2 Materials and methods

Sewage concentration was done by employing filtration, adsorption, and precipitation processes. Several configurations methods (A-D) were applied as dual-stage of filtration-ultrafiltration by using PVDF membrane with the pore size of 0.22 µm (Merck) followed with Amicon® Ultra 15K centrifugation filter and the molecular weight cut-off (MWCO) of 100kDa (Merck Millipore Ltd), filtration by PVDF membrane (0.22 µm) followed with purification by PIERCE Protein L Magnetic Beads (ThermoFisher), ammonium sulphate, ((NH₄)₂SO₄) precipitation (Kanto Chemical Co.Inc.), and polyethylene glycol (PEG 6000) precipitation (FUJIFILM Wako Pure Chemical Corp.). The best outcome of the concentration method will be used for human IgA recovery from an actual wastewater sample.

IgA concentration was initially using wastewater spiked with 30 µg of IgA (the final concentration 2 ng/mL) from human serum (Cat# I4038-5MG Sigma-Aldrich). Methods A and B began with filtrating 15 mL samples with PVDF membrane (0.22 µm). For method A, the supernatant was concentrated using Amicon® by centrifugation at 5000 x g for 30 min at 4°C in a bucket rotor. For method B, 50 µL (0.50 mg) of Pierce Protein L Magnetic Beads were washed by 150 µL Binding/washing buffer (Tris-buffered saline) in 1.5 mL microcentrifuge tube than by magnetic stand to discard the supernatant. The sample was diluted ten folds before incubation with magnetic beads for 1 hour at room temperature (RT). After the incubation, supernatant was removed, followed by 500 µL binding/wash buffer. IgA was recovered by adding 100 µL elution buffer (Pierce IgG elution buffer, pH 2) that was mixed and incubated for 10 min in RT. Neutralization was done by adding 15 µL neutralization buffer (1 M Tris, pH 8.5).

Chemical precipitation for methods C and D were done by precipitation by (NH₄)₂SO₄ and PEG 6000, respectively. A twenty-five-milliliter sample was spiked with 30 µg IgA (the final concentration 1.2 ng/mL). For method C, two-step (NH₄)₂SO₄ precipitation was done. After slow dilution of

12.5 mL 30% (NH₄)₂SO₄, incubation was done for 6 hours at 4°C. The solution free of low soluble protein was collected after centrifugation at 4000 x g for 30 min at 4°C. Further precipitation was done by adding 12.5 mL 50% (NH₄)₂SO₄ with overnight incubation. After centrifugation at 4000 x g for 30 min at 4°C, precipitated proteins were resuspended with 500 µL phosphate buffer saline (PBS). For the method D, 25 mL sample was stirred with 2 g PEG 6000 and 0.575 g NaCl and incubated for 16 hours at 4°C. The measurement of concentrated IgA in the samples was done by enzyme-linked immunosorbent assay (ELISA) using human IgA ELISA kit (Invitrogen) by following the manufacturers' instructions. Human IgA in wastewater was also detected by Western blot using iBind Flex western device according to the manufacturers' instructions (Thermo Fisher Scientific) after SDS-PAGE (BioRad) for 30 min at 180 V using Mini-PROTEAN TGX 4-20% polyacrylamide precast-gels (BioRad) and protein transfer using Trans-Blot Turbo transfer system with a 0.2 µm PVDF membrane (BioRad).

3 Results and discussion

Human IgA ranges from 10-15% of a human immunoglobulin and is abundant in serum, nasal mucus, saliva, breast milk, and intestinal fluids [10]. Human serum IgA is the second most abundant human Ig after IgG. It is the prevailing Ig in external secretion as mucosal surfaces. In human adults, IgA was estimated to be produced and selectively secreted by the gastrointestinal tract as in the small intestine and urine as up to 5,000 mg/day and 3 mg/day respectively, with a half-life 4 to 6 days [4,11].

Table 1. Concentration and recovery ratio

No	Concentration methods	Concentration (ng/mL)	Recovery Ratio (%)
1	Method A	454.3	22.7
2	Method B	226.0	11.3
3	Method C	-	-
4	Method D	56.7	2.8

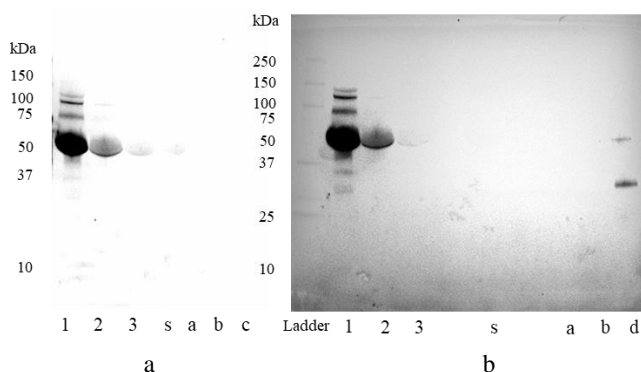


Figure 1. Western blot analysis of human IgA in sewage using Amicon® Ultra 15K: a). 100kDa MWCO; b). 30kDa MWCO.

Note: 1 = human IgA 100 µg/ml; 2 = human IgA 10 µg/ml; 3 = human IgA 1 µg/ml; s = negative control; a = raw wastewater; b = supernatant of PVDF membrane (0.22 µm) filtration; c = concentrated b sample with Amicon 100 kDa.

The concentration method is an essential step for the detection of human IgA from a wastewater sample. From various physical and chemical methods shown in Table 1,

method A gave the highest concentration recovery, 22.7%, with a concentration of 454.3 ng/mL. In contrast, the recovery method by chemical precipitation had a tiny recovery ratio of less than 3% for PEG 6000 precipitation. While, precipitation by (NH₄)₂SO₄ was under the detection limit. The further step of human IgA detection from wastewater were confirmed by western blotting. Concentrated wastewater by using Amicon® Ultra 15K 30 kDa MWCO results in detecting human IgA from wastewater as indicated in Figure 1.

4 Conclusions

In this study, concentration method which results highest recovery ratio was done by physical separation by combination of PVDF membrane 0.22 µm followed with Amicon® Ultra 15K 100kDa MWCO with recovery ratio 22.7%. The human IgA was successfully detected from real wastewater by using Amicon® Ultra 15K with 30kDa MWCO that was confirmed by western blotting.

Reference

- [1] Choi P M, Tschärke B J, Donner E, O'Brien J W, Grant S C, Kaserzon S L, Mackie R, O'Malley E, Crosbie N D, Thomas K V. and Mueller J F 2018 Wastewater-based epidemiology biomarkers: Past, present and future *TrAC - Trends Anal. Chem.* **105** 453–69
- [2] Dobler C C 2019 Biomarkers in respiratory diseases *Breathe* **15** 265–6
- [3] Jain K K 2017 Biomarkers of Infectious Diseases *The Handbook of Biomarkers* (New York, NY: Springer New York) pp 219–38
- [4] de Sousa-Pereira P and Woof J M 2019 IgA: Structure, Function, and Developability *Antibodies* **8** 57
- [5] Sterlin D, Fadlallah J, Adams O, Fieschi C, Parizot C, Dorgham K, Rajkumar A, Autaa G, El-Kafsi H, Charuel J L, Juste C, Jönsson F, Candela T, Wardemann H, Aubry A, Capito C, Brisson H, Tresallet C, Cummings R D, Larsen M, Yssel H, von Gunten S and Gorochov G 2020 Human IgA binds a diverse array of commensal bacteria *J. Exp. Med.* **217**
- [6] Rice J and Kasprzyk-Hordern B 2019 A new paradigm in public health assessment: Water fingerprinting for protein markers of public health using mass spectrometry *TrAC - Trends Anal. Chem.* **119** 115621
- [7] Foladori P, Cutrupi F, Segata N, Manara S, Pinto F, Malpei F, Bruni L and La Rosa G 2020 SARS-CoV-2 from faeces to wastewater treatment: What do we know? A review *Sci. Total Environ.* **743** 140444
- [8] Lu D, Huang Z, Luo J, Zhang X and Sha S 2020 Primary concentration – The critical step in implementing the wastewater based epidemiology for the COVID-19 pandemic: A mini-review *Sci. Total Environ.* **747** 141245
- [9] Goldring J P D 2019 Concentrating Proteins by Salt, Polyethylene Glycol, Solvent, SDS Precipitation, Three-Phase Partitioning, Dialysis, Centrifugation, Ultrafiltration, Lyophilization, Affinity Chromatography, Immunoprecipitation or Increased Temperature for Protein Isolation *Electrophoretic Separation of Proteins: Methods and Protocols* ed B T Kurien and R H Scofield (New York, NY: Springer New York) pp 41–59
- [10] Wang P 2021 Significance of IgA antibody testing for early detection of SARS-CoV-2 *J. Med. Virol.* **93** 1888–9
- [11] Mestecky J, Russell M W, Jackson S and Brown T A 1986 The human IgA system: a reassessment *Clin. Immunol. Immunopathol.* **40** 105–44

hollow fiber membrane elements, with a total membrane area of 72 m² (6 m² for each element). The hollow-fiber membrane is made of polyvinylidene fluoride (PVDF) and has a pore diameter of 0.4 μm and an outer diameter of 2.8 mm. The membrane filtration operation was 5 minutes per cycle (4 minutes for filtration, 1 minute for relaxation). The membrane maintenance method was the online back-wash applying sodium hypochlorite (NaClO) solution and citrate solution.

3 Results and discussion

Fig.2 shows the diurnal changes in COD and BOD concentrations and removal rates during the operation period.

In long-term continuous operation, the COD and BOD removal rates remained high at 85% and 90%, respectively, except for the unstable periods of 48h and 70h of HRT at an operating temperature of 25°C. In some cases, the COD removal rate was over 90%, and the BOD removal rate was over 95%.

It was found that lowering the temperature from 25°C to 20°C and then to 17°C during the stabilized operating period (HRT 8h) did not affect the anaerobic MBR or treated water quality.

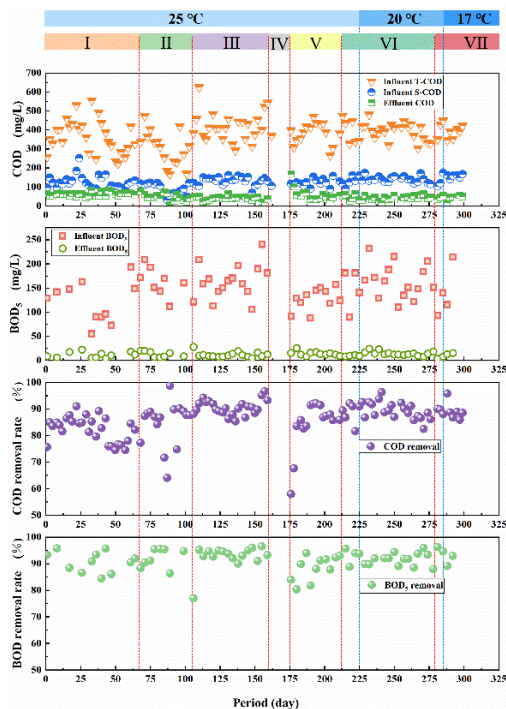


Fig. 2. Long-term performance of Pilot AnMBR.

The operation of AnMBR is divided into 7 RUNs according to the operating conditions, as shown in Table 1.

Fig.3 shows the diurnal changes in the amount and composition of biogas generated from AnMBR during the entire operating period.

The stabilized methane gas content in the whole period always reached 75%, and a high value of about 80% was also obtained. RUN I started operation at HRT 24h, and the recovery of methane gas content was slow, but in RUN II, III, VI, and VII, the recovery of methane gas content by resuming operation under the condition of HRT 12h or 8h was within one week. It was over 75%. It was found that the temperature lowering operation from 25°C to 20°C and then to 17°C had no effect on the biogas composition.

Table 1 Operating conditions for each RUN.

RUN	HRT (h)	Temperature (°C)
I	24	25°C
	48	
	70	
II	12	
	24	
III	8	
IV	-	
V	24	
	12	
VI	8	25°C
	12	20°C
VII	8	20°C
		17°C

The influence of temperature changes on the amount of biogas generated was also significantly observed from the operating results of the stabilized HRT 8h. At HRT 8h, the biogas generations at 25°C, 20°C, and 17°C were 1260.5 NL/d, 1165.1 NL/d, and 933.4 NL/d, respectively.

Biogas generation rates in stabilized AnMBR at HRT 8h were 0.084 NL/L (0.084 NL biogas generated from 1 L of raw water), 0.078 NL/L, 0.062 NL/L, respectively, from 25°C to 17°C.

The conversion rates of the removed COD to methane gas were 0.172 N L/g COD, 0.171 NL/g COD, and 0.133 NL/g COD, respectively, from 25 °C to 17 °C.

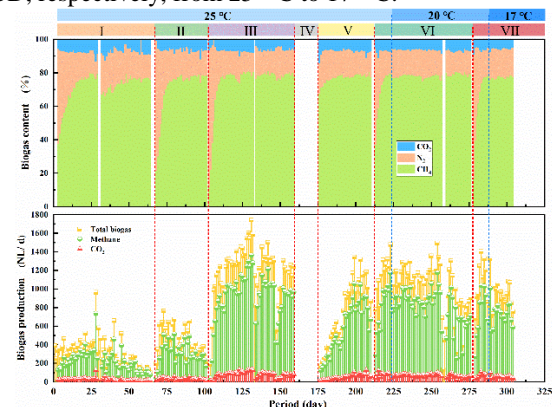


Fig. 3. Biogas production and content.

4 Conclusions

1) The performance at HRT 8h at water temperatures of 25°C, 20°C, and 17°C were stable, and the volume of raw wastewater treated was 15 m³. In addition, the COD of treated water was below 50 mg/L, the removal rate was over 89%, the BOD was below 15 mg/L, and the removal rate was over 91%.

2) The amounts of biogas generated at water temperatures of 25°C, 20°C, and 17°C were 0.084 NL/L, 0.078 NL/L, and 0.062NL/L, respectively. The methane content in the generated biogas was stable at about 78%. In the stable state of 20°C, biogas production decreased by about 8% compared to the condition of 25°C. At 17°C stable condition, biogas production decreased by 20% and 26%, respectively, compared to the 20°C and 25°C conditions.

Treating high-strength swine wastewater with AnMBR: Energy recovery efficiency and membrane fouling behaviors

○ Yu Li¹, Gaojun Wang^{1,2}, Guohao Liu¹, Rong Chen^{1,2,*}

¹Key Lab of Environmental Engineering (Shaanxi province), School of Environmental and Municipal Engineering, Xi'an University of Architecture and Technology, No.13 Yanta Road, Xi'an 710055, PR China.

²International S&T Cooperation Center for Urban Alternative Water Resources Development, Key Laboratory of Northwest Water Resource, Environment and Ecology (Ministry of Education), Xi'an University of Architecture and Technology, No.13 Yanta Road, Xi'an 710055, PR China.

Abstract

In this study, a lab-scale anaerobic membrane bioreactor (AnMBR) feeding with swine wastewater was operated over 190 days with increasing organic loading rate (OLR) gradually. The results showed that a stable COD removal rate higher than 97.0 % was achieved at high OLR of 20.5 g COD/L/d, during which the methane production rate maintained 0.23 L/L-reactor/d. Further increasing of OLR to 26 g COD/L/d declined the COD remove rate 92.1%, which resulted in a lower methane yield of 0.15 L/L-reactor/d simultaneously. What's more, the shortening of HRT aggravates membrane fouling. The filtration experiment results covered that cake layer resistance accounted for 98% of the total resistance, and the organic pollutants in cake layer were SMP and T-EPS with concentrations of 37.4 mg/gVS and 50.3 mg/gVS, respectively. Microbial community analysis uncovered that although the varied OLR altered microbial diversity, *Methanotrix*, *Methanobrevibacter* and *Methanoculleus* were always the dominant methanogens, which seemed responsible for the excellent methane yield. According, Our study confirmed that AnMBR was a promising technology for treating high-strength swine wastewater, which can not only guarantee the efficient pollution removal performance, but also achieve considerable energy recovery efficiency.

Keywords: Swine wastewater; Anaerobic membrane bioreactor; Energy recovery; Membrane fouling; Microbial community.

1 Introduction

The world's largest consumer of pork, China breeds more than 500 million pigs a year. Consequently, the industry produces a tremendous amount of swine wastewater. swine manure is a valuable soil regulator that nourishes crop production, but mismanagement and overuse can adversely affect the environment [1-2]. However, this waste also represents a valuable source for renewable energy production in the form of biogas. Biogas is produced during the anaerobic degradation of organic matter and can be used to replace fossil fuel in the production of heating/cooling, electricity, and transport fuel. In contrast to traditional biological process, the complete separation of hydraulic retention time (HRT) and solid retention time (SRT) can be achieved in AnMBR so that a high microbial activity can be maintained. However, so far, there are few studies on the treatment of swine wastewater by AnMBR.

Anaerobic digestion treatment is a complex biochemical process, and is usually affected by various environmental parameters such as types of wastewaters, chemical constituents, operational conditions, microbial activity, organic loading rate (OLR) and HRT [3]. Among these factors, HRT is a crucial parameter governing anaerobic treatment process for its significant effects on OLR, microbial diversity/activity and methane-conversion rate. Longer HRT is beneficial to the removal of pollutants whereas this causes larger reactor volume and higher capital cost. In different studies, the effect of HRT on the operational performance might vary greatly, probably resulting from the discrepancies in operational parameters, feed characteristics, biomass characteristics and reactor configuration.

Therefore, the purposes of this study were to: (i) comprehensively study the stability and long-term performance of AnMBR treatment of swine wastewater, especially pollutant removal and methane recovery; (ii) Analysis of the influence of high concentration of sludge on membrane fouling; (iii) To explore the response of microbial community under different HRT. To achieve these ends, a lab-scale AnMBR treating swine wastewater has been in operation for over 190 days. Different physicochemical parameters, including wastewater protein/polysaccharide, organic matter removal and biogas production, were investigated to evaluate the stability and long-term performance of the process. Key factors affecting membrane fouling were identified by detecting anaerobic biomass properties such as extracellular polymer content and filtration experiments. In addition, 16S rRNA gene sequencing was used to explore the evolution of microbial community structure over time.

2 Materials and methods

A lab-scale AnMBR, with an effective working volume of 2.5 L, was constructed for treating swine wastewater. The membrane module is PVDF flat membrane with an effective area of 0.0312 m² and a nominal pore size of 0.1 μm. The operational temperature was maintained at 37 ± 1°C by a thermostat water bath. Both the influent and effluent processes were controlled by rate-adjustable peristaltic pumps. All the pumps were controlled by digital timer to adjust the HRT in each stage. The pH was measured by pH meter. The COD, Polysaccharide, protein, total solids (TS) and volatile solids (VS) were measured according to the Standard Method [4]. Biogas composition was monitored by

a gas chromatography equipped with a thermal conductivity detector. Three types of EPS in anaerobic granular sludge were extracted in accordance with the heating extraction protocols. Other methods of analysis are omitted here.

3 Results and discussion

The time course of OLR, biogas composition, biogas composition, TS, VS and TMP during the long-term operation is shown in Fig. 1. With the shortening of HRT, the OLR increases gradually, and when the OLR is 20.5 ± 1.53 g-COD/L-reactor/d, the biogas production rate of AnMBR reaches 0.23 ± 0.02 L/L-reactor/d. However, when the organic load is increased to 27 g-COD/L-reactor/d, it can be seen from the figure that the biogas production decreases obviously. At this time, the effluent COD of AnMBR system also increased by nearly two times, and the COD removal rate also decreased significantly. The relevant data of effluent quality was omitted in this abstract. In the whole process, the biogas gas composition is always stable, and the methane and carbon dioxide gas composition is about 75.1% and 24.6% respectively.

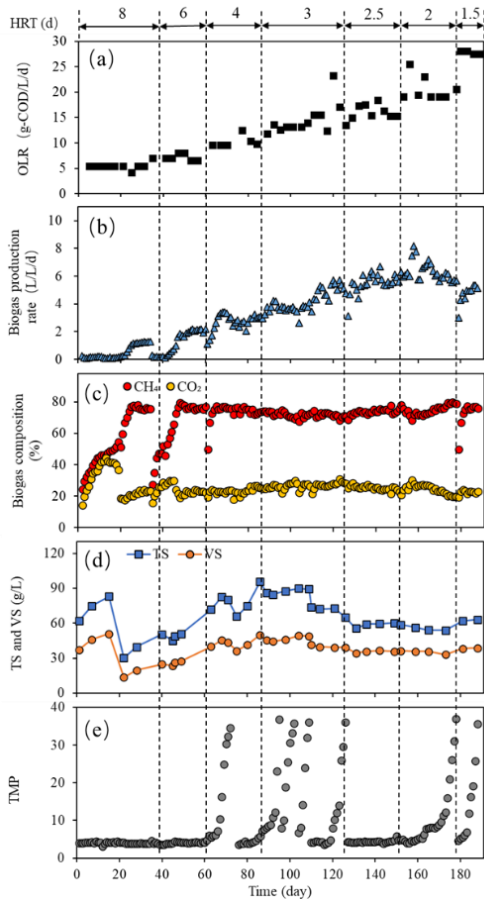


Fig. 1. Time course of OLR, biogas production rate, biogas composition, TS, VS and TMP.

On the 181th day, a methanogenic activity test with a different OLR was performed at 37 °C, and the results are shown in Fig. 2. As can be seen from the figure, with the increase of OLR, the methanogenic activity of sludge decreased significantly, which may be mainly due to excessive VFA generation inhibiting methanogenic activity. The results show that in AnMBR system, when the OLR is about 20 g-COD/L/d, the fermentation of swine wastewater is the most favorable.

As shown in Fig. 1e. The shortening of HRT significantly increases the fouling rate of membrane, so the operation performance of membrane must be improved by reducing sludge concentration and scour frequency. It is obvious from Fig. 1d. that the running time of membrane increases significantly with the decrease of sludge concentration. More membrane fouling characterization is omitted here.

To track the evolution of microorganisms within the AnMBR system, microbial community structure was analyzed by 16S rRNA high-throughput pyrosequencing during the whole process. The specific development of microbial structure with HRT shortening is omitted here.

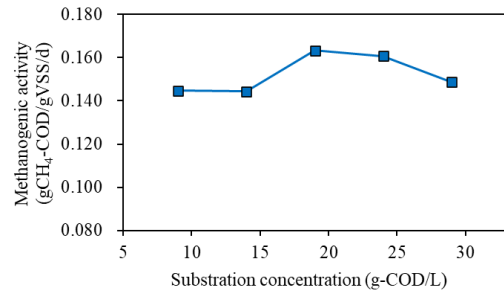


Fig. 2. Variation of methane production and methanogenic activity with substrate concentration.

4 Conclusions

This study demonstrated the great potential of AnMBR for swine wastewater treatment and methane recovery. The comprehensive results showed that under the condition of 20.05 g-COD/L/d and HRT of 2 d, the performance of AnMBR was the most stable with the average COD removal of $97.0 \pm 0.05\%$, and methane production rate was 0.23 ± 0.02 L/L-reactor/d with methane content of about 64%. In the treatment of high strength swine wastewater, the formation of cake layer is the main cause of membrane hole blockage. Cake layer formation can be effectively alleviated by reasonably increasing scouring frequency and decreasing sludge concentration. Microbial community structure showed that the suitable HRT could regulate the microbial diversity, promote the proliferation of bacteria and accelerate the biodegradation of swine wastewater;

Reference

- [1] Benyamin Khoshnevisan, Na Duan, Panagiotis Tsapekos, Mukesh Kumar Awasthi, Zhidan Liu, Ali Mohammadi, Irini Angelidaki, et al. A critical review on livestock manure biorefinery technologies: Sustainability, challenges, and future perspectives. *Renewable and Sustainable Energy Reviews* 2021;135: 1364-0321.
- [2] Mengmeng Jiang, Maria Westerholm, Wei Qiao, Simon M. Wandera, Renjie Dong. High rate anaerobic digestion of swine wastewater in an anaerobic membrane bioreactor. *Energy* 2020;193: 0360-5442.
- [3] Maaz, M., Yasin, M., Aslam, M., Kumar, G., Atabani, A.E., Idrees, M., Anjum, F., Jamil, F., Ahmad, R., Khan, A.L., Lesage, G., Heran, M., Kim, J., 2019. Anaerobic membrane bioreactors for wastewater treatment: novel configurations, fouling control and energy considerations. *Bioresour. Technol.* 283, 358–372.
- [4] APHA, 1998. *Standard Methods for the Examination of Water and Wastewater*, twentieth ed. A.P.H. Association, Washington, DC, USA.

Mitigation of membrane fouling in a thermophilic hybrid AnMBR treating food waste

○ Mengmeng JIANG¹, Min LIN¹, Wei QIAO^{1*}, Renjie DONG¹

¹College of Engineering, China Agricultural University, Beijing 100083, China

*E-mail: qiaowei@cau.edu.cn; wayqiao@sina.cn

Abstract

A hybrid anaerobic membrane bioreactor (Hy-AnMBR) was developed by incorporating polyurethane sponge carriers to mitigate membrane fouling and compared with a control AnMBR (Con-AnMBR) without carries under thermophilic condition (50±1) °C. The results showed that the TS, VS and operation time are essential parameters influencing membrane filtration. MLSS in the Hy-AnMBR was 20% lower than the Con-AnMBR, resulting in improved filtration performance. The scanning electron microscope (SEM) photograph shows the membrane pores could be observed on the Hy-AnMBR surface, which indicated that the cake layer pollution of Hy-AnMBR was less than Con-AnMBR. Adding sponge carriers mitigate 3.3%-9% pore-blocking analyzed by confocal laser scanning microscopy (CLSM).

Keywords: AnMBR; thermophilic anaerobic digestion; membrane fouling; sponge carriers.

1 Introduction

Anaerobic membrane bioreactor (AnMBR) is a promising technology that combined anaerobic digestion and membrane filtration technology, which has successfully been used to treat kinds of wastes. However, membrane fouling is one of the main obstacles to the development and application of AnMBR technology. The biomass concentration including mixed liquor suspended solids (MLSS), total solid (TS), and EPS has been concluded by some reports to harm membrane fouling in membrane bioreactors. As a result, lower sludge concentration in AnMBR is beneficial to membrane filtration performance, thus reducing membrane fouling.

Hybrid AnMBR by carrier addition can further retain microorganisms and decrease the biomass concentration in the bulk sludge, thereby improving membrane filtration performance, even improving the organic matter removal rate, which is a technology worth looking forward to. In this study, a hybrid-AnMBR (Hy-AnMBR) with polyurethane sponge carrier was investigated and compared with a control AnMBR (Con-AnMBR). Based on our latest report (Jiang et al., 2021), this study focuses on membrane fouling characteristics. The filtration performance and MLSS concentration in the bulk sludge were compared between the two systems, the fouled membrane surface and membrane pore morphology were investigated to evaluate the membrane anti-pollution performance after introducing carriers.

2 Materials and methods

The food waste used in this study was taken from a full-scale industrial project located in Jiangsu province. The food waste was produced after sorting, crushing, pulping, and solid-liquid-oil separation, then the liquid phase was collected and used. Trace elements were added with a concentration of Fe: 100 mg/L, Co: 1 mg/L and Ni: 1 mg/L before feeding. The inoculum was taken from a mesophilic sewage sludge digester and was diluted twice before use. The inoculum was kept at 50 °C before being fed with the substrate to get acclimated to the thermophilic temperature. The characteristics of food waste and inoculum were given

in Table 1, and the architecture of hybrid AnMBR was given in Fig. 1.

Table1 Characteristics of food wastewater and inoculum

Parameters	unit	Food waste (n=18)	Inoculum (n=2)
TS	g/L	80.0±4.0	62.7±0.0
VS	g/L	68.4±4.2	43.1±0.0
MLSS	g/L	41.4±7.9	56.5±0.4
MLVSS	g/L	39.1±7.6	22.9±0.1
TCOD	g/L	111.0±4.6	49.3±1.3
SCOD	g/L	63.3±7.5	10.4±1.3
NH ₄ ⁺ -N	mg/L	272±55	1034±11
VFA	mg/L	2078±109	1180±35

The hollow fiber membranes used in this study were made of polytetrafluoroethylene (PTFE) with a mean pore size of 0.1~0.2 μm and an effective filtration area of 0.1m² (Sumitomo Electric, Japan). The AnMBR system consists of a CSTR and a separated membrane chamber. Two systems were operated during this study: parallel operated during the startup period which was HRT 20 days; biofilm carrier was added in one CSTR bottom unit as the HRT was shortened to 15 days. The polyurethane biofilm carrier cube has a side length of 1 cm and a porosity of 98%. The filling volume of the biofilm carrier was around 3 L. The biogas recirculation pump has a sparging rate of 7 L/min. The filtration mode of the two AnMBR was 4 min on and 1 min off.

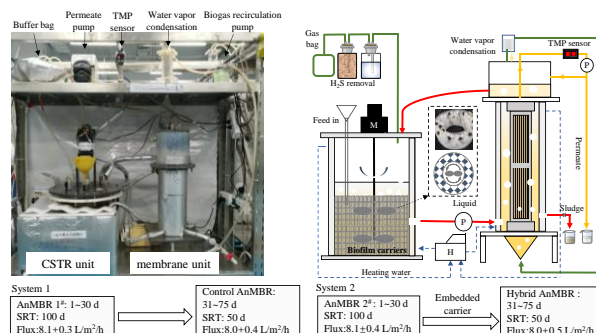


Fig. 1. Concept of the hybrid AnMBR

3 Results and discussion

Membrane filtration performance: In this study, the continuously TMP, Flux, MLSS and viscosity deviation were given in Fig. 2. The TMP and flux of both the two systems were almost the same before day 30, the MLSS and viscosity in the reactors showed not much difference. However, an increasing profile of TMP in both the Con-AnMBR and Hy-AnMBR after 30 days of operation was observed. From day 30 to day 50, the TMP of Con-AnMBR rapidly increased with a rate of 0.994 kPa/d (Fig. 2a). On the other hand, the adjustment of flux can be achieved to some extent in Hy-AnMBR but is difficult to sustain at a higher value in Con-AnMBR. The growth of TMP is relatively slow, with an increasing rate of 0.375 kPa/d (Fig. 2a). MLSS and viscosity showed a similar increasing trend after introduced carriers but were different in the two systems (Fig. 6c & d). After embedding the carriers, the MLSS in the Hy-AnMBR was 20% lower than the Con-AnMBR. In addition, the viscosity which typically used to characterize the rheological properties of sludge increased from 64 mPa·s to 96 mPa·s in AnMBR, and from 56 mPa·s to 60 mPa·s in hybrid AnMBR.

Principal component analysis was conducted among some possible factors shown in Fig. 2 (e & f). It can be concluded that in both the Con-AnMBR and Hy-AnMBR, the permeability showed a negative correlation with permeability, but the TS, VS and operation time are essential parameters that influence the membrane filtration.

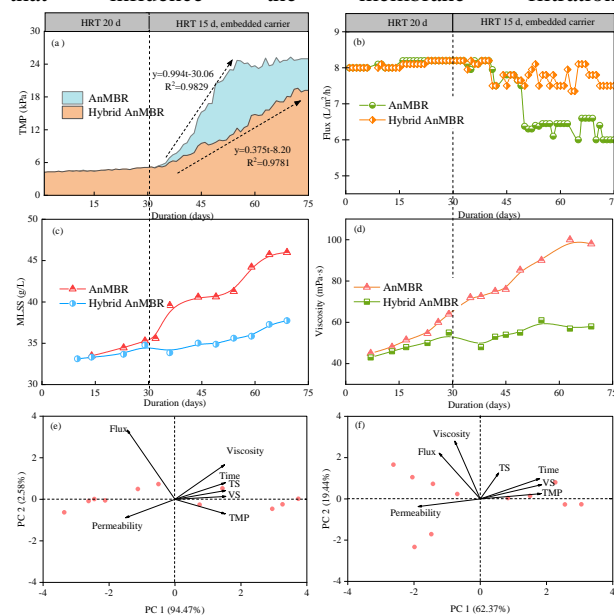


Fig. 2. Membrane filtration performance of the two systems

The SEM images and physical appearance of the membranes after fouling and cleaning are shown in Fig. 3. It can be seen from the photograph of the membrane surface that with upward hydraulic shear, the filamentous materials were entangled with the membrane fibers, especially in the Con-AnMBR. Observed by the SEM photograph, the fouled Con-AnMBR membrane surface was also covered with an obvious cake layer, the membrane pores were severely blocked and not visible after fouling, which increase filtration resistance and may be one of the main reasons for the reduction of membrane filtration performance. On the membrane surface of Hy-AnMBR, although there are some pollutants on the surface, the membrane pores were still clear.

Food waste is a substance with high protein and polysaccharide content belonging to biomacromolecules. Even if they are well decomposed in a high-solid AnMBR system, part of them may inevitably remain in the mixed liquid. The organic biomacromolecules block the membrane pores or form the cake layer and gel layer during long-term membrane filtration, leading to irreversible fouling.

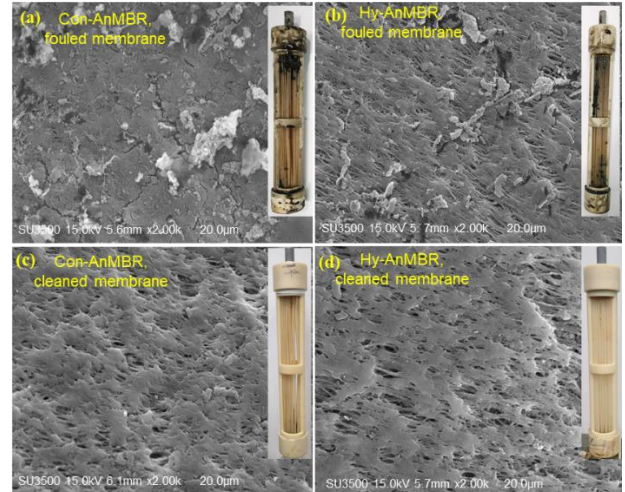


Fig.3 SEM images and physical appearance of the membrane module after fouling and cleaning

The dyeing area of protein, α -polysaccharide and β -polysaccharide through confocal laser scanning microscopy (CLSM) analysis are concluded in Table 2. The staining area of Hy-AnMBR is smaller than that of Con-AnMBR. Among them, the stained areas of protein, α -polysaccharide and β -polysaccharide accounted for (59.1±10.1) %, (47.9±4.3) % and (60.3±7.0) % of the total area respectively, which is 3.3%, 9% and 6.6% lower than that in Con-AnMBR, respectively. The main pollutants of Hy-AnMBR membrane pores are protein and β -polysaccharide.

Table 2 Ratio of dyeing area to sample area of CLSM fluorescent staining results

	Percentage of clogging surface of membrane (%)		
	Protein	α -polysaccharides	β -polysaccharides
Control AnMBR	62.4±10.4	56.9±7.5	66.9±2.9
Hybrid AnMBR	59.1±10.1	47.9±4.3	60.3±7.0

4 Conclusions

The Hy-AnMBR through adding biofilm carriers can effectively mitigate and delay the formation of membrane fouling by decreasing sludge concentration in the reactor. The cake formation and pore-blocking were therefore largely alleviated. The affecting factors identified by PCA analysis proved the advantages of the hybrid AnMBR for alleviating membrane fouling formation.

5 Acknowledgement

This work was partially supported by National Science Foundation of China (51778616).

Reference

[1] M. Jiang, Z. Wu, J. Yao, S.M. Wandera, D.E. Algapani, R. Dong, W. Qiao. Enhancing the performance of thermophilic anaerobic digestion of food waste by introducing a hybrid anaerobic membrane bioreactor, *Bioresource Technology*, 341 (2021) 125861.

Elucidating fouling characterization in a high solid anaerobic membrane bioreactor treating OFMSW leachate

○Zhiyue WU¹, Junqiang YAO¹, Wei QIAO^{1*}, Renjie DONG¹

¹ College of Engineering, China Agricultural University, 17 Qing hua East Road, Beijing 100083, China.

*E-mail: qiaowei@cau.edu.cn; wayqiao@sina.cn.

Abstract

Long-term scaling formation in a high solid anaerobic membrane bioreactor (AnMBR) has been a major challenge in treating the leachate from the municipal solid waste (MSW). In this study, the role of inorganic precipitation were evaluated. The chemical analysis exhibited that the mass balance and distribution of inorganic caions in the system, and inorganic mineral were identified by the XRD. Considerable results showed that calcite was the dominant inorganic precipitation, besides, the content of inorganic ash is more than 70% in bulk sludge, and it was higher on membrane surface. Moreover, around 17.4 mg Ca/cm², 1.3 mg-P/cm² and 0.4 mg-Mg/cm² were detected residual on the membrane surface. It is reasonable to assume that inorganic particles based on calcium carbonate scour the membrane surface and form a hard skeleton layer. Membrane permeability could be easily recovery with chemical cleaning, especially, and the precipitation layer retained until after 2% citric acid cleaning.

Keywords: Anaerobic membrane bioreactor, inorganic precipitation, OFMSW leachate, high solid, membrane scaling.

1 Introduction

The amount of municipal solid waste (MSW) in China has increased rapidly in the past three decades due to urban expansion. And more than 55% of MSW has been incinerate in big cities, before burying, 0.1-0.3 ton leachate per ton waste was produced during the storage period^[1]. Usually, in a combination of physical, chemical and biological methods, used to treat MSW leachate, anaerobic digester treatment has been demonstrated to be the most useful technology. However, the biggest challenges for AD process is low efficiency due to the loss of slow-growing methane microorganisms. Anaerobic membrane bioreactors (AnMBR) as a novel and efficient biotechnology can effectively retain key microorganisms inside the reactor by direct membrane rejection.

In fact, the effect of the presence of inorganic ions in the feed on the AnMBR system is very complex. Admittedly, inorganic elements are necessary for the growth of methanogens^[2], however, high concentration of inorganic ions in influent results in some problems, like membrane scaling. To date, most of the previous studies focused on membrane fouling due to organic matter. In this study, we investigated the fouling characterization in a high solid anaerobic membrane bioreactor treating OFMSW leachate.

2 Materials and methods

Briefly, a flat sheet membrane (Kubota, Japan) with the total area of 0.116 m² and an average pore size of 0.2 μm was immersed in the bioreactor, and operated at 37± 1°C, which running at a constant average flux of 6 L/MH. During the operation, trans-membrane pressure (TMP) was monitored with a pressure sensor and tracked TMP trend by a online recorder, as shown in Fig. 1. As the influent, the leachate of OFMSW contained: total chemical oxygen demand (TCOD) 57±4 g/L, ammonium nitrogen (NH₄⁺-N)

860±120 mg/L, calcium (Ca) 2350±540 mg/L, magnesium (Mg) 708±304 mg/L and total phosphorus (TP) 94±5 mg/L.

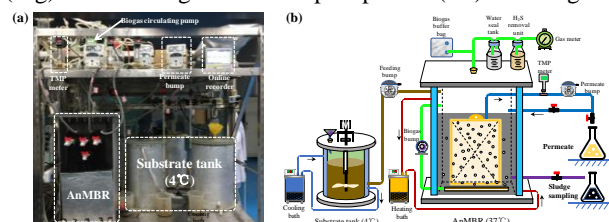


Fig. 1. Photograph(a) and schematic diagram(b) of the AnMBR.

The calcium and magnesium concentration were measured by an Atomic Absorption Spectrophotometer after acidizing treatment. A Loss on Ignition test is performed to determine the inorganic content of foulant on loose cake layer and precipitation layer.

Carry out a cleaning mode to analyze the membrane resistance distribution and the characteristics of pollutants. As the following three core steps: (1) Gas washing; (2) NaClO cleaning; (3) Citric acid cleaning.

3 Results and discussion

In the high-solid AnMBR, the membrane operation performance at continuous flux of 6 LMH was evaluated, and the results were shown in Fig 2. Variation curves of instantaneous Max-TMP and Min-TMP were obtained shown in Fig. 2a. After 61 days running, Max-TMP was remained at a low level and increased by only 1.1kpa, when Min-TMP did not show an increasing trend. Reversible fouling caused by cake layer and resulted in the Max-TMP increased gradually, and the stability of Min-TMP reveals that irreversible fouling was not obvious.

Permeability was calculated as a ratio of the average flux and TMP in order to evaluate changes in membrane filtration performance. It was observed that membrane

permeability was gradually decline by 2.7% within 44 days, while the TS in bulk sludge was increased from 3% to 5%.

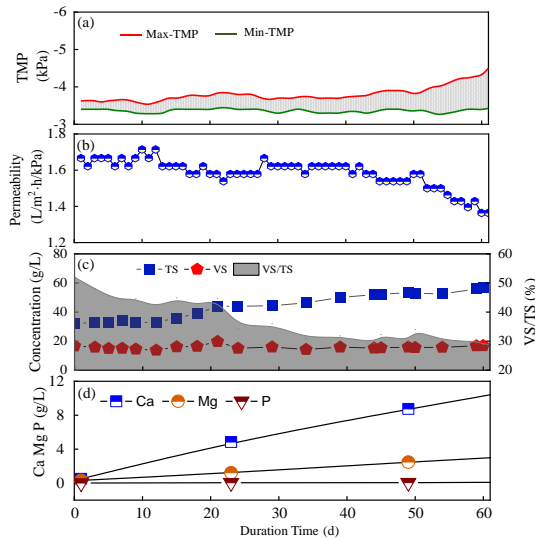


Fig. 2. Evolution of the membrane performance during the operation time with different concentration of TS and inorganic ions.

Additionally, a submerged membrane permeability was decreased significantly with an increase TS, especially after more than 4%. A similar result was shown until after 44 days with a 15.5% reduction. It was suggested that a better membrane filtration performance was obtained in a TS below 5%. The AnMBR rejected calcium, phosphorus and magnesium reach to 94.4±5.3%, 84.5±7.8% and 73.1±6.8%, respectively. And about 63%, 61%, 46% were rejected in the reactor, when the 4%, 23%, 11% embedded in permeate, and 33%, 16%, 43% discharge with sludge, respectively.

Table 1 The concentration of Ca, Mg and TP in feed, bulk sludge and permeate.

Parameter	Item	1st day	23th day	49th day	61st day
Ca (mg/L)	Feed	2050	1620	2942	2450
	Permeate	189	65	114	59
	Bulk sludge	834	3056	8878	11892
Mg (mg/L)	Feed	689	810	1010	797
	Permeate	331	259	177	246
	Bulk sludge	110	210	651	1180
TP (mg/L)	Feed	58	91.6	93	87
	Permeate	10	5	6.6	18
	Bulk sludge	490	856	923	521

Based on the XRD analysis, calcite was the dominant inorganic precipitation, and a complex precipitate containing calcium and phosphorus was found by analyzing a software, and its molecular formula was $\text{Ca}_{15}(\text{PO}_4)_2(\text{SiO}_4)_6$, merely it was a small amount.

Fig.3 shows the concentrations distribution of the inorganic elements on membrane detected in the solution of water cleaning, NaClO cleaning and citric acid cleaning. There are no obvious P and Mg characteristic peaks in the cake layer, but they are obtained 1.3 mg-P/cm² and 0.4 mg-Mg/cm² remain on surface of membrane by chemical analysis.

The results from LOI (Table 2) shown that the loose cake layer on the membrane surface consisted of 23.9%~26.7%

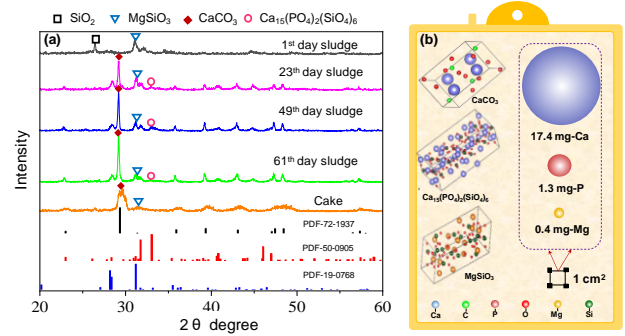


Fig. 3 XRD analysis and Ca, P, Mg distribution on membrane.

organic matter and 73.3%~76.1% inorganic matter, and about 6% organic foulant was detained in precipitation layer. As the inorganic foulants accumulated on the membrane surface with flux decline, inorganic-organic interaction became stronger.

Table 2 LOI result for foulant from the loose cake layer and precipitation layer.

Item	Loose cake layer			Precipitation layer		
	Top	Middle	Bottom	Top	Middle	Bottom
Loss on Ignition/%	26.7	25.1	23.9	6.2	6.1	5.9
Organic Content/%	26.7	25.1	23.9	6.2	6.1	5.9
Inorganic Content/%	73.3	74.9	76.1	93.8	93.9	94.1

4 Conclusions

This study focuses on the fouling characterization of leachate with high calcium concentration in HS-AnMBR system. The results show that AnMBR was a practicable technology for the treatment of OFMSW leachate rich in calcium. A significant accumulation of inorganic precipitation at high alkalinity was observed due to the accumulation of calcium carbonate precipitation. During the operation, membrane fouling may not be a challenge since it can work long-term before cleaning due to the calcite precipitate layer with a hard skeleton on the membrane surface. Moreover, phosphorus was partially anaerobically removed in AnMBR benefit by the precipitation.

5 Acknowledgement

This work was partially supported by National Science Foundation of China (51778616).

Reference

- [1] Zhou L, Zhuang WQ, Ye B, et al. Inorganic characteristics of cake layer in A/O MBR for anaerobically digested leachate from municipal solid waste incineration plant with MAP pretreatment. *Chem Eng J.* 2017;327:71-78.
- [2] Tian L, Chen XD, Yang QP, Chen JC, Shi L, Li Q. Effect of calcium ions on the evolution of biofouling by *Bacillus subtilis* in plate heat exchangers simulating the heat pump system used with treated sewage in the 2008 Olympic Village. *Colloids Surfaces B Biointerfaces.* 2012;94:309-316.

Effective enrichment of anammox granules for high-loading landfill leachate treatment: Research progress

○ Jinghuan LUO* & Jianyong LIU

School of Environmental and Chemical Engineering, Shanghai University, 333 Nanchen Road, Shanghai 200444, China.

*E-mail: jhuanluo@shu.edu.cn.

Abstract

Anammox is an autotrophic nitrogen removal process and sludge granulation has been an effective approach to achieve abundant slow-growing anammox bacteria in the reactor, while the floatation and wash-out of anammox granules was usually occurred in particular at high loading rates. Our research demonstrates that anammox granules could be effectively enriched with hydroxyapatite (HAP), granular activated carbon (GAC) or calcium carbonate (CaCO₃) as the inner core, thus achieving a satisfactory biomass retention. Anammox granules could be also quickly cultured from anaerobic digestion (AD) granules by the layered inoculation. The mature anammox granules were then successfully employed to treat landfill leachate for advanced nitrogen removal.

Keywords: anammox; granulation; biomass retention; landfill leachate; nitrogen removal.

1 Introduction

Compared with conventional nitrification-denitrification process, anammox requires no external organics and much less aeration demand, and also largely reduces waste sludge production and carbon dioxide emission [1]. As an environmentally-friendly technique, it has been drawing much attention worldwide to treat ammonium-rich wastewaters [1]. Nonetheless, there are also some limitations in anammox operation, one of which is the slow growing rate (e.g., 0.21 d⁻¹) and the low biomass yield (e.g., 0.071 mol C/mol NH₄⁺) [2] for anammox bacteria with a doubling times reported at 4~15 days [3]. In order to achieve abundant anammox bacteria, sludge granulation has been demonstrated as one of the most effective approaches [1]. However, the granules floatation and wash-out from anammox reactors has been a notorious issue in particular at high loading rates [4], which easily causes sludge loss and process deterioration.

To ensure an efficient biomass retention for the slow-growing anammox bacteria, our research was dedicated to enriching anammox granules with HAP, GAC or CaCO₃ as the inner core and culturing anammox granules from AD granules. The mature anammox granules were then employed to treat landfill leachate for advanced nitrogen removal.

2 Results and discussion

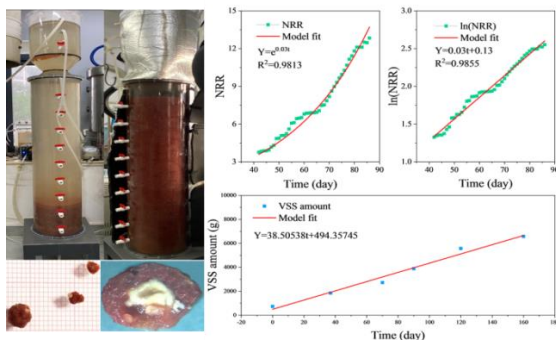


Fig. 1. Effective enrichment of anammox-HAP granules.

Under a high NLR and an efficient mass transfer, anammox-HAP granules were successfully enriched with a cell yield of 0.23 g VSS/g NH₄⁺-N. The biomass was increased from 732 g to 6,577 g and anammox bacteria jumped from 18.6% to 82.8% after 140 days of operation.

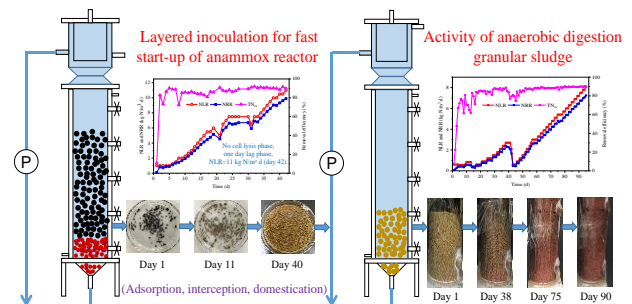
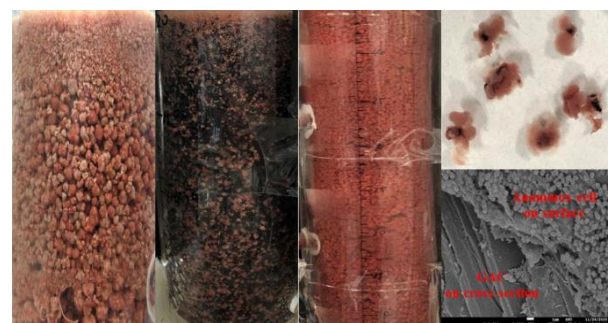


Fig. 2. Anammox granules cultured from AD granules by layered inoculation.

Anammox granules were cultured from AD granules by their layered inoculation in R1 reactor with both cell lysis phase and lag phase being shortened. The maximum NLR and NRR were 11 kg N/m³/d and 9.9 kg N/m³/d on day 42, respectively. The domesticated AD granules on the upper layer were later transferred to R2 reactor to investigate their anammox activity. AD granules in R1 did perform anammox activity and could be cultured into anammox granules. Adsorption, interception and domestication all contributed to anammox biomass in AD sludge bed in R1, thus accelerating the start-up of the reactor.



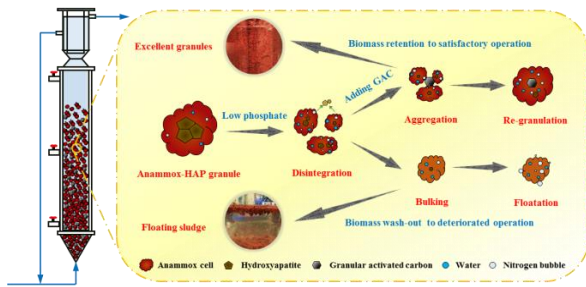


Fig. 3. GAC promoting re-granulation of anammox-HAP granules at low phosphate concentration.

A reactor inoculated with mature anammox-HAP granules and fed with low phosphate (5 mg P/L) was added with GAC to maintain sludge granulation and nitrogen-removing stability. At influent total nitrogen >800 mg/L and NLR ~9.8 kg/m³/d, a satisfactory nitrogen removal of around 88% was maintained during 140 days of operation. Insufficient phosphate supplement resulted in a sludge bulking, with suspended solid and sludge density decreased whereas sludge water content and expansion ratio increased due to HAP loss. Nevertheless, the sludge re-granulation was found at the later stage as the proportion of granules in 2.8~3.35 mm went up to 37.4% after large granules disintegrated into small pieces at the initial stage. The settling velocity was finally ranging from 129.8 to 182.2 m/h. In addition, *Candidatus Brocadia* was increased from 2.1% to 20.1% and dominated in the microbial community. These findings suggest GAC was able to promote re-granulation of anammox-HAP granules at low phosphate concentration, which avoids sludge flotation and widens their application as an inoculum.

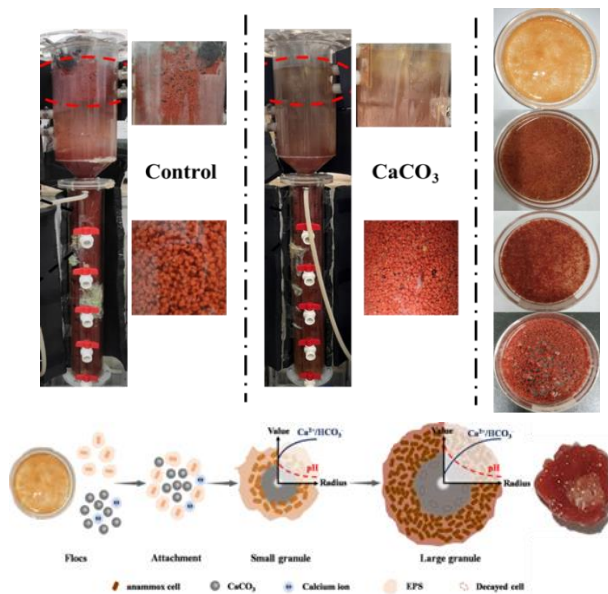


Fig. 4. Effective enrichment of anammox-CaCO₃ granules.

Anammox-CaCO₃ granules were successfully enriched with an anammox abundance above 80%. Compared to severe sludge flotation and wash-out of anammox granules in the control reactor, anammox-CaCO₃ granules were well settled even under a high NLR up to 36 kg N/m³/d. A satisfactory biomass retention was thus achieved.

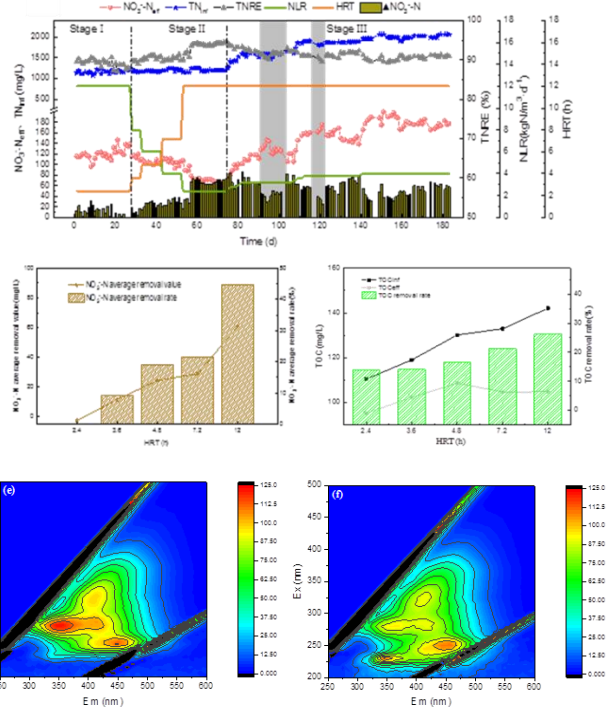


Fig. 5. Anammox granules for advanced nitrogen removal from landfill leachate.

A stable advanced nitrogen removal from mature landfill leachate was achieved by anammox granules with refractory organics used to further reduce anammox by-product nitrate. Soluble microbial products, polycarboxylic acid and fulvic acid were found to be removed, and the unsaturated functional groups such as carboxyl, hydroxyl and carbonyl on aromatic compounds were transformed into aliphatic ones. In addition to anammox bacteria, microbial groups to degrade macromolecules and refractory organics were also detected in anammox granules.

3 Conclusions

Anammox granules were effectively enriched with HAP, GAC or CaCO₃ as the inner core, thus avoiding sludge flotation or wash-out and achieving satisfactory biomass retention. Anammox granules could be also cultured from AD granules by the layered inoculation strategy. The mature anammox granules were successfully employed to treat landfill leachate for advanced nitrogen removal.

References

- [1] Lackner et al. Full-scale partial nitritation/anammox experiences - An application survey. *Water Research* 2014; 55: 292-303.
- [2] Lotti et al. Physiological and kinetic characterization of a suspended cell anammox culture. *Water Research* 2014; 60: 1-14.
- [3] van der Star et al. The membrane bioreactor: A novel tool to grow anammox bacteria as free cells. *Biotechnology and Bioengineering* 2008; 101: 286-294.
- [4] Chen et al. Flotation of flocculent and granular sludge in a high-loaded anammox reactor. *Bioresource Technology* 2014; 169: 409-415.

of nutrient solution and 1 g of biochar were added into the serum bottles, and 50 ml of deionized water was added to obtain a working volume of 100 ml. There were three groups in total and two parallel replicates in each group. Each of the three groups had nutrient solutions consisting of: 0.47 g/L (NH₄)₂SO₄, 0.49 g/L NaNO₂, and 1.44 g/L KNO₃.

The seed sludge used in this study was collected from a stable operating UASB anammox reactor in the laboratory. Batch tests were performed in serum bottles with working volumes of 100 mL. Biochar 1 g, seed sludge 25 mL, and nutrient solution 50 mL were added into serum bottles and then deionized water (25 mL) was added to obtain a 100 mL working volume. All batch tests were performed in a thermostatic shaker with the shaking speed and temperature controlled at 120 rpm and 35°C, respectively.

3 Results and discussion

3.1 Effects of biochar on nitrogen removal

Batch adsorption experiments were conducted to assess the overall aqueous NH₄⁺, NO₂⁻, and NO₃⁻ sorption ability of biochar. As illustrated in Figure 1(a), the biochar rapidly adsorbed NH₄⁺ for the first 4 h. However, the biochar did not adsorb NO₂⁻ and NO₃⁻, which may have been related to the negative charge on the biochar surface, which can only be associated with cation exchange in the adsorption solution^[16,17]. Quasi-first-order and quasi-second-order dynamics equations were used to fit the experimental data and the results are shown in Figure 1(b). The quasi-second-order kinetic equation better described the adsorption process of NH₄⁺ by biochar.

Although biochar has a certain capacity to adsorb NH₄⁺, biological nitrogen removal still dominated the overall nitrogen removal of the reaction. As shown in Figure 1(d), when the substrate was ammonium and nitrite (Group A), the total nitrogen removal rate of the BC was 97.4% over 45 hours, while that of the control was only 87.3%. Furthermore, during the reaction, the cumulative N₂ production of the BC was higher than that of the control group [Fig. 1(c)]. It can be seen from the change in the three nitrogen contents at the end of the reaction that nitrate was the main reason that the nitrogen removal efficiency was significantly different between the biochar group and control group. The nitrate concentration of the biochar group was much lower than that of the control group. Therefore, it was concluded that biochar improved the efficiency of anammox nitrogen removal and dinitrogen production by promoting the degradation of nitrate. Furthermore, the N₂O released by the denitrification reaction was detected during the reaction. As shown in Figure 1(c), at the initial stage of the reaction, the N₂O concentration of the biochar group was higher than that of the control group. The BC had a 95% reduction in N₂O within 12 h, while the N₂O in the CT only decreased by 73%, indicating that the biochar group had higher N₂O production and degradation capabilities. Therefore, the addition of biochar promoted the denitrification process, and also improved the activity of N₂O reductase, thus reducing the risk of N₂O spillover.

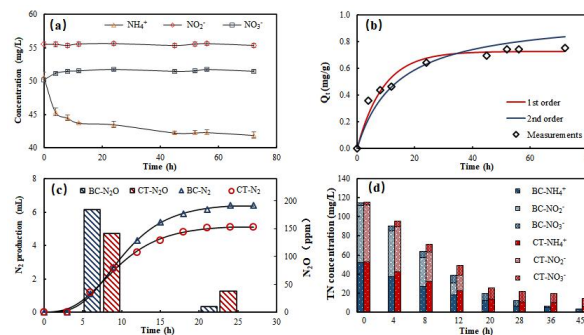


Figure 1. (a) Adsorption of NH₄⁺, NO₂⁻, and NO₃⁻ by biochar; (b) adsorption kinetics of NH₄⁺ by biochar; (c) change in N₂ and N₂O during the reaction; and (d) change in total nitrogen during the reaction in Group A.

3.2 Effect of biochar on electron transport system

The results showed that [Fig. 2(c)], during the stage of rapid ammonium decline (stage 1), electron transfer in BC reached 0.89 mmole·L⁻¹, nearly 3 times that of CT, and the electrons were mainly utilized for denitrification. In the second stage, due to the lack of suitable substrates, the reaction rates of denitrification and partial denitrification gradually declined and the quantity of electrons consumed also decreased. From the third stage, the nitrite substrate was depleted and the remaining nitrate was partially reduced. The amount of electrons consumed for partial denitrification in BC reached 0.23 mmole·L⁻¹, twice that of CT. Denitrification consumes almost no electrons, which was evident in the above results, suggesting that when the nitrite supply was limited, the anammox reaction outcompeted the denitrification reaction for nitrite. At the end of the reaction, the total electron transfer in BC was 1.56 mmole·L⁻¹, twice as much as that of CT. In the first two stages, the electron consumption by denitrification NO₂⁻→N₂ accounted for 85% of the total electron consumption, while in the latter two stages partial denitrification (NO₃⁻→NO₂⁻) accounted for 94% of the total electron consumption. This corresponded to the reaction rates of denitrification and partial denitrification shown in Figure 2(a). In conclusion, the addition of biochar affected the reduction rate of nitrate and nitrite by altering electron transfer. During the reaction period, INT initially exhibited an increasing trend, and then decreasing [Fig. 2(b)], which was mainly related to the change in substrate availability. In addition, the INT value of BC was always higher than the control, indicating that the addition of biochar improved the electron transport efficiency of the system, which may explain the rapid decrease in nitrate in BC.

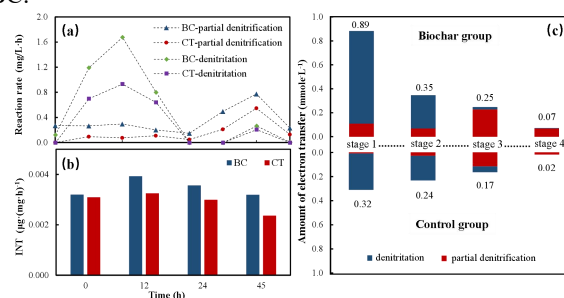


Figure 2. (a) Reaction rates of partial denitrification and denitrification in the biochar and control groups; (b) changes in electron transfer activity (INT) at different stages in the biochar and control groups; and (c) the

amounts of electrons consumed by denitrification and partial denitrification during the reaction in the biochar and control groups.

3.3 Impact of electrochemical properties of biochar on electron transfer

The EDC and EAC of biochar were 2.64 and 0.79 mmole·g⁻¹, respectively, indicating that biochar was a redox mediator that tended to supply electrons [Fig. 3(a)]. FTIR analysis was carried out to characterize the functional sites of the biochar. As shown in Figure 3(b), sawdust biochar pyrolyzed at 300°C contains a large number of oxygen-containing functional groups, among which electron-donating groups (C-O) account for a relatively large amount. These results indicated that the presence of reducing groups in biochar prepared at 300°C provides plenty of electron sources for the reduction of nitrite and nitrate. Among them, phenolic hydroxyl (-OH) and ether (C-O-C) were the strong and weak electron-donating groups, respectively, which were the main electron-donating functional groups that were the source of the reducing ability of biochar^[18, 19].

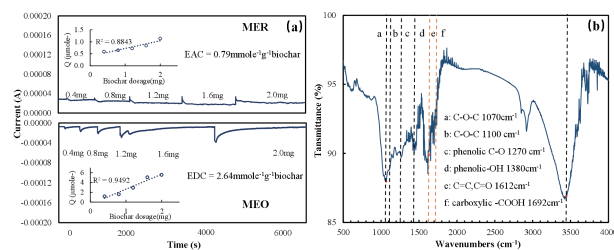


Figure 3. (a) The slopes of the linear regressions of current versus biochar dosage correspond to the electron accepting capacity (EAC) and electron donating capacity (EDC). (b) FTIR spectrum of biochar.

4 Conclusions

This study demonstrated that as an additive, the oxygen-containing functional groups on the surface of biochar have higher electron donating ability. During the reaction, biochar acts as an electron pool, continuously providing electrons for the reduction of nitrate. The reduction of nitrate is accompanied by the progress of the entire reaction. Under the action of denitrification, it is synchronized with the anammox reaction to achieve nitrogen removal. In the case of insufficient nitrite in the system and restricted anammox reaction, priority is given to providing secondary nitrite for the anammox reaction, so that the nitrogen removal efficiency of the system is significantly improved.

Reference

[1] Wang, X., et al., Characteristics and mechanism of anammox granular sludge with different granule size in high load and low rising velocity sewage treatment. *Bioresour Technol*, 2020. 312: p. 123608.
 [2] Zhang, J., et al., Start-up and bacterial communities of single-stage nitrogen removal using anammox and partial nitrification (SNAP) for treatment of high strength ammonia wastewater. *Bioresour Technol*, 2014. 169: p. 652-657.
 [3] an der Star, W.R., et al., Startup of reactors for anoxic ammonium oxidation: experiences from the first full-scale

anammox reactor in Rotterdam. *Water Res*, 2007. 41(18): p. 4149-63.

[4] Wang, T., et al., Efficient nitrogen removal in separate coupled-system of anammox and sulfur autotrophic denitrification with a nitrification side-branch under substrate fluctuation. *Sci Total Environ*, 2019. 696: p. 133929.

[5] Lackner, S., et al., Full-scale partial nitrification/anammox experiences--an application survey. *Water Res*, 2014. 55: p. 292-303.

[6] Winkler, M.K., et al., Segregation of biomass in cyclic anaerobic/aerobic granular sludge allows the enrichment of anaerobic ammonium oxidizing bacteria at low temperatures. *Environ Sci Technol*, 2011. 45(17): p. 7330-7.

[7] Zheng, Z., et al., Enhanced nitrogen removal of the simultaneous partial nitrification, anammox and denitrification (SNAD) biofilm reactor for treating mainstream wastewater under low dissolved oxygen (DO) concentration. *Bioresour Technol*, 2019. 283: p. 213-220.

[8] Wang, D., et al., Roles and correlations of functional bacteria and genes in the start-up of simultaneous anammox and denitrification system for enhanced nitrogen removal. *Sci Total Environ*, 2019. 655: p. 1355-1363.

[9] Wu, Z., et al., Highly efficient nitrate removal in a heterotrophic denitrification system amended with redox-active biochar: A molecular and electrochemical mechanism. *Bioresour Technol*, 2019. 275: p. 297-306.

[10] Zhang, M., et al., Evaluating biochar and its modifications for the removal of ammonium, nitrate, and phosphate in water. *Water Res*, 2020. 186: p. 116303.

[11] Sathishkumar, K., Y. Li, and E. Sanganyado, Electrochemical behavior of biochar and its effects on microbial nitrate reduction: Role of extracellular polymeric substances in extracellular electron transfer. *Chemical Engineering Journal*, 2020. 395.

[12] Kappler, A., et al., Biochar as an Electron Shuttle between Bacteria and Fe(III) Minerals. *Environmental Science & Technology Letters*, 2014. 1(8): p. 339-344.

[13] Oh, S.Y., et al., Microbial reduction of nitrate in the presence of zero-valent iron and biochar. *Bioresour Technol*, 2016. 200: p. 891-6.

[14] Ye, S., et al., The effects of activated biochar addition on remediation efficiency of co-composting with contaminated wetland soil. *Resources, Conservation and Recycling*, 2019. 140: p. 278-285.

[15] Saquing, J.M., Y.-H. Yu, and P.C. Chiu, Wood-Derived Black Carbon (Biochar) as a Microbial Electron Donor and Acceptor. *Environmental Science & Technology Letters*, 2016. 3(2): p. 62-66.

[16] Tan, Z., et al., Mechanism of negative surface charge formation on biochar and its effect on the fixation of soil Cd. *J Hazard Mater*, 2020. 384: p. 121370.

[17] Yao, Y., et al., Effect of biochar amendment on sorption and leaching of nitrate, ammonium, and phosphate in a sandy soil. *Chemosphere*, 2012. 89(11): p. 1467-71.

[18] Li, S., et al., Quantifying the contributions of surface area and redox-active moieties to electron exchange capacities of biochar. *J Hazard Mater*, 2020. 394: p. 122541.

[19] Wu, S., et al., Redox-Active Oxygen-Containing Functional Groups in Activated Carbon Facilitate Microbial Reduction of Ferrihydrite. *Environ Sci Technol*, 2017. 51(17): p. 9709-9717.

Enhancing phosphorus recovery from sewage sludge using anaerobic-based processes: Current status and perspectives

Bohan Yu ^a, Xiangmin Xiao ^b, Jianwei Wang ^b, Meng Hong ^b, Chao Deng ^b, Yu-You Li ^c, Jianyong Liu ^{a,*}

^a School of Environmental and Chemical Engineering, Shanghai University, 333 Nanchen Road, Shanghai 200444, China

^b Cangzhou Water Supply and Drainage Group Company Limited, 15 West Jiuhe Road, Cangzhou, Hebei Province 061001, China

^c Department of Civil and Environmental Engineering, Graduate School of Engineering, Tohoku University, 6-6-06 Aza, Aramaki, Aoba-ku, Sendai, Miyagi 980-8579, Japan

Email: liujianyong@shu.edu.cn

Abstract

Anaerobic-based processes are green and sustainable technologies for phosphorus (P) recovery from sewage sludges economically and are promising in practical application. However, the P release efficiency is always not satisfied. In this paper, the P release mechanisms (regarding to different P species) from sewage sludge using anaerobic-based processes are systematically summarized. The obstacles of P release and the updated achievements of enhancing P release from sewage sludges are analyzed and discussed. It can be concluded that different P species can release from sewage sludge via different anaerobic-based processes. Extracellular polymeric substances and excessive metal ions are the two main limiting factors to P release. Acid fermentation and anaerobic fermentation with sulfate reduction could be two promising ways, with P release efficiencies of up to 64% and 63%. Based on the summarization and discussion, perspectives on practical application of P recovery from sewage sludge using anaerobic-based processes are proposed.

Keywords: phosphorus recovery; sewage sludge; anaerobic-based process; acid fermentation; sulfate reduction.

1 Introduction

Phosphorus (P), a necessary and irreplaceable resource for global food production, which is geographically concentrated and nonrenewable, is going to be depleted in 100-200 years. As well known, anaerobic fermentation (AF) is a traditional and widely used technology for sewage sludge treatment economically, with carbon source or bioenergy recovery and sludge amount reduction. Meanwhile, anaerobic microorganisms play a crucial role in P release from natural media, e.g., soil and sediment. Thus, using anaerobic-based processes to recover P from sewage sludge is highly feasible.

However, the release efficiency of P is not satisfied, which is an obstacle to practical application. The problems are summarized. First of all, extracellular polymeric substances (EPSs) and cell structures in waste activated sludge (WAS) reduce the mass transfer efficiency and thus organic P (OP) release is limited. Secondly, several limiting factors that influence release of inorganic P (IP) are found, including excessive metal ions in sewage sludge, solubility difference and aging process of IP species. Thirdly, high P concentration in sludge is a common obstacle to all P species release.

In this review article, the P release mechanisms (regarding to different P species) from sewage sludge using anaerobic-based processes are systematically summarized. The obstacles of improving P release efficiency from sewage sludge using anaerobic-based processes are analyzed with solutions proposed. The state-of-the-art

achievements of enhancing P release from sewage sludge are discussed and compared. Based on the above summarization and discussion, two items of perspectives are put forward, which advance the insights of improving the economic feasibility of P recovery and necessity of a comprehensive assessment of wastewater treatment & P recovery.

2. Release of different P species from sewage sludge via anaerobic-based processes

Anaerobic release of OP from WAS commonly relies on the microbial hydrolysis stage, and could be identified as two steps. At first, the anaerobic decomposing bacteria (fermenting bacteria), e.g., proteolytic bacteria, lipolytic bacteria, starch decomposing bacteria, and cellulose decomposing bacteria, makes sludge disintegrate by secreting extracellular hydrolytic enzymes. In the second step, the intracellular components are massively leached after the first step; the intracellular di-ester P like deoxyribonucleic acid and ribonucleic acid are further used by microbial metabolism.

Poly-phosphate accumulating organisms play a key role in the release of poly-P in WAS (Fig. 1). Under anaerobic conditions, PAOs get energy from breaking poly-P chains. The obtained energy is used to uptake volatile fatty acids (VFAs) and synthesize polyhydroxyalkanoates through tricarboxylic acid cycle. When the anaerobic duration is short, poly-P is released into liquid phase positively by PAOs under anaerobic conditions, so it can be considered that there is no obstacle to release poly-P under anaerobic condition.

When the anaerobic duration is long, it is observed that all poly-P was hydrolyzed to ortho-phosphate after 12 days of AF, which indicated a cell lysis happened

There are three main pathways of IP release under anaerobic condition. Microbial acidogenic process is an important anaerobic process with system acidified; apart from acid-dissolving, sulfide is found as a novel way to release Fe-P under neutral conditions with generation of FeS; moreover, dissimilated iron reduction bacteria cause reduction of ferric phosphate to ferrous phosphate. Taking the release pathways of all P species into consideration, it is clear that anaerobic-based processes are capable of accommodating all P species release.

3. Obstacles to P release via anaerobic-based processes

OP release is usually insufficient due to poor mass transfer efficiency between intracellular OP and bacteria, which is also regarded as rate-limiting step of acidogenic process.

For obstacles to IP release, excessive metal elements and aging structure of IP are main problems. The metal ions in thickened WAS are highly-concentrated about 3~50 fold than that in WAS without thickening, whereas the total P is only about 2~3 fold. The highly-concentrated metal ions may be attributed from sludge dewatering agents. As for aging structure, when phosphate is combined (removed) by ferric salts, the generated Fe-P can be further identified as innersphere complex, outersphere complex, and surface precipitation, according to the combination way between hydrous iron oxides and PO₄³⁻; normally, innersphere and outersphere complex is easier to release than surface precipitation complex. Ca-P is proved to easily form granular Ca-P, which is an aging structure of Ca-P. Besides, the complex and strong structure of Al-P is also a barrier in P release. Toor et al also found that most of the phosphate bound with Al was innersphere complex through ligand exchange; under acid conditions, the phosphate bound with Al was mainly outersphere complex due to highly protonated surface, which can adsorb phosphate efficiently [1].

High concentration of sludge P (usually >500 mg/L) is found as a serious inhibiting factor of P release. It can be inferred that when the equilibrium concentration of liquid phosphate is high, the metal ions are more likely to combine phosphate, and the adsorbed metal ions in sludge floc may also capture P to form IP precipitates.

4. Enhancing P release via anaerobic fermentation

Pretreatments at WAS can mitigate the low mass transfer efficiency. At the aspect of P release, the significance of pretreatments should be release of cellular P (OP and poly-P) into liquid phase and improve mass transfer efficiency of sludge. As a conclusion, acid/alkali and hydrothermal treatment are more efficient to release cellular P than the other pretreatment by comparing the residual content of OP and poly-P in solid phase after pretreatment and disintegration efficiency.

For enhancing IP release from sewage sludge via anaerobic fermentation, acid fermentation and anaerobic fermentation with sulfate reduction are two promising ways for future application. As shown in Fig. 3, it is assumed to use biological + Fe for P removal, the properties of WAS can be summarized as followed: 19-35 g/L total suspended

solid, 10-30 g/L total chemical oxygen demand, 300-500 mg P/L total P, Fe/P=0.3-1.5. The P species and fractions are quoted from the previous study [2], in which the fractions of Fe-P, Ca-P, OP, and poly-P are 5-24% of TP, 2-11% of TP, 10-30% of TP, and 30-80% of TP, respectively. The total P release efficiency of each step was calculated by summarizing the efficiencies from literatures and the previous studies. In acid fermentation, Fe-P is reduced to Fe²⁺-P by dissimilated iron reduction, then dissolved by low pH. The increase of Fe-P fraction (33-50% TP) after acid fermentation is attributed to conversion of released OP and poly-P to Fe-P. After the post acid extraction (pH=3-4), almost all of Fe²⁺-P is released, and the total release efficiency reaches up to 90% of TP. In AF with sulfate reduction, Fe-P is substantially released under neutral condition, and Fe/P in WAS greatly influences the release efficiency (19-63% of TP). After extracting Ca-P by post acid extraction, the total release efficiency reaches up to 79% of TP. After P recovery, a concentrated VFAs stream can be obtained, and thus carbon source and biogas production are two options for carbon recovery. For the reason that that both acid fermentation and sulfate reduction may cause decrease of methane production. Methanogenic process should be carried out in another reactor.

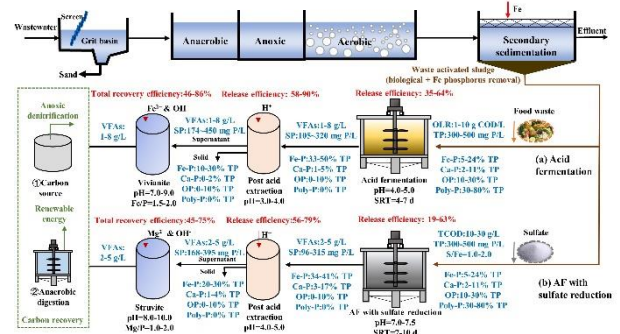


Fig. 1. Enhancing P release from sewage sludge by acid fermentation and AF with sulfate reduction for practical application.

5. Conclusion and perspectives

Anaerobic-based processes can accommodate all P species release, especially AF technology. EPSs and excessive metal ions in sludge are two main limiting factors of P release, and medium P concentration (<500 mg P/L) is preferable for anaerobic P release. Acid fermentation and AF with sulfate reduction could be two promising ways, with P release efficiency up to 64% and 63%. With simultaneous recovery of carbon and P, anaerobic-based processes are economically feasible for application. Comprehensive life cycle assessment is required for synthetically evaluating the wastewater treatment and P recovery process, as well as its environmental and human health impact.

Reference

[1]Toor, U.A., H. Shin, and D.-J. Kim, *Mechanistic insights into nature of complexation between aluminum and phosphates in polyaluminum chloride treated sludge for sustainable phosphorus recovery*. Journal of Industrial and Engineering Chemistry, 2019. **71**: p. 425-434.
 [2].Yu, B., et al., *Species, fractions, and characterization of phosphorus in sewage sludge: A critical review from the perspective of recovery*. Sci Total Environ, 2021. **786**: p. 147437.

Mainstream nitrogen removal by a one-stage partial nitritation-anammox reactor with HAP syntrophic granules after an AnMBR

○ Gaoxuefeng FENG^{1*}, Yujie CHEN¹ & Yu-You LI^{1,2}

¹Department of Civil and Environmental Engineering, Tohoku University, Miyagi 980-8579, Japan.

²Department of Frontier Science for Advanced Environment, Tohoku University, Miyagi 980-8579, Japan.

*E-mail: feng.gaoxuefeng.q1@dc.tohoku.ac.jp

Abstract

The anaerobic ammonium oxidation (anammox) process has attracted attention because of its advantages over traditional biological nitrogen removal processes. Although the anammox process for the treatment of high nitrogen concentration wastewater has been widely used worldwide, the treatment of mainstream wastewater is mainly carried out at laboratory scales, and the full scale application is limited. A one-stage partial nitritation-anammox (PN/A) reactor with hydroxyapatite (HAP) syntrophic granules was setup to treat the mainstream wastewater after an AnMBR. In this study, the nitrite-oxidizing bacteria (NOB) was successfully suppressed by the free ammonia (FA) treatment and low dissolved oxygen (DO), the nitrogen removal rate (NRR) of 0.35 kg-N·m⁻³·d⁻¹ with 79% nitrogen removal was achieved in a one-stage PN/A reactor in mainstream wastewater treatment and the feasibility of operating a one-stage PN/A reactor in mainstream wastewater treatment was demonstrated in this study.

Keywords: anammox; PN/A; mainstream; HAP

1 Introduction

Wastewater treatment mainly includes physical, chemical and biological methods. Generally speaking, biological methods rely on the metabolic capacity of microorganisms, and are lower in cost compared with physical and chemical methods. Elements such as nitrogen and phosphorus can lead to eutrophication which can affect the quality of water for daily life and production.

Many sewage treatment plants use the nitrification-denitrification process for nitrogen removal, which requires a large amount of aeration and the supply of organic carbon. The anammox process was discovered to be an advanced technology for nitrogen removal which can significantly reduce energy consumption and sludge production compared to the nitrification-denitrification process^[1].

Although the anammox process for the treatment of high nitrogen concentration wastewater has been widely used worldwide, the treatment of mainstream wastewater is mainly carried out at laboratory scales, and the full scale application is limited^[2]. Due to the high C/N ratio of mainstream wastewater, a high C/N ratio will cause a large amount of heterotrophic bacteria in the sludge resulting in the inhibition of ammonium-oxidizing bacteria (AOB) and reduce the nitrogen removal rate. However, due to the low concentration of ammonium nitrogen in the influent, the concentration of FA is low, making the suppression of NOB which is a major challenge in mainstream PN/A process more difficult. Low DO and FA treatment is widely used to suppress NOB^[3].

The addition of calcium and proper pH can generate HAP crystals, which are effective conditions for improving the sludge settleability of the anammox process and the PN/A process^[4]. HAP particles have the quality of small particles and good sedimentation. Using HAP as a sludge carrier is a good means to stabilize the operation of the reactor.

In this study, a one-stage partial nitritation-anammox reactor was setup to evaluate the nitrogen removal

performance of the one-stage PN/A reactor with HAP syntrophic granules in mainstream wastewater treatment. The NOB suppression and the stable operation of PN/A reactor in mainstream wastewater treatment was studied.

2 Materials and methods

2.1 Reactor setup and operation

The one-stage partial nitritation-anammox system was comprised of a air-lifting reactor (effective volume:2L), a substrate tank, two pumps and a water bath heater, as shown in Fig.1. Influent was pumped by a peristaltic pump. An air pump with a dispenser which was fixed to the bottom was used to oxygenate and stir the mixed liquid. The flow rate is controlled by the flow meter. The operation temperature is kept at 25°C by a water bath heater.

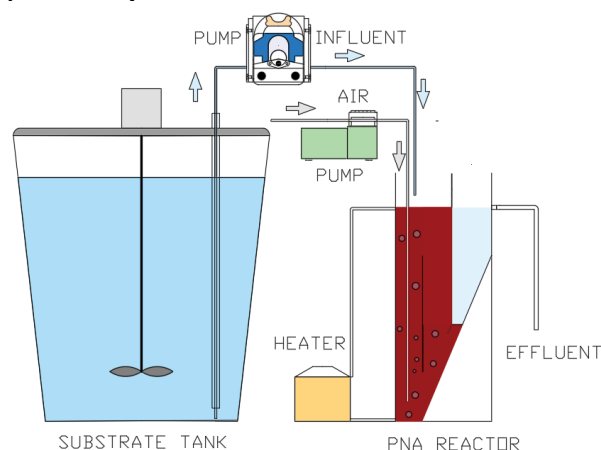


Fig. 1. Reactor configuration.

As shown in Table 1, the whole experiment was divided into 3 parts.

- 1) Phase 1 (0-10d): Using artificial mainstream wastewater, the influent nitrogen concentration

gradually decreased from 178 mg·L⁻¹ to 60 mg·L⁻¹ and the HRT was adjusted from 5h to 3h. Phase 1 served as the start up period.

- 2) Phase 2 (11-72d): Using the real mainstream wastewater after an AnMBR instead of the artificial mainstream wastewater. Adding calcium to generate HAP as a carrier of sludge.
- 3) Phase 3 (73-153d): Adjust the HRT from 3h to 2h. Increase the calcium concentration of the influent from 25 mg·L⁻¹ to 55 mg·L⁻¹.

Table 1. Experimental condition.

Period	Phase 1	Phase 2	Phase 3
Time(d)	0-10	11-72	73-153
NH ₄ ⁺ -N(mg·L ⁻¹)	178-60	42	36
HRT(h)	5-3	3	2
NRR(kg·N·m ³ ·d ⁻¹)	0.56	0.26	0.35
NRE(%)	80.9	77.1	79
MLVSS(g·L ⁻¹)	4.2	3.6	5.8
Ca(mg·L ⁻¹)		25	55

2.2 Analysis method

The influent and effluent samples which were filtered through 0.45μm filters were measured daily to know the exact situation of the reactor. Ammonium, nitrite and nitrate were analyzed by capillary electrophoresis (Agilent 7100). The mixed liquor volatile suspended solid (MLVSS) and mixed liquor suspended solid (MLSS) were analyzed according to APHA standard methods.

3 Results and discussion

The nitrogen removal performance during the whole experiment is shown in Table 1 and Fig. 2. The influent nitrogen concentration decreased from 178 mg·L⁻¹ to 36 mg·L⁻¹. The average NRR reached 0.33 kg·N·m³·d⁻¹ and the nitrogen removal efficiency (NRE) reached 78.1%.

The average ΔNO₃⁻-N/ΔN was 11% and during every period of the experiment, the average ΔNO₃⁻-N/ΔN was under 12%. In the end of the period 2, the ΔNO₃⁻-N/ΔN was over 20% and the maximum reached 49%. It means that the NOB appeared in the sludge which seriously affected the removal efficiency of nitrogen. At the begging of period 3, the HRT was adjusted from 3h to 2h, ammonium bicarbonate were putted into the reactor every day, and the influent pH was increased by sodium hydroxide from 7.9 to 8.7, thereby the FA concentration was increased to inhibit the activity of NOB, the DO concentration was under 0.05 mg·L⁻¹ through the whole experiment to suppress the NOB, and stop adding ammonium bicarbonate after a few days. The NOB was successfully inhibited, proving that inhibiting NOB through FA and low DO is a successful strategy.

ΔNO₃⁻-N/ΔN was below 12% for most time of the phase 3 which indicates that DNB consumed part of NO₃⁻ and enhance the nitrogen removal rate of this system.

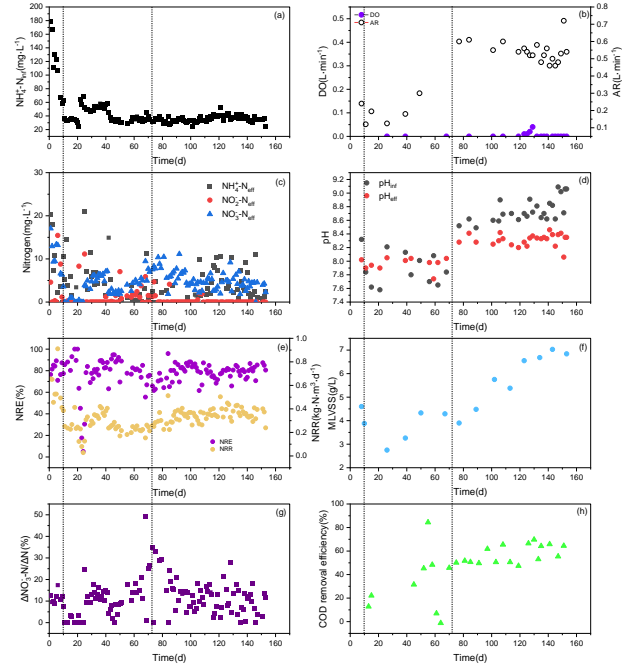


Fig. 2. The operation performance of the one-stage PN/A reactor at mainstream conditions ((a) the influent nitrogen concentration, (b) DO and AR, (c) the effluent nitrogen concentration of ammonium, nitrite and nitrate, (d) pH, (e) NRE and NRR, (f) MLSS, (g) ΔNO₃⁻-N/ΔN, (h) COD removal rate).

4 Conclusions

- (1) The use of FA treatment and low DO is an effective way to stably suppress NOB.
- (2) A stable operation with the nitrogen removal efficiency of 79% and nitrogen removal rate of 0.35kg·N·m³·d⁻¹ was achieved in a one-stage PN/A reactor in mainstream wastewater treatment.

Reference

- [1] TRINH, Hoang Phuc, et al. Recent Development of the Mainstream Anammox Processes: Challenges and Opportunities. *Journal of Environmental Chemical Engineering*, 2021, 105583.
- [2] CHEN, Yujie, et al. High nitrogen removal performance of anaerobically treated fish processing wastewater by one-stage partial nitrification and anammox process with hydroxyapatite (HAP)-based syntrophic granules and granule structure. *Bioresource Technology*, 2021, 338: 125526.
- [3] WANG, Zhiyao, et al. Unravelling adaptation of nitrite-oxidizing bacteria in mainstream PN/A process: Mechanisms and counter-strategies. *Water Research*, 2021, 200: 117239.
- [4] GUO, Yan, et al. Achieving superior nitrogen removal performance in low-strength ammonium wastewater treatment by cultivating concentrated, highly dispersive, and easily settleable granule sludge in a one-stage partial nitrification/anammox-HAP reactor. *Water Research*, 2021, 200: 117217.